TECHNISCHE UNIVERSITÄT MÜNCHEN

Wissenschaftszentrum Weihenstephan für Ernährung, Landnutzung und Umwelt

Lehrstuhl für Renaturierungsökologie

In Kooperation mit

Fachgebiet für Vegetationsökologie

Hochschule Weihenstephan-Triesdorf

Understanding CO₂ fluxes in peatlands: What can we learn from process-oriented modelling?

Christine Metzger

Vollständiger Abdruck der von der Fakultät Wissenschaftszentrum Weihenstephan für Ernährung, Landnutzung und Umwelt der Technischen Universität München zur Erlangung des akademischen Grades eines Doktors

der Naturwissenschaften (Dr. rer. nat.)

genehmigten Dissertation.

Vorsitzender: Prof. Dr. H. Pretzsch
Prüfer der Dissertation: 1. Prof. Dr. J. Kollmann
2. Prof. Dr. M. Drösler (Hochschule Weihenstephan-Triesdorf)
3. Prof. Dr. P.-E. Jansson (Royal Institute of Technology, Stockholm, Schweden)

Die Dissertation wurde am 21.12.2015 bei der Technischen Universität München eingereicht und durch die Fakultät Wissenschaftszentrum Weihenstephan für Ernährung, Landnutzung und Umwelt am 07.04.2016 angenommen.

Table of contents

List of figures

List of tables

Summary

Over millennia, peatlands have accumulated a huge amount of carbon (C) in peat. Drainage for e.g. cultivation, leads to release of the stored carbon and makes them hot spots for carbondioxid (CO_2) emissions. Process based models can help to understand and predict such changes. The overall aim of this dissertation project was to improve the knowledge and understanding of the processes involved in the carbon cycle and their contribution to CO_2 emissions from treeless peatlands. This is a precondition for correct quantifications and predictions on a larger scale or at sites and under scenarios where no measurements are possible or available. This work consists of three studies: in the first study, the process oriented CoupModel was calibrated to fit to measurements from five European peatland sites to explore differences in CO_2-related processes between the sites. The second study focuses on interactions between the different processes on another site. The third study investigates the derivation of plant parameters from satellite data as model input. An additional aim of study I and II was to test if the available data is sufficient to reduce parameter uncertainty and consequently model output uncertainty. Further, gaps between modelled and measured fluxes should be identified to indicate open issues in process understanding.

Most of previous CO_2 modelling studies on peatlands have focused on how well a certain set of data can be described by the model, while data comparisons between sites are usually done with statistical or data-oriented approaches. However, the latter are of limited benefit if sites differ in several factors. Study I aimed to find out whether the large differences in measured CO_2 fluxes between the various treeless peatland sites are solely explained by the model input data (i.e. differences in meteorology, water table, soil C stock and management) or to what extent a site-specific parameterisation is necessary (i.e. the sites differ in their response to the input drivers). Therefore, the model was calibrated to fit to the measurements and the resulting parameterisation was analysed. The results revealed the importance of site-specific vegetation parameters and soil conditions, while for most other parameters a site-independent configuration was applicable. The photosynthetic efficiency and the ratio of C stored during litter fall for regrowth in the next year differed greatly between the different sites, as well as the soil respiration rate coefficients representing substrate quality and land-use history. The identification of these parameters is highly relevant for upscaling issues and model predictions.

Further, several strong correlations between parameters were detected. To investigate interactions within and between different processes the model

was applied in study II to another open peatland site with long term flux measurements of 12 years. This study was further meant to act as validation for the constrained parameters from study I, with an independent data set. Unlike previous CO_2 modelling studies on peatlands that usually focus on net ecosystem exchange (NEE) as the only process and calibration variable, study II included all data available and parameters from several biotic and abiotic processes. Many interactions between different processes and between their parameters were revealed. Resulting parameter ranges were found to be dependent on the variable and the performance index (e.g. correlation coefficient or mean error) chosen to quantify the fit of the model output to measured data. Further, they depended on other calibrated parameters (equifinalities). This implies that transferring parameter ranges between models need to be done with caution, especially if such ranges were achieved by considering only few processes. Further, the high importance of the uncertainty in unsaturated soil water distribution was shown: the calibrated shape parameter of the water retention curve correlated with the model performance in all measured variables, which hindered constraining other parameters by overlaying their correlations. The parameterisation for C uptake versus losses strongly derivate from those in study I, indicating that the plants at this very nutrient poor site were much more efficient in building biomass and storing C with relatively little assimilates compared to plants from the more nutrient rich sites in study I. The findings of this study can improve future model calibrations and experimental setups, and are of high interest for comparisons with results from other sites and models.

Study I showed the great impact of vegetation on CO_2 fluxes due to site-specific differences in photosynthetic efficiency. However, this parameter could be derived by fitting the model to measured above-ground biomass or leaf area index (LAI). Several studies had indicated a great potential to derive photosynthesis as well as LAI and biomass from remote-sensed NDVI on several different types of ecosystems, which would make this parameter available on a large scale. Testing such possibilities on temperate fen grasslands was the aim of the third study. Therefore, NDVI, LAI and biomass were sampled at several sites in a fen in South Germany and compared with each other and with NDVI calculated from satellite images. A special interest was to explore how land-use intensity affects the relationships between the different indices and vegetation characteristics. The results revealed high uncertainties in using NDVI as predictor for LAI, and NDVI or LAI as predictor for biomass on such ecosystems. A likely explanation is the high amount of standing brown biomass which was unevenly distributed within the canopy, especially at extensively managed meadows. NDVI was shown to be a better proxy for photosynthesis than

LAI, as its relation to photosynthesis potential was nearly linear and site-independent. Further research should therefore investigate the use of NDVI as input for CO_2 models.

By using process-oriented modelling and observation data, this work could explain several observed phenomena, identify many open issues for further research and suggest several model improvements including proxies for site-specific parameters. The presented results will be of interest for both, modellers and experimentalists in designing their model and measurement setup.

Zusammenfassung

Moore haben über Jahrtausende Kohlenstoff (C) in Form von Torf akkumuliert. Der gespeicherte Kohlenstoff wird in großen Mengen als CO_2 freigesetzt, wenn die Moore entwässert werden, z.B. für die landwirtschaftliche Nutzung. Prozessbasierte Modelle können dazu beitragen solche Änderungen zu verstehen und Emissionen vorherzusagen. Das Ziel dieser Doktorarbeit ist im Allgemeinen Wissen und Verständnis über die Prozesse des Kohlenstoffzyklus und ihren Beitrag zu CO_2 Emissionen aus waldfreien Mooren zu verbessern. Dies ist Voraussetzung für eine zuverlässige Quantifizierung und die Vorhersage von CO_2 Emissionen auf einem größeren Maßstab, oder auf Standorten oder unter Bedingungen für die keine Messwerte vorliegen oder erhoben werden können. Die Arbeit besteht aus drei Studien: Um Standort-Unterschiede in CO_2 bezogenen Prozessen zu erforschen, wurde in der ersten Studie das prozess-orientierte CoupModel an Daten von fünf verschiedenen, europäischen Moorflächen kalibriert bis modellierte und gemessene Werte zusammenpassen. Die zweite Studie hat ihren Schwerpunkt auf den Interaktionen zwischen verschiedenen Prozessen an einem weiteren Standort. In der dritten Studie wird die Herleitung von Pflanzen-Parametern aus Satellitendaten untersucht, die als Modell-Eingabe dienen könnten. Ein weiteres Ziele der ersten und zweiten Studie war der Test, ob die vorhandenen Daten ausreichend sind um Modellparameterwerte einzugrenzen. Des Weiteren sollten Lücken zwischen modellierten und gemessenen Flüssen identifiziert werden, die auf ein unvollständiges Prozessverständnis hinweisen.

Die meisten der bisherigen Studien über die Modellierung von CO_2-Flüssen in Mooren konzentrieren sich darauf, wie gut ein bestimmter Datensatz vom Modell beschrieben werden kann, während Emissionsunterschiede zwischen verschiedenen Standorten üblicherweise mit statistischen oder datenorientierten Ansätzen ausgewertet werden. Letztere sind jedoch begrenzt nützlich, wenn sich die Standorte in mehreren Faktoren unterscheiden. Um herauszufinden, inwiefern sich die großen Unterschiede in gemessenen CO_2 Flüssen zwischen den verschiedenen Moorstandorten der Studie I allein durch die unterschiedliche Meteorologie, Wasserstand, Boden-Kohlenstoffgehalt und Landnutzung erklären lassen, wurde das Modell an den Messdaten kalibriert und die resultierenden Parametrisierung analysiert. Dabei stellte sich die Wichtigkeit von standortspezifischen Vegetationsparametern und Bodeneigenschaften heraus, während für die meisten anderen Parameter auch eine standortunabhängige Konfiguration zu guten Modellergebnissen führte. Die photosynthetische Effizienz und der Anteil an C, welcher während dem Laubfall eingelagert und für den

x

Neuaustrieb im nächsten Jahr verwendet wird, variierten stark zwischen den verschiedenen Standorten. Das traf auch auf die Zersetzungsratenkoeffizienten zu, welche Substratqualität und Nutzungsgeschichte widerspiegeln.

Außerdem wurden mehrere, starke Korrelationen zwischen Parametern aufgedeckt. Um die Interaktionen innerhalb und zwischen verschiedenen Prozessen zu untersuchen, wurde das Modell in der zweiten Studie an einem weiteren waldfreien Moor angewandt, für das eine lange Zeitreihe von Messdaten über 12 Jahre hinweg vorlagen. Diese Studie war außerdem als Validierung der aus Studie I resultierenden Modellkonfiguration mit unabhängigen Daten gedacht. Entgegen bisheriger CO_2-Modellierungsstudien, welche sich häufig auf den Netto Ökosystemaustausch (NEE) als einzigen Prozess und als einzige Kalibrierungsvariable beschränken, wurden in Studie II alle verfügbaren Daten verwendet und Parameter von verschiedenen biotischen und abiotischen Prozessen untersucht. Viele Interaktionen zwischen verschiedenen Prozessen und ihren Parametern wurden aufgedeckt. Es stellte sich heraus, dass resultierende Parameterwertebereiche von der Messvariable und dem Performanceindex (z.B. Korrelationskoeffizient oder Mittlerer Fehler) abhingen, welche als Kriterium für die Auswahl von den zu den Messdaten passenden Modellläufen gewählt wurde. Des Weiteren hingen sie von anderen, kalibrierten Parametern ab (Equifinalities). Das bedeutet eine eingeschränkte Übertragbarkeit von Parameterwertebereichen zwischen Modellen, insbesondere, wenn solche Wertebereiche unter Berücksichtigung von nur wenigen Prozessen ermittelt wurden. Außerdem wurde die enorme Wichtigkeit der Unsicherheit in der ungesättigten Bodenwasserverteilung gezeigt: der kalibrierte Parameter, der den Verlauf der Wasserrückhaltekurve beschreibt, korrelierte mit der Modellperformance in allen Messvariablen und behinderte dabei die Eingrenzung der Wertebereiche anderer Parameter, indem deren Korrelationen überlagert wurden. Die Parametrisierung für die Aufnahme und Freisetzung von Kohlenstoff unterschied sich deutlich von den Ergebnissen aus Studie I, was darauf hindeutet, dass die Pflanzen dieses sehr nährstoffarmen Standorts, im Vergleich zu den Pflanzen der nährstoffreicheren Standorte aus Studie I, einen sehr viel effizienteren Kohlenstoffhaushalt haben, um mit den relativ wenigen Assimilaten zurecht zu kommen. Die Ergebnisse dieser Studie sind für Entwurf und Planung zukünftiger Modellkalibrationen und Feldexperimente hilfreich und für Vergleiche mit Ergebnissen von anderen Modellen und Standorten von großer Bedeutung.

In Studie I wurde der starke Einfluss der Vegetation auf CO_2-Flüsse durch die standortspezifischen Unterschiede in der photosynthetischen Effizienz gezeigt. Dieser Parameter kann jedoch ermittelt werden, in dem man das Modell an Messwerte von Biomasse oder Blattflächenindex (LAI) anpasst. Mehrere Studien weisen auf die Möglichkeit hin, Photosynthese sowie Blattflächenindex und Biomasse aus Fernerkundungsdaten (insbesondere dem sogenannten Normalized Difference Vegetation Index, NDVI) abzuleiten, so dass der Parameter auch großskalig verfügbar wäre. Entsprechende Korrelationen wurden auf verschiedenen Ökosystemen ermittelt und sollten in Studie III auf temperaten Niedermoorstandorten getestet werden. Hierfür wurden NDVI, LAI und Biomasse an verschiedenen Standorten im Freisinger Moos, einem süddeutschen Niedermoor, gesammelt und untereinander, sowie mit Satelliten-NDVI verglichen. Insbesondere sollte untersucht werden, wie sich die Landnutzungsintensität auf die Beziehungen zwischen den verschiedenen Indizes und Vegetationseigenschaften auswirken. Es stellte sich heraus, dass die Verwendung von NDVI als Schätzer für LAI, sowie NDVI oder LAI als Schätzer für Biomasse mit hohen Unsicherheiten behaftet ist. Wahrscheinlich ist dafür der hohe Anteil an stehender, brauner Biomasse verantwortlich, welche besonders in extensiv genutzten Wiesen sehr heterogen verteilt war. Für die Schätzung von Photosynthese war der NDVI geeigneter als der LAI, da seine Beziehung zum Photosynthese-Potential nahezu linear und standortunabhängig war. Zukünftig sollte daher der Nutzen von NDVI als Input für CO_2-Modelle untersucht werden.

Mit Hilfe von prozessorientierter Modellierung und Messdaten konnten in dieser Arbeit verschiedene Phänomene erklärt, offene Punkte für zukünftige Forschung identifiziert und verschiedene Modellverbesserungen vorgeschlagen werden, welche die Schätzung standortspezifischer Parameter mit einschließt. Die vorgestellten Ergebnisse sind für sowohl Modellanwender, als auch Experimentalisten in der zukünftigen Gestaltung von Modell- und Messaufbau von Bedeutung.

Table 1. Abbreviations and technical terms as used in this study. A description of the used parameter symbols can be found in the appendix, Table A1.3-1.6.

Term	Definition
Bog	A peatland without connection to ground water and mineral soil. Plants are only fed by rain water, while the vegetation is typically dominated by *Sphagnum* mosses. Therefore, conditions are usually very nutrient poor and acid. Typically they establish from fens, when the layer of *Sphagnum* mosses has grown to such an extent that plant roots cannot reach the ground water and mineral soil anymore.
C	Carbon
CO_2	Carbon dioxide
EC	Eddy covariance. A technique to measure turbulent fluxes (e.g. heat, gases like CO_2) between atmosphere and biosphere (cf. Baldocchi et al., 1988).
Fen	A peatland with connection to ground water and mineral soil. Fens are nutrient richer and usually more alkaline than bogs, with a vegetation of usually tall sedges (*Carex*) or reed. They are often agriculturally used as grass- or cropland or for forestry.
GAI	Green area index, corresponds to LAI in a narrower sense and includes only the green (photosynthetically active) plant parts.
GHG	Greenhouse gas
GPP	Gross primary production: Uptake of CO_2 by the ecosystem via e.g. photosynthesis. As CO_2 is removed from the atmosphere towards the ecosystem, this flux is labelled with a negative sign in this study.
GWP	Global warming potential. Stocker et al. (2013): "An index, based on radiative properties of greenhouse gases, measuring the radiative forcing following a pulse emission of a unit mass of a given greenhouse gas in the presentday atmosphere integrated over a chosen time horizon, relative to that of carbon dioxide. The GWP represents the combined effect of the differing times these gases remain in the atmosphere and their relative effectiveness in causing radiative forcing. The Kyoto Protocol is based on GWPs from pulse emissions over a 100-year time frame."
H	Sensible heat: Energy transfer resulting in a temperature change of the system (temperature fluxes)

Term	Definition
LAI	Leaf area index. Total one-sided area of leaf tissue per unit ground surface area (Watson, 1947).
LE	Latent heat: Energy fluxes from the Earth's surface to the atmosphere, caused by processes without a temperature change of the system, e.g. evaporation, transpiration, or snow melt.
ME	Mean error. When used as performance index it quantifies the difference between the average of the simulated compared to the average in the measured, i.e. it shows the error in the magnitude.
Mire	Natural peatland without remarkable land-use management.
NDVI	Normalized differenced vegetation index, indicating the greenness of the vegetation. It is calculated from wavebands in the red (R_{RED}, 760 – 850 nm) and near infrared (R_{NIR}, 630 – 685 nm) wavebands: $$\text{NDVI} = \frac{R_{NIR} - R_{RED}}{R_{NIR} + R_{RED}}$$
NEE	Net ecosystem exchange is the balance of photosynthesis, and respiration from plants and microbes: NEE = GPP + R_{eco} A negative value indicates ecosystem uptake, i.e. the GPP component (negative) is larger than the respiration losses.
NSE	Nash-Sutcliff efficiency (Nash and Sutcliffe, 1970). It accounts for both, deviation of dynamics (R^2) and magnitude (ME). It ranges from $-\infty$ to 1, whereas 1 means the best agreement of two variables (e.g. best fit of modelled to measured data). Values < 0 indicate that the mean measured value is a better predictor than the simulated value (Moriasi et al., 2007).
PAI	Plant area index, corresponds to LAI as measured with non-destructive methods and therefore includes also brown (photosynthetically inactive) plant parts like senescent leaves.
PAR	Photosynthetically active radiation. Radiation in the light spectrum that could be used by plants for photosynthesis.
Peatland	Soil type, characterised by a high content of organic carbon (e.g. at least 30% dry mass of dead organic material in the upper most 30 cm of the soil according to Sponagel, 2005. Typically formed by incomplete decomposition of plant litter due to high water levels causing anoxic conditions.

Term	Definition
Performance	The ability of the model to simulate an output variable in the way that it fits to the corresponding observation variable. This ability is quantified by performance indices like e.g. R^2 or ME.
PP	Potential photosynthesis: The possible assimilation of a plant in its current developmental stage. This corresponds to the photosynthesis derived from the GPP light response curve at a theoretical photosynthetic photon flux density of 2000 µmol m^{-2} s^{-1}.
PPFD	Photosynthetic photon flux density
R^2	Coefficient of determination: An index between 0 and 1, indicating the strength of a correlation. When used as performance measure (study I and II), it assesses the correlation between measured and modelled values, i.e. how well the dynamics in the measurement derived values are represented by the model. When used as measure for a relationship (study III) it indicates the slope of the regression line.
R_{eco}	Ecosystem respiration: Sum of autotrophic (from plant) and heterotrophic (from microbes) respiration.
Rn	Net radiation
SE	Residual standard error: indicates the distances between the observed data points and the regression line, i.e. the scatter in the relationship, under consideration of the number of data points (degree of freedom).
SPA	Specific plant area: Total one-sided area of plant tissue per unit ground surface area, divided by plant weight.
SOC	Soil organic carbon
Ts	Soil temperature
VI	Vegetation index, e.g. LAI or NDVI
WT	Water table. A negative value indicates the distance from the below ground water level to the soil surface, while a positive value indicates flooded conditions.

Publications and the candidates contribution

This PhD thesis is based on three studies, which have been published or are in preparation for publishing:

The site comparison (study I; chapter 2.1 to 2.4, 3.1 to 3.3, 4.1 and 4.2) was published under the Creative Commons Attribution 3.0 License as: Metzger, C., Jansson, P. E., Lohila, A., Aurela, M., Eickenscheidt, T., Belelli-Marchesini, L., Dinsmore, K. J., Drewer, J., van Huissteden, J., and Drösler, M.: CO_2 fluxes and ecosystem dynamics at five European treeless peatlands – merging data and process-oriented modeling, Biogeosciences, 12, 125–146, doi:10.5194/bg-12-125-2015, 2015. My contribution included analysing of possible data sets and models, selecting the most suitable ones for that study, raising the scientific question, setting up and running the model, setting up and performing the calibration procedure, analysing and interpreting the results and writing the drafts of the manuscript including all graphs and tables, incorporating comments from the co-authors and revising the manuscript.

The process interaction study (study II, chapter 2.1 to 2.4, 3.1 to 3.3, 4.3 and 4.4) is in review for publication as Metzger, C., Nilsson, M. B., Peichl, M., and Jansson, P.-E.: The importance of process interactions and parameter sensitivity for modelling the carbon dynamics in a natural peatland, Geosci. Model Dev. Discuss., doi:10.5194/gmd-2016-116, in review, 2016. My contribution included analysing the data, raising the scientific question, setting up and running the model, setting up and performing the calibration procedure, analysing and interpreting the results and writing the drafts of the manuscript including all graphs and tables. Further, I incorporated the comments from the co-authors and revised the manuscript.

The study about the relationships between vegetation indices and vegetation characteristics (study III, chapter 2.5, 3.4, 4.5 and 4.6) is accepted for publication in Grass and Forage Science, as: Metzger, C., Heinichen, J., Eickenscheidt, T., and Drösler, M.: Effects of management intensity on the relationships of NDVI to GPP, LAI and plant biomass on grassland fens. My contribution included designing the measurement setup and performing most of the sampling and processing of LAI, NDVI and biomass data and calculating NDVI from satellite images. I performed the statistical tests, analysed and interpreted the data and wrote all versions of the manuscript under the consideration of the comments from the co-authors. All graphs and tables were created by me.

1   Introduction

"Warming of the climate system is unequivocal, and since the 1950s, many of the observed changes are unprecedented over decades to millennia. The atmosphere and ocean have warmed, the amounts of snow and ice have diminished, sea level has risen, and the concentrations of greenhouse gases have increased." (IPCC, 2013).

In the Kyoto protocol, 191 countries committed to reduce their greenhouse gas emissions. Germany aims to reduce its emissions until 2050 by at least 80 to 95 percent compared to the base year 1990 (BMUB, 2015). Peatland restoration has a high potential for reduction of climate-damaging carbon-dioxide (CO_2) emissions that need to be reported for peatlands and might be accounted for CO_2 mitigation in future (Section 1.1). Restoration investments require a correct quantification of action benefits which, in turn, requires a solid process understanding and reliable model predictions. Process-based models are further necessary to upscale the process dependencies gained from site measurements, to identify emission hotspots and locate areas with need for action (Section 1.2). Process models are built on physical equations which require site or ecosystem specific parameters, which are often unknown and therefore need to be retrieved from calibration (Section 1.3).

In the last decades, a lot of models have been developed based on physical equations, representing the current knowledge in process understanding (Section 1.4). Progresses in computer technology allow constantly faster computation and therefore more detailed models with extensive calibration algorithms. At the same time a huge amount of detailed measurements became available, allowing calibration, validation and further improvement of current models.

Also, technology in remote sensing is continuously improving, providing new possibilities for using satellite data in high resolution as model input (Section 1.5).

The overall aim of this PhD project was to gain further knowledge on processes involved in the carbon cycle by making use of the available data and an existing model (Section 1.6). This knowledge will help to improve model predictions on peatlands, whereas model improvement does not exclusively refer to new or modified model equations, but also includes model parameterization. Further, the possibility of using remote sensed vegetation indices as model input data on managed peatlands was investigated.

1.1 Why peatland CO_2 emissions?

Natural peatlands are usually sinks for CO_2, but can turn into emission sources due to management practices. During photosynthesis, plants take up CO_2 from the atmosphere and incorporate the carbon into plant material. Some carbon is again released as CO_2 during plant respiration, while another part turns into litter. In mineral soils, most of the litter is usually soon mineralised by decomposition through microbes. However, undisturbed peatlands typically have a high water level, causing anoxic conditions which depress the decomposition process and organic material accumulates in the soil (Clymo, 1984). Over millennia, this had led to huge carbon accumulations of at least 550 Gt of carbon, stored in peat (Yu, 2012 and references therein). This is equivalent to 30% of all global soil carbon (Gorham, 1991), twice the carbon stock in the forest biomass of the world (Parish, 2008) and almost half the total atmospheric content (Byrne et al., 2004). Peatlands are the top long-term carbon store in the terrestrial biosphere (Fig. 1) – a hypothetical sudden release would result in an instantaneous 50% increase in atmospheric CO_2 (Byrne et al., 2004). If drained, the stored carbon stock becomes exposed to oxygen and accessible for enhanced decomposition, leading to CO_2 emissions. Peatlands were widely drained for forestry, agricultural production and peat extraction. In Germany, 95% of the peatlands are drained, causing 2–5% of the total greenhouse gas emissions (Drösler et al., 2013b). This makes them the largest single emission source beside the energy sector (Drösler et al., 2013b). Worldwide, about 14–20% of peatlands are currently used for agriculture and the great majority of these are used as meadows and pastures (Strack, 2008).
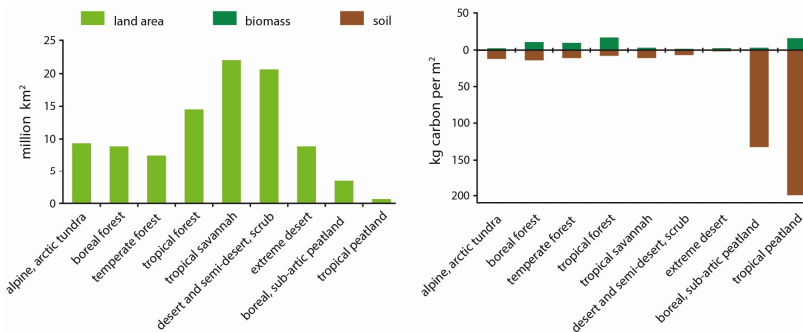
Figure 1. Extent and carbon density of terrestrial biomes. From UNEP year book (2012).

Many investigations have shown that CO_2 emissions from peatlands increase with increasing land-use and drainage intensity (e.g. Drösler et al., 2008; Petrescu et al., 2015). The GHG fluxes of drained peat soils depend on soil properties (Klemedtsson et al., 2005; Updegraff et al., 1995), groundwater level (e.g. Reichstein et al., 2003) and management practices, like fertilization and ploughing (e.g. Aerts and Toet, 1997, Maljanen et al., 2010 and references therein). Rewetting of a peatland can stop the enhanced decomposition and even turn it back into a CO_2 sink (e.g. Tuittila et al., 1999; Waddington et al., 2010). The restoration of peatlands is one of the most cost-effective ways of avoiding anthropogenic greenhouse gas emissions (Parish, 2008), without noteworthy limiting production or constraining economy as the affected area is small: Only 3% of the global land mass is covered by peatlands (Lappalainen, 1996).

Additionally, rewetting has positive effects on other ecosystem service functions: Both, rainwater-fed bogs and groundwater-fed fens host many endangered species which were specialised to tolerate nutrient-poor, acid or wet conditions and are important for biodiversity (Parish, 2008). On ecosystem scale, they are important for flood mitigation, storm abatement, aquifer recharge, drought prevention, water quality protection and improvement, aesthetics and subsistence use (Mitsch and Gosselink, 2000). Undisturbed peatlands have a cleaning function by filtering nitrate, ammonium and phosphate, and the high cation exchange capacity of *Sphagnum*-mosses makes them suitable for trapping aerial heavy metal pollutants (Clymo and Hayward, 1982).

However, peatland restoration takes costs and efforts. Therefore, a precise quantification of gained emission prevention is a perquisite for rewarding and accounting them in respect to the CO_2 mitigation commitment. A detailed understanding of the connected processes, drivers and dependencies is essential to assess actual emissions and quantify the effect of potential restoration efforts and management practices.

1.2   Why process-oriented modelling?

Process-oriented models predict CO_2 emissions under different conditions, climate change and different management scenarios, based on current process understanding and knowledge gained from measurements. Many extensive measurements have been made and are currently ongoing to investigate CO_2 emissions from peatlands, providing valuable information about responses to climatic conditions and management effects. However, such measurements are cost intensive, site-specific and provide only limited possibilities for up scaling and predictions and are therefore only feasible

for selected pilot sites to develop, calibrate and verify models (Joosten and Couwenberg, 2009).

Process models allow transferring the gained knowledge between sites and therefore contribute to better understanding. They provide extended comparison and evaluation possibilities and could act as plausibility check or cross validation to data-oriented (empiric) modelling approaches, which use statistical methods. Models can quantify explicitly and consistently how climate and soil drivers control the sources and sinks of different gases, their spatial distribution and their temporal variability (Vuichard et al., 2007). Process models can predict CO_2 fluxes under different climate and management scenarios or at different locations. Therefore, they are useful to quantify emissions on a larger scale (e.g. St-Hilaire et al., 2010), to predict emissions under future climate scenarios (e.g. Cramer et al., 2001; Gong et al., 2013) or to assess the effect of change in management practices and restoration efforts (e.g. St-Hilaire et al., 2010; Schneider et al., 2003). They might help to identify hot spots and regions with high potential for emission reduction, as well as provide recommendations for management actions. Comparisons of measured flux data are usually done with statistical or data-oriented approaches (e.g. Humphreys et al., 2006; Lund et al., 2009). They are useful to explore the effect of single variables if the site conditions are similar or differ only in few variables (like in e.g. Ward et al., 2013; Chojnicki et al., 2010). However, they are uninformative when trying to distinguish between responses of several individual factors. Processes are usually linked and interact with each other. Therefore, important drivers at one site might not play a significant role on another site (e.g. Lafleur et al., 2005). Process oriented modelling provides a method to identify to what extent observations at different sites can be described by the same processes, while accounting for such interactions. Thereby, they help explaining observed phenomena in the data and increase process understanding. In contrast to previous CO_2 modelling studies on peatlands that usually focus on model performance, the main aim of the first study in this thesis was to explore the differences between various peatland sites in their responses to driving variables. Still, this requires (1) that the model can reasonably describe the observations and (2) that the parameters used in the model to describe the observations can be estimated from available data.

1.3 Why parameterisation, sensitivity analysis and investigation of interactions?

Processes in the real world, as well as parameters defining the processes in the models are strongly interlinked. Process models are based on a conceptual basic understanding of phenomena related to specific processes. They are represented in the models as physical equations, including a number of coefficients. Those coefficients are called parameters. Only few of them are known as site-independent, unambiguous constants from laboratory experiments. All other parameters need to be either assumed, or gained from calibration procedures. But not all parameters have a strong impact on model output and performance. Monte Carlo based sensitivity analysis are used to identify the key parameters for both, the performance and the impact on various major model outputs (e.g. Verbeeck et al., 2006; Santaren et al., 2014).

Many studies investigated single processes and their parameters, while only few consider different biotic and abiotic processes and multiple calibration variables. Several modelling studies have explored peatland hydrology (e.g. Dimitrov et al., 2010; Dettmann et al., 2014) and heat fluxes in peatlands (e.g. Keller et al., 2004; Granberg et al., 1999), while others concentrate on carbon fluxes (e.g. Verbeeck et al., 2006) where the focus is sometimes on heterotrophic respiration only (e.g. Abdalla et al., 2014). Some studies consider several variables for model calibration and conclude the usability of such multiple constraint approaches, but were not performed on peatlands (e.g. Santaren et al., 2014; Carvalhais et al., 2010). Only few models applied to peatlands have a holistic approach, accounting for interactions between water and heat fluxes, soil hydraulic properties and the carbon cycle, including an explicit simulation of the plant (e.g. Wetland-DNDC, Zhang, 2002; *ecosys*, Grant et al., 2012; CoupModel, Jansson and Karlberg, 2010). Holistic ecosystem models are needed, because processes in the real world are strongly interlinked: Net ecosystem exchange (NEE) is the balance of photosynthesis and respiration from plants and microbes. All components of NEE are strongly interconnected in several ways with the amount of plant biomass, temperature, radiation, nutrients and moisture availability (e.g. Clymo, 1984, Lindroth et al., 2007). Photosynthesis, soil temperature and moisture depend among others on incoming radiation, transpiration and plant coverage. Heterotrophic respiration further depends on quality and quantity of plant litter (e.g. Yeloff and Mauquoy, 2006). In addition, phenological events such as the timing of snow melt are important for soil temperature dynamics and biologic activity (Aurela, 2004).

Such processes interactions are realised in ecosystem models, but lead to inter-correlation between the different parameters and complicate the

parameter constraint to an unambiguous solution: several combinations of different parameter values can lead to a similar good fit of model output to measured variables which is defined as equifinality (Beven and Freer, 2001). The model sensitivity to such parameters might be hidden if equifinalities are not considered. Constraining a model based on multiple variables can help to resolve or reduce equifinalities (Carvalhais et al., 2010). Therefore, unlike previous peatland modelling studies, the second study of this thesis investigates the sensitivity of parameters from several different modules, not only on NEE, but also on latent heat (LE), sensible heat (H), net radiation (Rn), leaf area index (LAI), soil temperatures (Ts), water table (WT) and snow. However, criteria based on multiple variables imply a subjective weighting of variables and performance indices. Fitting the model to a certain variable might improve or worsen the performance in another variable (Carvalhais et al., 2010) and might therefore have implications for the parameter range judged as valid (e.g. Schulz and Beven, 2003). In the second study of this thesis, the effects of selecting a certain criteria on the resulting parameter range will be investigated.

1.4   Why CoupModel?

A large number of different process models have been developed, with different degree of complexity and included processes, and for different purposes. A detailed approach was chosen for this PhD project by applying the well-established, ecosystem independent CoupModel (Jansson and Karlberg, 2010). The CoupModel combines multiple sub modules representing many different biotic and abiotic processes and supports sensitivity analysis techniques.

On peatlands, some attempts have been made to consider site differences using simplified process models on national (e.g. ECOSSE, Smith et al., 2010) and global scales (e.g. InTec, Ju and Chen, 2005; McGill, St-Hilaire et al., 2010) and up to millennial timescale (HPM, Frolking et al., 2010; JSBACH, Schuldt et al., 2013). However, I am not aware of any studies comparing differences in parameter distributions of CO_2-related processes between treeless peatland sites, using an uncertainty-based approach and a detailed process-oriented model running on site scale.

Many carbon ecosystem models are available for site scale application such as Biome-BC (Feng et al., 2011), DNDC (Reichstein et al., 2003), PaSim (Contant et al., 2008), PIXGRO (Clymo, 1973), CANDY (Reich et al., 1994) or DAYCENT (CENTURY) (Price, 1994). Some models were explicitly created or adapted to peatlands such as PDM (Frolking et al., 2001), PCARS (Frolking et al., 2002), CASA (Potter et al., 2001), *ecosys*

(Grant et al., 2012), wetland-DNDC (Zhang 2002), peatland DOS-TEM (Potter et al., 2001), PEATLAND-VU (van Huissteden et al., 2006), PEAT-BOG (Wu and Blodau, 2013), LPJ-WHy (Wania et al., 2009a, 2009b) or GUESS-ROMUL (Yurova et al., 2007).

In this work, the CoupModel was chosen for the following reasons: The model was designed for a wide range of soil types and different ecosystems and applications (see Jansson, 2012 for review) which might be useful as some of the sites in the present study are already quite degraded and might not respond like a typical, undisturbed peatland anymore. The model has been shown to be capable of simulating all three main greenhouse gases from peatlands: CO_2 (Klemedtsson et al., 2008), nitrous oxide (N_2O) (Norman et al., 2008) and methane (CH_4) (Ravina, 2007). Further, the CoupModel includes detailed sub modules for the most relevant processes in the carbon cycle, including related abiotic processes: It predicts plant growth, plant transpiration and autotrophic respiration, soil nitrogen (N) and C processes, energy and heat fluxes, soil temperature, soil frost and snow depth. It supports an hourly time step for input and output data and can run in even finer time resolution, which is necessary for analysing e.g. chamber flux data. The user can select between different sub models, different equations and different complexities and easily access all parameters via a user interface. Calibration procedures with randomized parameter values and methods for visualisation and detailed analysis of the model output are supported. An extensive model description can be found in Jansson and Karlberg (2010). The model and its documentation as well as several tutorials for its application can be downloaded from the CoupModel homepage (CoupModel, 2015).

1.5   Why LAI and NDVI?

Leaf area index is connected to many factors and parameters needed for modelling CO_2 fluxes. LAI might be estimated from normalized difference vegetation index (NDVI), which is available on a global scale from satellite data. Optical vegetation indices (VIs) are usually much less expensive and are easier to measure compared with more direct variables like carbon uptake or biomass, and do not destruct the vegetation.

Vegetation was identified as crucial factor for both, process-oriented modelling (Running and Coughlan, 1988; Bonan, 1993), and empirical modelling (Lund et al., 2009; Lindroth et al., 2008), and plays a major role in many processes involved in the carbon cycle. This is reflected by several indicators that are commonly used to represent various plant functionalities in ecosystem and carbon models, including the CoupModel as used in study

I and II. LAI or amount of biomass affect for example, plant respiration (De Vries, 1975), evapotranspiration (e.g. Leuning et al., 2008), microclimate (Peacock, 1975), temperature isolation between soil and atmosphere (e.g. Kätterer and Andrén, 2009) and amount of litter and root exudates, providing fresh substrate for decomposers (Kuzyakov et al., 2000). The potential of the plant to absorb radiation is a key component for modelling photosynthesis (Monteith, 1972) and is related to greenness indices like NDVI (e.g. Gamon et al., 1995). Actual accumulated photosynthetic net production is reflected by biomass (Monteith, 1972). The importance of LAI was also emphasized in plant productivity models (Cowling and Field, 2003). LAI might be estimated from satellite-derived indices like NDVI (e.g. Rossini et al., 2012). NDVI has also been shown to be related to photosynthesis (e.g. Gianelle et al., 2009), biomass (e.g. Vescovo et al., 2012) and fraction of green to total biomass (green-ratio) (Gianelle and Vescovo, 2007). However, these dependencies are known to be specific to biomes (Heinsch, F. A. et al., 2006), plant species and vegetation types (e.g. Anderson, 1995; Wilson et al., 2007), plant architecture and background soil (e.g. Darvishzadeh et al., 2008), as well as site conditions (Kross et al., 2013). Therefore, shape parameters of the relationships need to be developed and the dependencies need to be validated for each ecosystem type.

Many studies have investigated dependencies between satellite-derivable VIs and plant characteristics or photosynthesis on different types of grasslands (e.g. Fan et al., 2009; Wohlfahrt et al., 2010) and some on northern peatlands (e.g. Kross et al., 2013 and references therein). There have been only a few such studies that have included nutrient-rich wetlands (e.g. Rendong and Jiyuan, 2002). To my knowledge, there are no reported investigations of these relationships on managed temperate grassland fens, which commonly differ from boreal peatlands due to their high productivity, while they are less intensively managed compared with many types of grasslands on mineral soils. Especially managed fens in the temperate region can act as hot spots for greenhouse gas emissions, due to their often intensive land-use management (e.g. Drösler et al., 2008). Therefore, their carbon balance and consequently the relationships between vegetation indices and biophysical vegetation characteristics as e.g. input for carbon models and statistical analysis are of extraordinary importance.

The aim of the third study in this PhD project was therefore to investigate the relationships between LAI, NDVI and vegetation characteristics on several grasslands in a temperate fen to find out whether in particular NDVI can be used as proxy for LAI and other vegetation characteristics required by carbon models. A special focus was on the effect of management

intensity as this was expected to affect the relationship: Harvest, fertilisation and drainage affects plant productivity and plant community composition (e.g. Wedin, 1996) whereas plant communities and different species vary in spectral reflectance (Anderson, 1995) and temporal patterns in reflectance (e.g. Gamon et al., 1995).

1.6 Objectives

The overall aim of this thesis was to improve process understanding for less uncertain quantifications and predictions of CO_2 emissions from peatlands, by making use of existing observation data and a well-established ecosystem model. Thereby, three core areas are investigated, represented by one study each:

1. Differences between sites in their response to driving variables (study I)
2. Interactions between different processes related to the carbon cycle (study II)
3. Potential of vegetation indices as model input data (study III)

Study I: The main aim of the first study was to find out to what extent the large differences in measured CO_2 fluxes between five data rich European flux measurement sites can be solely explained by the differences in meteorology, water table, soil C stock and management. Therefore, the process-oriented CoupModel was applied using an uncertainty-based Monte Carlo approach. Specific objectives were:

- To identify differences and similarities between various sites in CO_2-related processes, corresponding parameters and responses to forcing data.
- To identify and discuss the impact of available data for estimating key parameters in CO_2 flux models in general.
- To identify problems related to the model representation of the different ecosystem processes for open peatlands.

Study II: The second study aimed to identify and explore the connections within and between biotic and abiotic processes and parameters which are relevant for modelling NEE in a natural open peatland, by investigating several different output variables. Of particular interest was:

- To identify the processes and parameters that have the strongest impact on model performance.

- To evaluate implications of different criteria selection choices on model performance and resulting parameter ranges.
- To identify and describe equifinalities between parameters from different processes.
- To test the usability of all available observation data for model constrain and identify missing measurement variables.

Study III: The objective of the third study was to explore the potential of VIs as model input. Thus, the impact of management intensity on the relationships between VIs and vegetation characteristics including potential photosynthesis (PP) on temperate fen grasslands was investigated. Specifically, the potential should be tested of using:

- NDVI as a proxy for PP, LAI, biomass, and green-ratio.
- LAI as a proxy for biomass and PP.

Therefore, biomass, LAI, PP and ground-measured and satellite-derived NDVI were investigated at five selected locations with different management regimes in a fen in southern Germany.

2 Methodology

In study I and II, the process-based CoupModel was calibrated to fit to measurement data from different treeless peatland sites with a wide gradient in land-use intensity, water level, soil nutrient status and mean annual temperature (cf. Section 2.1). Together with the climatic gradient from North Finland to South Germany and different growing season lengths, this lead to great differences in amplitude and dynamics of observed gross primary productivity (GPP), ecosystem respiration (R_{eco}) and different amounts of biomass. In study I, the resulting parameterisation was analysed for site-specific differences, and tested to what extent a site-independent configuration could be used. In study II, the resulting parameterisation was analysed for connections and interactions between different processes, between different parameters and between parameters and processes. In both studies, the fitted model output was compared with the measurements to identify needs for model improvement. Parameter uncertainties were investigated to identify needs for further data collection. The configuration of CoupModel (Section 2.2) differed slightly between the two studies, mainly by the inclusion of an additional moss layer in study II. Model parameters were calibrated using a MonteCarlo based algorithm and multiple criteria for selecting runs with acceptable performance (Section 2.3). To identify possibilities for receiving important plant physical parameters from remote sensing (study III), biomass, LAI, PP and ground-measured and satellite-derived NDVI was investigated at five selected locations with different management regimes in a fen in southern Germany (Section 2.4).

2.1 Study sites and available data

All sites of this thesis were treeless peatlands. They differed in respect to climate, hydrology, current and former land management, vegetation and soils (Table 2). The gradient ranged from natural mires (Lom and Deg) in North Europe to managed grasslands in a fen in South Germany (Freisinger Moos, FsA and FsB) and from continuous sinks for CO_2 emissions to relative strong CO_2 emission sources (Fig. 2).

Table 2. Characteristics of the different treeless peatland sites used for model calibration and evaluation (study I and II), and analysis of vegetation indices and characteristics (study III)

Site-Code	Lom	Amo	Hor	FsA, FsB and all sites of study III	Deg
Used in study	I, IV	I, IV	I, IV	I, III; IV (FsA)	II
Country	Finland	UK	Netherlands	Germany	Sweden
Site name	Lompolojänkkä	Auchencorth moss	Horstermeer	Freisinger Moos	Degerö
Area [ha]	12	25	12	0.04	65
Latitude; longitude	67°59'83"N; 24°12'55"E	55°47'34"N; 3°14'35"W	52°14'25"N 5°4'17"E	48°22'50"N 11°41'12"E	64°10'55" N 19.33'24" E
Peatland type	fen	bog	fen	fen	poor fen
Dominant vegetation	mosses, sedges, shrubs	grasses, sedges, soft rush, mosses	grass, reed, small shrubs	sedges, herbs, grasses (A), tall sedges (B)	cottongrass, tufted bulrush, *Sphagnum* mosses
Maximum LAI					
Land use and management	natural mire	restored; grazed	restored; nature reserve	drained, 1 cut a^{-1} [b]	natural mire
Mean temperature / range[a] [°C]	−1.4/−15-13	10/4-15	9.8/3-17	7.5/−2-17	1.2/−12-15
Mean water table [cm]	+1.2	−12.5	~ −10	−25 (FsA) −20 (FsB)	−11.6
Annual precipitation [mm]	484	1155	797	788	523
N deposition [kg ha^{-1} a^{-1}]	8.13	1.59		7.1	
Peat depth [m]	2–3	0.5–5	2	3	3–4 (8)
pH	5.5–6.0	4.4	4.8–6.0	5.5–6.7 [b]	4.1

[a] annual range of mean monthly temperatures
[b] this applies to site FsA and FsB only. The management of the other sites in the Freisinger Moos that are used in study III are described in Table 4.
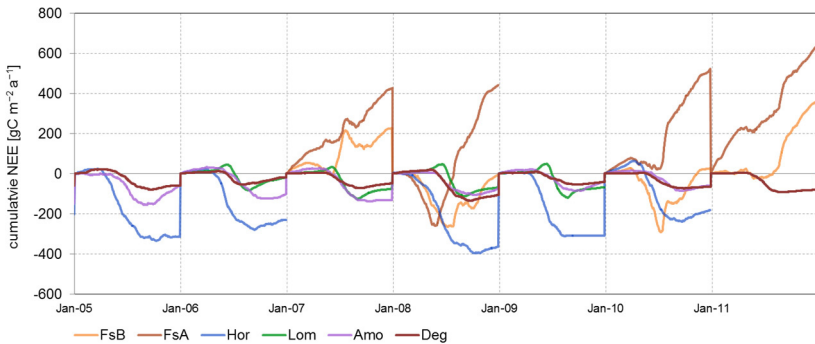
Figure 2. Annual net ecosystem exchange of the sites of study I and II as measured by Eddy covariance or chamber technique and interpolated to annual balances by empiric approaches. Positive values indicate CO_2 emissions, negative values indicate CO_2 uptake.

For the modelling studies, measured meteorological data, water table and C content per soil layer were used as model input (Table 3). In study II, water table was simulated while measured data was used for calibration. Dry and wet N deposition, latitude and thickness of the organic layer were used as constant site-specific input.

In study I, water retention parameters were assigned to each soil layer according to soil data from each site. However, at Amo and Lom, water retention, and at all sites unsaturated conductivity, was assigned from the CoupModel soil database as suggested by Lundmark (2008) for peat soils. Measured total soil organic carbon (SOC) per layer was partitioned to the two SOC pools per layer on the basis of the measured total C:N ratio per layer (Table A1.1 in the appendix), whereas the initial C:N ratios of the slow decomposing pools were assumed to be 10, while for the fast pools 27.5 was chosen according to measured C:N of leaf tissues at FsA and FsB. In study II, water retention parameters were calibrated. Measured C content per layer was used as input, but partitioning to the different pools was done by a spin-up procedure.

13

Table 3. Input data for the process oriented modelling.

Site Code	Variable	Period	Resolution of measurement / as used for calibration
Lom	water table depth	mid 2006-2010	half-hourly/hourly
	meteorology (temperature, global radiation, precipitation, wind speed, relative humidity)	mid 2006-2010	half-hourly/hourly
	soil organic C per layer	2007	once
Amo	water table depth	April 2007-2010	half-hourly/hourly
	meteorology (temperature, global radiation, precipitation, wind speed, relative humidity)	mid 2006-2010	half-hourly/hourly
	soil organic C per layer	2008	once
Hor	water table depth	2004-2006	half-hourly/hourly
	meteorology (temperature, global radiation, precipitation, wind speed, relative humidity)	2004-2011	half-hourly/hourly
	soil organic C per layer	2007	once
	water retention curve parameters	2007	
FsA and FsB	water table depth	2007-2011	biweekly, since April 2010 half hourly / hourly
	meteorology (temperature, global radiation, precipitation, wind speed, relative humidity)	2007-2011	half-hourly/hourly
	soil organic C per layer	2010	once
	water retention curve parameters	2011	
Deg	meteorology (temperature, global radiation, precipitation, wind speed, relative humidity)	1991-20013	half-hourly/hourly
	soil organic C per layer	1995	once

The measurement data used for model calibration (Table A1.2 in the appendix) included NEE, partitioned by empiric modelling into R_{eco} and GPP. NEE was measured with either Eddy covariance (Amo, Hor, Lom, Deg) or transparent chambers (FsA, FsB). R_{eco} was measured with opaque chambers or taken from night-time NEE measurements. In the empirical models, R_{eco} was interpolated between measurements, respectively

extrapolated to day-time, by a temperature dependent function (Lloyd and Taylor, 1994). Light level based functions (Falge et al., 2001) were used for GPP calculations. The empiric modelling, as well as corrections and filling of gaps due to instrument failure or low turbulence at flux tower sites was done by the project partners according to the methods described in Reichstein et al. (2005). A detailed description is given in the references listed in Table 3. Though R_{eco} and GPP were not explicitly measured, this will be called measured data in the following for simple distinction from the fluxes simulated by CoupModel. Gap-filled data and in case of chamber sites interpolated data between measurement days were only used for comparisons, but not for calibration.

In study II, the model was fitted to NEE (but not to GPP and R_{eco}) and additionally to sensible (H) and latent (LE) heat fluxes, as well as to net radiation (Rn), snow and water table depth. In study I and in particular in study II, variables for certain sub periods were introduced additional to the calibration data for the whole simulation periods. In study II, NEE was separated into night time values (22:30–02:30), representing ecosystem respiration, and day time values (09:30–15:30), representing the sum of the respiration component and the assimilation component. Additionally, spring time values were considered separately for NEE and snow depth, and spring and winter time values for Rn, Ts, H, and LE. This is justified as low values with little dynamic during winter and the critical transition of plant emerge and snow melt in spring might not be properly accounted for, if only the whole period was considered. In study I, only winter fluxes were considered additionally. WT in study II was calibrated and analysed in the whole profile and additional in lower soil layers (< -0.15 m and < -0.2 m), as WT in the upper soil layers showed high fluctuations in the modelled, and also partly the measured WT, while a good overall water table with good representations of dry summer periods should be achieved.

LAI or above-ground biomass data was available at all sites of study I and II, and used for calibration. At Hor, also below ground biomass was an available calibration variable. At the sites in the Freisinger Moos, LAI, biomass and NDVI were collected as part of this PhD project (cf. Section 2.4). This includes the sites FsA and FsB in study I and all sites of study III. The Freisinger Moos is a fen complex, divided into many land parcels with different land management intensity. For study III, five grassland sites were selected, ranging from three cuts per year and a fertilization rate of up to 252 kg N ha^{-1} yr^{-1} down to extensively managed grasslands, including a protected biotope with only one management cut every second year in late autumn and no fertilization (Table 4).

Table 4. Vegetation and management characteristics of sites used in the vegetation indices study (study III)

Parcel	Management	Mean water table [cm]	Dominant vegetation in June 2012 at the chamber plots	Comment
E1	natural monument, water level restored, 1 cut every second year during late autumn	-11	*Carex panicea (43%), Allium suaveolens* (9%), *Potentilla erecta* (4%), *Schoenus ferrugineus* (4%), *Phragmites australis* (4%), *Cirsium palustre* (2%)	Two sites with slightly different elevation, but no clear difference in vegetation. The mean of both sites was used.
E2	protected biotope, drained, 1 cut per year during late autumn	−32	*Filipendula ulmaria* (30%), *Poa pratensis* (20%), *Anthoxanthum odoratum* (17%), *Galium mollugo* (11%), *Carex nigra* (7%), *Luzula campestris* (5%), *Cirsium oleraceum* (3%), *Peucedanum palustre* (3%), *Rumex acetosella* (2%), *Cerastium holosteoides* (2%)	Four sites with water and temperature manipulation, but only the control site was used.
E3a ≙ FsA	hay meadow, drained, 1 cut per year during summer	−25	*Anthoxanthum odoratum* (40%), *Carex nigra* (40%), *Plantago lanceolata* (5%), *Ajuga reptans* (3%), *Galium mollugo* (2%), *Rumex acetosella* (2%)	Same parcel as E3b, but clearly different vegetation
E3b ≙ FsB	hay meadow, drained, 1 cut per year during summer	−20	*Carex vesicaria* (87%), *Galium uliginosum* (3%), *Alopecurus pratensis* (2%), *Poa trivialis* (2%), *Phragmites australis* (2%)	Same parcel as E3a, but clearly different vegetation
I1	intensive meadow, 2-3 cuts per year, drained, fertilized with 50 kg N ha^{-1} yr^{-1}	-21	*Poa trivialis* (43%), *Ranunculus repens* (20%), *Trifolium pratense* (17%), *Alopecurus pratensis* (8%), *Festuca pratensis* (4%)	GPP data not available in 2011
I2	intensive meadow, 2-3 cuts per year, drained, fertilized with 110-252 kg N ha^{-1} yr^{-1}	-57	*Dactylis glomerata* (29%), *Poa trivialis* (26%), *Lolium perenne* (14%), *Taraxacum officinalis* (8%), *Cerastium holosteoides* (4%), *Galium mollugo* (4%), *Alopecurus pratensis* (4%), *Trifolium pratense* (4%)	Four sites, differing in fertilization, but only the control site was used.
I3	intensive meadow, 3 cuts per year, drained, fertilized 181 kg yr^{-1}	−41	*Alopecurus pratensis* (63%), *Poa trivialis* (29%)	Four sites with water and temperature manipulation, but only the control site was used.

2.2   CoupModel description

CoupModel v4 from 12th April 2013 was used for the simulations in study I, v5 from 12th December 2014 for study II. The current version can be downloaded from (CoupModel homepage, 2015). A detailed description can be found in Jansson and Karlberg (2010). The model represents the ecosystem by a description of C and N fluxes in the soil and in the plants. It includes the main abiotic fluxes, such as soil heat and water fluxes that represent the major drivers for regulation of the biological components of the ecosystem.

The model setup differed slightly between study I and II to incorporate model improvements suggested by study I and to account for differences in sites and available data. An additional plant layer was introduced in study II to represent mosses, which were abundant at the Deg site. Therefore, a third type of soil organic matter (SOM) pools, representing litter from mosses was included. Due to the long simulation period, peat depth growth was accounted for in study II. Water table was used as input in study I, but simulated by CoupModel in study II.

The soil profile was divided into 12 (16 in study II) layers with an increasing layer depth of 4 or 5 cm for the upper layer to 60 or 100 cm in the lowest layer. The exact depth for each layer differed between sites according to the measurement depths and total depths of the peatlands.

The simulations were started two (study I) or ten (study II) years prior to the evaluation period, so the system (in particular the plant, in case of study II also the SOM pool sizes) could adapt to the site conditions and become more independent of initial values. Model performance was only evaluated for the years when meteorological data was available. The input data from the available years were copied to previous years if not available from an adjacent climate station. The model internal time step was half-hourly for abiotic processes and hourly for nitrogen and carbon related processes.

The most important equations and the corresponding calibrated parameters can be found in Table A1.3-5 in the appendix. The major model assumptions relating to the model application to the peatland are described below. Detailed assumptions in respect to fixed parameter values can be found in Table A1.6 and A1.7 in the appendix.

2.2.1 Radiation interception, evapotranspiration and snow

An interception sub-model for both, radiation and precipitation, a snow model and a surface pool model was used to provide boundary conditions at the soil surface. Cloud fraction was calculated from global radiation input and latitude. Incoming radiation was partitioned between the plant canopy and the soil according Beer's law (cf. Impens and Lemeur, 1969). The radiation absorbed by the canopy was partitioned between the two plant layers in study II (Fig. 3), depending on their height and surface cover, whereas it was assumed that leaves are uniformly distributed within the total height of the canopy.

Interception and plant evaporation depended on the simulated leaf area index of the plants as well as the degree of area coverage. Transpiration depended additionally on the simulated plant water uptake. Soil evaporation was derived from an iterative solution of the soil surface energy balance of the soil surface, using an empirical parameter for estimating the vapour pressure and temperature at the soil surface. Vapour pressure deficit was calculated from the input for relative humidity. Snow fall was simulated from precipitation and air temperature, snow melt from global radiation, air temperature and simulated soil heat flux.
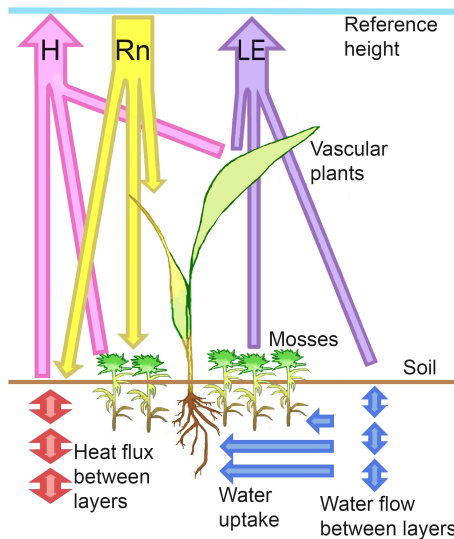
Figure 3. Energy flux partitioning and related soil water flows in the CoupModel as applied in the investigation of interactions (study II), using two plant canopies and root systems. For the sites in the site comparison (study I), only one plant layer was applied. Rn: Incoming radiation, LE: latent heat fluxes, H: sensible heat fluxes.

2.2.2 Soil temperatures and heat fluxes

Surface temperature was simulated based on an energy balance approach, where the radiation reaching the soil equals the sum of sensible and latent heat flux to the air and heat flux to the soil. The same approach was used for the snow surface temperature. Heat flow between adjacent soil layers were calculated based on thermal conductivity functions accounting for the content of ice and water. The heat flow equation is based on a coupled equation accounting for the freezing and thawing in the soil (Jansson and Halldin, 1979). Convection heat flows were not accounted for. The lower boundary temperature was calculated based on a sine variation including parameters for the annual mean temperature and amplitude at the site.

2.2.3 Soil hydrology

Soil water flows and water contents were calculated for each of the soil layers. Soil water depended on infiltration to the soil, soil evaporation, water uptake by plants, and ground water flow. Soil moisture represented as liquid water content, is calculated based on the water storage and temperature in the corresponding soil layer. Water flows between adjacent soil layers were calculated based on Richards' equation (Richards, 1931), considering hydraulic conductivity, water potential gradient and vapour diffusion. In study I, soil water characteristics were used as input from measurements or, at Amo and Lom from the CoupModel soil database. In study II, they were calibrated. Saturation conductivity was assigned depending on the mean measured dry bulk density values of the corresponding layers (cf. Päivänen, 1973).

The soil water characteristics were described by the Brooks & Corey equation (Brooks and Corey) and unsaturated conductivity by the Mualem function (Mualem, 1976). When the current simulated ground water table is above the assumed drainage level, outflow of saturated layers above that level was simulated, based on a linear model. In case of study I, saturation was forced to the measured ground water level, by adding or removing water from the corresponding layer.

Surface runoff was controlled by a surface pool of water that covers various fractions of the soil surface. During periods of a fully saturated soil profile the flow of water in the upper soil compartment could be directed up-wards, towards the surface pool. Surface runoff was calculated as a function of the amount of water in the surface pool.

2.2.4 Plants

In case of study II, two plant layers were simulated, representing vascular plants and mosses. They differed in their parameters for size, shape, C allocation, litter fall and temperature response for assimilation and respiration. For study I, only one plant type was used, which complies with the description of the vascular plant in the following.

Vascular plants consisted of three functional parts: roots, photosynthetically active biomass (i.e. green leaves and green stems that are labelled as leaves in equations and parameter names), and photosynthetically passive biomass (i.e. brown, senescent leaves and stems that are labelled as stems). Mosses were considered to consist of two parts: an upper, photosynthetically active part (labelled as leaves) and a lower, photosynthetically passive part (labelled as roots) representing white or brown, belowground leaves and stems that are still living. Each plant constitutes a biomass pool for each of its parts. Vascular plants had additionally a pool for mobile reserves. LAI was proportional to leaf biomass by using a constant specific leaf area as conversion factor. Vascular plants were assumed to have a maximal height of 50 cm compared to 2 cm for mosses.

Plant development started every spring when the accumulated sum of air temperatures above a threshold value reached a certain value. The accumulation of temperatures started when the day length exceeded 10 hours. Snow cover hindered leafing-out by reducing the radiation passing through to the plant, while low soil temperatures reduced plant water uptake.

Senescence and litter fall differed between the two plant types. For vascular plants, beside a small amount of litter fall occurring during the whole plant growth period (cf. Fulkerson and Donaghy, 2001), senescence was assumed to start after the plant reached maturity and therefore depended on growth stage (cf. Thomas and Stoddart, 1980) and dormancy temperatures (cf. Davidson and Campbell, 1983). New assimilates were constantly allocated to the roots and to the photosynthetically active part. After maturity, existing green biomass was reallocated to the photosynthetically passive part. A third stage of litter fall was configured depending on a temperature threshold: Five consecutive days in the autumn with day lengths shorter than 10 hours and with temperatures below a threshold temperature parameter terminated the growing season; Increased litter fall took place and vascular plants went to dormancy. During vascular plant litter fall, part of the carbon was stored in the mobile pool, which could be then reused for leafing-out in the next year (cf. White, 1973; Wingler, 2005). The litter from above-ground biomass was inserted to a surface litter pool, while root

litter was inserted to the corresponding litter pools of the soil layers in which the roots were located. The litter in the surface pool was inactive and transferred with a constant rate to the litter pool of the uppermost layer.

A different approach for senescence and litter fall was applied for mosses, as they largely differ in these processes from vascular plants: *Sphagnum* mosses produces new leaves on the top, while litter fall occurs on the lower leaves, when they become shaded and die (cf. Clymo and Hayward, 1982). This leads to a permane leaf area index (LAI nt moss cover and a litter fall that is proportional to assimilation. In the model, this was realised by keeping the photosynthetically active part of mosses to a fixed static value. Any losses (i.e. respiration and litter fall) or gains (incorporation of assimilates) were restricted to the belowground moss parts. Moss litter was produced with a constant rate coefficient throughout the year and was directly inserted to the corresponding soil litter pools. The dormancy period for mosses was initiated in the same way as for vascular plants, but affected only assimilation.

For both plant types, assimilation was simulated using the light use efficiency approach (cf. Monteith, 1972), at which total plant growth is proportional to the net of global radiation absorbed by the canopy but limited by unfavourable temperature and limited soil water. The response to soil water was defined from the ratio of actual to potential transpiration. Potential transpiration depended on vapour pressure, temperature, wind speed and aerodynamic resistance of the plant. Actual transpiration was assumed to equal water uptake from soil layers, depending on relative amount of roots, the specific response to soil water potential, and soil temperature of each layer. Both plant layers were assumed to be well-adapted to wet conditions (cf. Keddy, 1992; Steed et al., 2002) and therefore experiencing water stress only due to too dry conditions, which was supported by pre-study modelling results.

Plant respiration was assumed to be proportional to assimilation (growth respiration) and to amount of biomass (maintenance respiration) in active leaves and roots. In case of mosses, maintenance respiration took place only in belowground parts, therefore a higher range for the parameter scaling growth respiration was calibrated (cf. Table A1.5 in the appendix). A simple Q10 approach was used to simulate the response of plant maintenance respiration on temperature.

2.2.5   Soil organic matter and decomposition

The organic substrate was represented by three (two in case of study I, Fig. 4) C and N pools for each of the soil layers: one representing more stable, partly decomposed material (SOC_{slow}), one representing fresh or little decomposed moss litter ($SOC_{fast,m}$, not existing in study I) and one representing fresh or little decomposed litter from vascular plants ($SOC_{fast,v}$). Initial conditions were selected to fulfil the measured total carbon per layer. In case of study I, they were partitioned to the two SOC pools per layer on the basis of the measured total C:N ratio per layer whereas the initial C:N ratios of the slow decomposing pools were assumed to be 10, while for the fast pools 27.5 was chosen according to measured C:N of senescent leaf tissues at FsA and FsB. Due to the high C:N ratios measured at Deg and the third SOC pool type, this was not possible in study II. Therefore, SOC per layer in study II was partitioned into the pools in the way that they were approximately in equilibrium for a certain parameter combination that produces a reasonable fit to NEE (prior calibration). Additionally, the longer spin-up time of 10 years was chosen for study II.

Decomposition products from the SOC_{fast} pools were partitioned into CO_2 which was released to the atmosphere and C which is partly moved to the SOC_{slow} pools and partly returned to the $SOC_{fast,}$ pools. Decomposition products from the SOC_{slow} pools were partly released as CO_2 and partly returned to the SOC_{slow} pools. The rate at which carbon was transferred between pools was pool specific and reduced under unfavourable soil temperature and moisture conditions. Temperature dependence was described by a simple Q10-approach in case of study I. For study II, a more sophisticated function was used which was developed by Ratkowsky et al. (1982) for bacteria, but has also been applied to fungal growth (Bazin and Prosser, 1988). The response to moisture was assumed to be zero at moisture contents below the wilting point, rising to 100% between two threshold moisture contents and falling to a certain level under saturated conditions.

Due to the strong uptake and long simulation period, peat depth growth during the simulation period was considered in study II: The initial organic concentration was preserved for each layer but the lowest in the profile. Instead, the difference in the total amount of C in all pools in one layer between start and end of each year was moved to or from the layer below, to simulate growth or decrease of the peat depth. Thereby, carbon was taken from the different pools according to the relative abundance of each pool in the source layer and inserted to the corresponding pool in the target layer to allow dynamic changes in litter quality. The lowest layer (−2.8 to −3.4 m below the surface) represented the entire depth change of the whole profile,

but was excluded from a constant concentration to avoid adjustments of the number of layers.

Nitrogen and methane related processes were considered by a model including the most important pathways and fluxes. However, no emphasize on the calibration of these processes were made in this thesis since the current objective was on CO_2 fluxes.
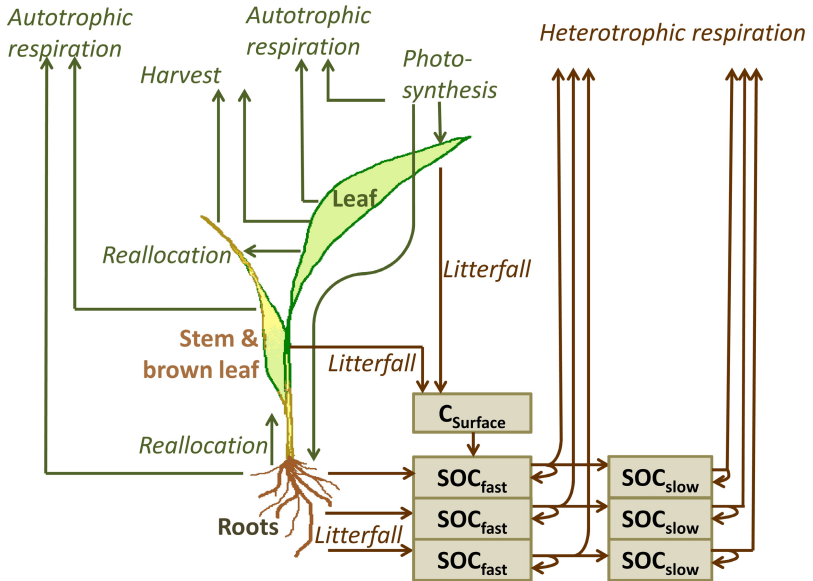
Figure 4. Scheme of carbon fluxes and pools in the current CoupModel setup as applied in the site comparison (study I).

2.3   Calibration strategies

The model was calibrated based on a Monte Carlo approach: Multiple runs were performed with random values for various parameters (see Table A1.4 and A1.5 in the appendix). Thereby, each run corresponds to a certain combination of values for each parameter. Several different criteria based on various measurement variables were chosen to define runs with an acceptable performance. Different performance indices (Section 2.3.1) were used to quantify the reduction in the discrepancy between simulated and measured variables.

Calibration strategies, calibrated parameter and parameter ranges were different for study I and II due to the different aims, available data and experience gained from the results of study I that could be applied to study II. The aim of study I was to find a single set of parameter values (i.e. one certain run) to ensure that for all parameters, that were not identified to be site-specific, a single value representation leads to similar good results for all sites. This was achieved by a stepwise approach including several sets of multiple calibration runs as described in Section 2.3.3. Finding site-independent model parameters would mean that differences in the measured fluxes could be explained solely by model input data: water table, meteorological data, management and soil inventory data.

The aim of study II was to find several sets of runs, selected by different criteria, to explore interactions between parameters within these sets of runs and to examine the effect of criteria selection. Therefore, a simpler approach was chosen, based on one multiple run and a repeated selection of different criteria (Section 2.3.4). Resulting parameter ranges were compared between the different applied criteria, and trade-offs and supporting effects in the performance in different variables were identified. Parameter sensitivities and equifinalities were analysed. The usefulness of the available observation variables for model constrain were evaluated and missing data identified.

2.3.1   Performance indices

In both modelling studies, the selection of runs and evaluation of performance was based on three indices: coefficient of determination (R^2) asses how well the dynamics in the measurement derived values are represented by the model. Mean error (ME) is the difference between the average of the simulated compared to the average in the measured, i.e. it shows the error in the magnitude. Nash-Sutcliff efficiency (NSE) (Nash and

Sutcliffe, 1970) accounts for both, deviation of dynamics and magnitude. It ranges from $-\infty$ to 1, whereas 1 means the best fit of modelled to measured data. Values < 0 indicate that the mean measured value is a better predictor than the simulated value (Moriasi et al., 2007). As NSE may be understood as a combination of R^2 and ME, it was only evaluated in study II, if R^2 and ME alone did not narrow the parameter range.

NEE in study II, showed a spiky record, especially during night time. To attenuate the effect of the spikes, the simulated and measured values were transformed to cumulated total amounts, starting from the beginning of the observation period. An additional R^2 value was calculated for the cumulated values (AR^2).

2.3.2 Model calibration for site comparison (study I)

To find out to what extent the same parameter values could be used for all sites compared to a site-specific representation, a stepwise approach was carried out starting with finding the best site-specific parameter representations and then trying to merge them to common values, valid for all sites. Finally the common representation was revised to some few parameters showing great site-specific effect on model performance. An overview of the different steps can be found in Fig. 5, details on the calibration procedures are presented in the appendix.

For the basic calibration (step I, Fig. 5) 350'000 to 700'000 runs were performed for each site. 45 parameters which were suspicious of eventually being site-specific were selected and calibrated with an assumed uniform random range (Table A1.4 in the appendix). Parameter ranges were then constrained based on selected runs (step I and II, Fig. 5), showing acceptable performance to multiple variables (Table A1.8 in the appendix), measured at the sites.

Several additional multiple calibration runs were performed, with few selected parameters each, to unravel parameter interactions (step III, Fig. 5). A number of simulations were also made by single value representations of parameters (step IV, Fig. 5) to visualize the impact of certain parameter values on interacting parameters and on performance. These runs are called single runs in the following, numbered with C1 to C7 and described in Table A1.9 in the appendix. The C1 scenario was the base for simulation setup in study II.
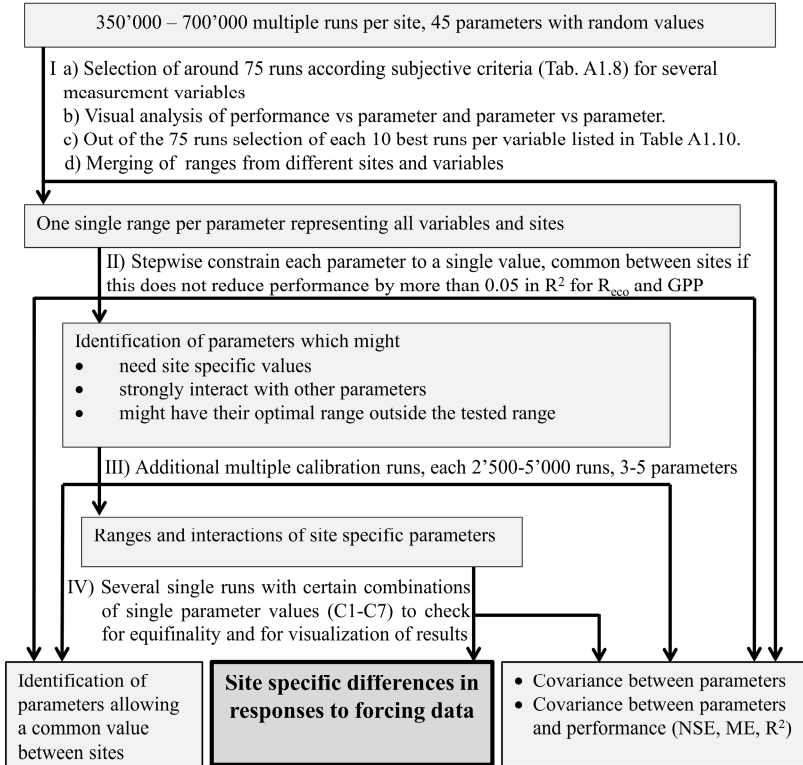
Figure 5. Stepwise parameter calibration as applied in study I. Boxes show the outcome of each step. Description for scenarios C1-C7 can be found in Table A1.9 in the appendix.

2.3.3   Model calibration for identification of interactions (study II)

To explore interactions between parameters and to examine the effect of criteria selection, several multiple criteria were applied to a multiple run selecting several sets of runs with acceptable performance in different variables. The multiple run consisted of 50.000 runs, using a uniform random distribution within assumed prior ranges for 54 selected parameters from different modules. The parameters were selected as candidates to demonstrate the role of various regulating processes. Many parameters were still considered with fixed single values (Table A1.7 in the appendix). Prior ranges for calibrated parameters were selected according to literature values or experiences from previous model runs, in most cases a certain range

around the default values (Table A1.5 in the appendix). Model outputs were compared with measured field data including many variables in high temporal resolution, spanning up to 12 years of observations (Table A1.2 in the appendix). Several combined criteria were defined to select runs (behavioural models) with an acceptable performance in different variables. Resulting parameter value ranges of the accepted runs were then compared with the prior ranges and between the different criteria selections to examine the effect of criteria selection. Correlations between parameter values and model performance in the different measurement variables were analysed, as well as between accepted values of different parameters. Parameters were ranked in their effect on model performance, their correlation with other parameters and their constrain-ability from the available data.

Criteria were applied in two steps. In the first step, a basic set of 1285 behavioural models was selected. Out of these, several sets of 50 runs each were selected in the second step in two different ways: one for sensitivity analyses and parameter ranges which was based on single criteria and the other for identification of equifinalities, based on multiple criteria.

Basic selection

A basic selection was applied, as the lowest summer water levels and a reasonable representation of the plant was assumed to be crucial for most of the processes of interest. Criteria were on performance in WT of lower layers and vascular plant LAI (Table A1.11 in the appendix). The criteria on ME in LAI of ±0.2 m^2 m^{-2} was a relatively wide range, as the mean of measured values was 0.4 m^2 m^{-2}, i.e. a underestimation of LAI by -0.2 m^2 m^{-2} would result in a maximum LAI of 0.2-0.4, which was close to the minimum for being able to re-establish new biomass after a low productive year. A wide range of day-time NEE ME was additionally applied to exclude outliers due to numerical problems, which reached an ME in NEE up to $8 \cdot 10^{27}$ gCO_2-C day^{-1} in the prior. The criteria on water level below 0.2 m was chosen, as correctly capturing summer drought conditions was of higher interest in the present study than a correct water level during e.g. frozen conditions in winter, causing water table drops down to 0.15 m.

Single criteria to identify parameter range

The best 50 behavioural models for each performance index of each variable were selected out of the basic selection for sensitivity analyses and to test if, and how, parameter ranges depend on the selected criteria. Thereby, best means highest in case of R^2 and NSE, but closest to zero in

case of ME. Posterior parameter ranges were defined as the interval between the 5% and the 95% percentile of the distribution of parameter values of the runs selected. Posterior parameter ranges were compared with the ranges resulting from the basic selection. If the upper or lower limit of a posterior parameter range of the final selections differed by ≥10% from the upper or lower limit of the posterior range of the basic selection, the parameter was assumed to be sensitive to the selected criteria and further analysed.

The same was done for each best 200 behavioural models, but as the results were similar, they were only plotted in respect to parameter ranges. Further, all parameters were plotted against all performance indices of each variable and checked visually for discrepancies with the resulting ranges (results are not shown).

Multiple criteria to for identify parameter correlations

For identification of equifinalities, a set of multiple criteria for each variable (Table A1.11 in the appendix) was applied to select sets of 50 behavioural models each. Again, these selections were based on the basic selection. Parameter ensembles of these accepted behavioural models were then analysed to identify covariance between parameters. A pair of parameters was considered to interact, if their values correlated with an R^2 of at least 0.1 in the basic selection, respectively 0.2 in the final selection. If a pair showed correlations in several criteria sets, the highest R^2 value was reported in the results.

2.3.4 Evaluation and measures (study II)

Several measures were introduced in study II to quantify parameter sensitivities and constrain-abilities, as well as equifinalities and therefore to be able to rank the parameters in their concern.

The sensitivity (S) of a parameter to each performance index of each variable was quantified by the sum of the differences between posterior range and prior range (range reduction). If a parameter was sensitive to more than one period of each variable, the highest value for each variable was chosen for further analysis. To identify trade-offs and supporting effects between different criteria, correlations of the performances between different variables and indices were plotted and visually analysed. Due to limited computer capacity, this was based on a random set of 3200 runs. Further, the parameter value ranges resulting from the different criteria were compared with each other and determined how well they were overlapping,

i.e. how unambiguously they could be constrained. Overlap (O) for each parameter was defined as the difference between the minimum of the upper limits of the posterior ranges of the different criteria, minus the maximum of the lower limits of posterior ranges and therefore become negative, if ranges were not overlapping. Further it was compared how well overlapping ranges differed between performance indices within the same variable and between different variables. The overlapping range of each parameter was normalized by dividing it by the average of the posterior ranges of this parameter, so that a value of 1 would be reached if all posterior ranges of that parameter would be identical for all performance indices and variables. Equifinalities were quantified by the R^2 value of the correlation between each parameter pair. Parameter concern (P) was defined based on three components: the sensitivity of the parameter, how unambiguously it could be constrained and the sum of correlation coefficients of equifinalities with other parameters:

$$P = (S_{R^2} + S_{ME}) \times (1 - O) + \sum 2 \times \frac{2^{10 \times R_{equi}^2}}{10}$$

Thereby, sensitivity was the sum of the range reduction for R^2 and for ME, respectively NSE in case no sensitivity was detected for R^2 and ME but NSE. The sensitivity was multiplied by the factor one minus the normalized overlapping range, so that the sensitivity of parameters which could be unambiguously constrained are down weighted, and such with high uncertainty due to different results for different performance indices or variables are up weighted. Equifinalities were considered by the sum of R^2 values for each correlation of that parameter with another parameter, displayed in exponential form and weighted, so that strong correlations were emphasised and the contribution of equifinalities were in a comparable scale to the sensitivity measures.

2.4   Data sampling (study III)

To evaluate possibilities of using optical vegetation indices as model input, the relationships between vegetation characteristics and optical vegetation indices were investigated in study III. Ground measurements of LAI, NDVI as well as green and brown biomass were performed at several grasslands in the Freisinger Moos (Fig. 6) and compared with satellite data and available CO_2 flux measurements.
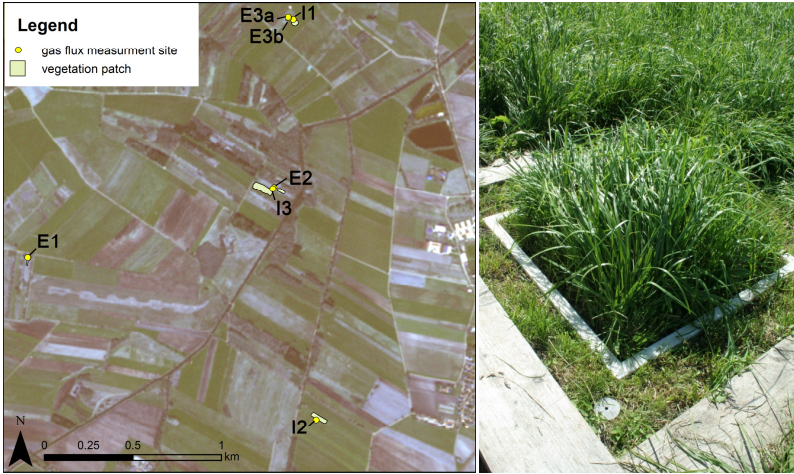
Figure 6. Left: overview of the investigated sites and vegetation patches in the Freisinger Moos. Right: chamber plot at the intensive managed meadow I2.

Each site of study III consisted of gas measurement plots and a small area outside the plots (vegetation patch) where PAI, NDVI and biomass were sampled. The vegetation patches were necessary, because the chamber plots were surrounded by boardwalks, storage for chambers and other instruments, which could bias the satellite NDVI. Further, the vegetation around the chamber plots was kept short for easy chamber handling, and the soil collars of the chamber plots, which had a height of 3 cm, can bias the ceptometer measurements. The patches were selected to represent similar vegetation as in the plots. They were located at a distance of at least 5 m from the detracted areas and had a minimum size of 50 m^2. Due to high spatial variability in the vegetation on extensive meadows, some additional patches were selected that did not represent a chamber site, but included other dominant vegetation types on the parcel. PAI and NDVI were measured in the patches and additionally in the chamber plots, but values from the plots were only used for correlations with PP.

2.4.1 Photosynthesis

Flux data collection and empiric modelling for NEE and GPP as described in this section (2.4.1) were performed by my colleagues, in particular Tim Eickenscheidt and Jan Heinichen. They performed the flux sampling campaigns during 2010 and 2011 (site I1 only 2010) according to the methods described by Eickenscheidt et al. (2015). NEE and ecosystem respiration were measured with transparent and opaque chambers (closed dynamic manual chamber system) at three replicated plots of 75 x 75 cm^2 on each site under clear sky conditions. CO_2 fluxes, photosynthetically active radiation (PAR) and soil temperatures were sampled repeatedly from sunrise to late afternoon to cover the full range of these parameters in the course of the day. CO_2 fluxes were derived from CO_2 concentrations, measured with infrared gas analysers (LI-820, LI-COR, Lincoln, USA). For each site and each sampling day, a temperature-dependent ecosystem respiration model was calculated according to Lloyd and Taylor (1994). Modelled respiration was then subtracted from measured NEE to obtain GPP. A GPP model based on a Michaelis-Menten-type rectangular hyperbolic function as proposed by Falge et al. (2001) was fitted for each measurement day. From the GPP model, the photosynthesis at a theoretical photosynthetic photon flux density (PPFD) of 2000 µmol m^{-2} s^{-1} was derived. This corresponds to the photosynthesis potential (PP) of the plant in its current development stage at the specified light level and was used in all comparisons with vegetation indices.

2.4.2 Satellite NDVI

From April 2010 until November 2011, a total of 23 RapidEye images of Level 3A were provided by the RapidEye Science Archive Project (RESA, 2015) with a spatial resolution of 5 m, with 16 images from 2011. Geometric and atmospheric correction was performed by my colleagues from the Institute of Forest Management, TUM, using ATCOR 3 implemented in PCI Geomatica 10.3, as described by Elatawneh et al. (2013). Only cloud-free pixels were taken into account. Values within three days after harvest were not included to avoid effects from hay drying on the fields.

The normalized difference vegetation index was calculated in ArcGis (ESRI) version 10.2.0.3348 by the equation

$$\text{NDVI} = \frac{R_{NIR} - R_{RED}}{R_{NIR} + R_{RED}},$$

<div align="right">Eq. (1)</div>

where R_{NIR} and R_{RED} indicate the reflectance in the near infrared (760 – 850 nm, channel 5) and the red (630 – 685 nm, channel 3) wavebands, respectively.

For comparisons with photosynthesis potential, NDVI values were gap-filled by linear interpolation between two consecutive measurements if no harvest or year shift took place.

2.4.3   Ground NDVI and PAI

LAI can be estimated by direct and indirect techniques (see reviews of methods in Breda, 2003 and Jonckheere et al., 2004). Direct measurements are destructive and workload-intensive, but allow measuring the green (photosynthetically active) plant parts (in the following labelled as green area index, GAI). An easy-to-measure and commonly used indirect method is the determination of LAI by measuring the light transmission through a canopy by a ceptometer, which also includes dead and senescent (brown) above-ground parts of the vegetation (in the following labelled as plant area index, PAI). Plant area divided by the plant weight is labelled as specific plant area (SPA).

Sampling campaigns for NDVI and PAI were performed every 2 to 4 weeks between April 2011 and July 2012. Samples were taken less frequently at those vegetation patches not representing a gas flux measurement site. At each sampling day, NDVI and PAI were measured at five randomly selected locations per vegetation patch and on each of the three chamber plots per flux measurement site. NDVI, PAI and biomass samples were taken from the same spots in the vegetation patches. Three replicative measurements were taken for LAI and NDVI at each spot and resulting values were averaged. Measurements were performed within 3.5 (2.5 in winter) hours either side of solar noon under clear sky conditions. PP and satellite-derived NDVI were often sampled on different dates. Therefore, NDVI and LAI values were linear interpolated between each pair of measurement points to match the dates of PP sampling. In cases where was a harvest or year shift between two measurement points, the data were not taken into account.

Ground-based NDVI was sampled using a handheld spectroradiometer (Fig. 7) with two four-channel sensors (SKR 1850, Skye instruments Ltd, Powys, UK). It was configured to measure simultaneously incident and reflected light in the same wavebands as RapidEye for the red and the near infrared channel. The sensor was held 160 cm above the soil to capture a surface with a diameter of 70 cm to fit the dimensions of the chamber plots. In the chamber plots, the pole on which the sensors were mounted was placed on a

marked position, to make sure that the white soil frames for the chambers were not inside the captured surface. NDVI was calculated according to Equation 1.

A ceptometer-based canopy analysis system (SunScan system SS1, Delta-T Devices Ltd, Cambridge, UK) was used for PAI measurements. The SunScan system measures both diffuse and direct radiation. It includes a beam fraction sensor, placed above the vegetation for sampling incident PAR (Fig. 7). Simultaneously, PAR under the canopy is collected by a 1-m-long probe including 64 photodiodes. The average of all 64 diodes was used for PAI calculation. A leaf absorption value of 0.85, a random spherical distribution of leaves and a correction term of 0.3 to account for the height of the probe were assumed for PAI calculations as suggested in the user manual (Webb et al., 2008). A detailed description of how the system calculates PAI can be found in the user manual (Webb et al., 2008).

At the chamber plots, three replicative measurements at each diagonal of the plot were averaged. To account for the bias due to the soil frames and shorter vegetation around the plots (cf. Fig. 6), the values were corrected by the slope of a linear regression between PAI from chamber plots and PAI from the corresponding patch, whereas the regression line was forced through zero (cf. Fig. A4.1 in the appendix). Only PAI values from spots in a patch were used for the correction, which did not differ in NDVI by more than 0.05 compared to the average NDVI of the corresponding replicated plots. The corrected PAI values were only used for comparison with PP. For all other correlations, PAI and NDVI values from the vegetation patches were used.

Figure 7. Left: Handheld spectroradiometer for NDVI measurements. Middle and left: Canopy analysing system for LAI measurements: The probe of the ceptometer is put underneath the vegetation (middle), whereas the beam fraction sensor (right) measures simultaneously the incoming light. The field computer (middle) calculates the LAI automatically.

2.4.4　Biomass, green-ratio, GAI

A total of 186 biomass samples were collected between April 2011 and July 2012 on the same dates and spots as the PAI and NDVI measurements. Three samples were taken at each vegetation patch on each measurement date. Green mosses and all aboveground plant parts attached to a plant were cut with a knife within a frame spanning 20 cm on both sides of the SunScan probe, leading to a sample size of 100 cm x 40 cm. In case of very homogenous vegetation and PAI values lower than 1.5 m^2 m^{-2}, a smaller sample size of 40 cm x 40 cm was chosen. The samples were kept in plastic bags and frozen until further processing. Each sample was mixed to achieve a homogenous distribution of brown and green leaves. Then, around one quarter of each sample was sorted into green and brown plant parts, weighed separately and later multiplied by the total weight to estimate the dry weight of brown and green biomass. The samples were oven-dried at 60 °C for at least 48 h before weighting. GAI was calculated from PAI by multiplying it by the percentage of green leaves. To receive GAI at the chamber plots, where destructive sampling was not possible, PAI was multiplied by the green-ratio. Thereby the green-ratio was derived from NDVI by applying the relationship between green-ratio and NDVI over all samples.

2.4.5 Analyses and statistics

All statistical analyses were carried out in the R software, version 3.03 (R Core Team, 2013). The relationships between each variable pair were analysed with respect to regression coefficients, residual standard errors (SE) and a partial t-tests providing the coefficients of determination (R^2) by simple linear regression (lm function in the stats package; R Core Team, 2014). Therefore, nonlinear relationships were linearised by simple exponential or logarithmic transformations. The coefficients for these transformations were derived by fitting a nonlinear least-squares model (fitModel function in the mosaic package; Pruim et al., 2014). Each relationship was tested without transformation, and with logarithmic and simple power transformations: those equations were applied that resulted in the highest R^2 value. If R^2 values were similar, no transformation was applied. The assumption for a t-test of normality of model residuals was tested using the Kolmogorov-Smirnov test (ks.test function in the stats package; R Core Team, 2014) (Lilliefors, 1967). In the case that the data did not satisfy the necessary requirements, the nonparametric pairwise Wilcoxon rank-sum test (wilcox.test function in stats package; R Core Team, 2014) (Bauer, 1972) was used instead of the partial t-test. For all statistical tests, a significance level of 0.05 was chosen. Box plots were used to compare the values from intensive and extensive meadows. In case of time series, the data were classified into groups of one month. For the relationships between PAI and NDVI as well as GAI and NDVI, the NDVI data were classified into intervals of width 0.1. The absence of overlapping notches of two boxes was used as an indication of a significant difference in mean values (McGill et al., 1978).

3 Results & Discussion

3.1 Results of site comparison (study I)

To screen for site-specific differences in the response to model input (meteorological data, water table depth and soil C stock), the model was calibrated to fit to observations (CO_2 fluxes, soil temperature, snow depth and LAI) and resulting differences in model parameters were analysed. For most processes, the responses to input drivers did not differ between the five sites, while only few parameters needed a site-specific configuration. Seasonal variability in the major fluxes was well captured (Section 3.1.1), when a site-independent configuration was utilized for most of the parameters. Parameters that differed between sites included the rate of soil organic decomposition, photosynthetic efficiency, and regulation of the mobile carbon pool from senescence to leafing-out in the next year (Section 3.1.2). The largest difference between sites was the rate coefficient for heterotrophic respiration. Setting it to a common value would lead to underestimation of mean total respiration by a factor of 2.8 up to an overestimation by a factor of 4. The respiration rate coefficient showed correlations with parameters defining plant respiration and water and temperature responses (Section 3.1.3), however, none of the tested parameter sets cancelled out the observed site-specific differences.

3.1.1 Model performance – results of basic calibration and selected common configuration

Model performance showed distinct differences between the sites, depending on the investigated variable and on the number of considered runs (Table 5). Figure 8 shows the differences between measurements and model C1.

Table 5. Best fits between modelled and measured data in the site comparison study, expressed as the highest values achieved for selected performance indices.

Variable	Index	Lom all/selected runs	Lom single run	Amo all/selected runs	Amo single run	Hor all/selected runs	Hor single run	FsA all/selected runs	FsA single run	FsB all/selected runs	FsB single run
NEE	R^2	0.61/0.60	0.59	0.59/0.58	0.55	0.53/0.51	0.48	0.20/0.16	0.15	0.25/0.21	0.19
	ME	0.00	0.05	0.00	0.04	0.00	0.02	0.00	1.43	0.00	−0.05
GPP	R^2	0.66/0.66	0.65	0.68/0.68	0.66	0.58/0.57	0.55	0.38/0.35	0.34	0.40/0.39	0.35
	ME	0.00	0.05	0.00	−0.09	0.00	0.04	0.00	0.06	0.00	−0.03
R_{eco} EC	R^2	0.79/0.74	0.69	0.71/0.71	0.66	0.78/0.77	0.75	n.a.	n.a.	n.a.	n.a.
	ME	0.00	0.00	0.00	−0.05	0.00	−0.06	n.a.	n.a.	n.a.	n.a.
Reco chamber	R^2	0.73/0.71	0.64	0.67/0.57	0.38	0.52/0.48	0.45	0.73/0.66	0.69	0.87/0.81	0.85
	ME	0.00	−0.06	0.00	0.04	0.00/−4.74	−5.38	0.00	−0.01	0.00	−0.08
Reco winter	R^2	0.67/0.63	0.63	0.14/0.08	0.06	0.28	0.28	0.51/0.43	0.32	0.92/0.89	0.89
	ME	0.00	0.01	0/0.04	0.13	0.00	−0.26	0/1.60	3.21	0.00/0.73	2.11
upper soil temperature	R^2	0.88/0.87	0.87	0.86	0.84	0.92	0.91	0.88/0.86	0.84	0.88/0.86	0.84
	ME	0.00	−0.01	−0.03	−0.08	−1.37/−1.51	−1.77	0.00/0.58	0.35	0/1.20	0.35
lower soil temperature	R2	0.95	0.95	0.90	0.89	0.89	0.89	0.97/0.96	0.94	0.92/0.91	0.94
	ME	0.00	−0.03	0.00	0.02	0.00	−0.08	0.00	−0.15	0.00	−0.15
Snow depth	R^2	0.75	0.75	n.a.	n.a	n.a.	n.a.	n.a.	n.a.	n.a.	n.a.
	ME	-0.1	-0.06	n.a.	n.a	n.a.	n.a.	n.a.	n.a.	n.a.	n.a.
LAI	R^2	0.65/0.51	0.53	n.a.	n.a	0.36/0.31	0.33	0.75/0.69	0.61	0.82/0.76	0.61
	ME	0.00	0.11	n.a.	n.a	0.00/−0.61	−1.49	0.00	0.12	0.00	0.05
Above-ground living biomass	R^2	n.a.	n.a.	n.a.	n.a	0.02/0.00	0.00	0.31/0.26	0.24	0.47/0.43	0.32
	ME	n.a.	n.a.	n.a.	n.a	0	−112	0/−20	−21	0/−36	−48
Root biomass	R^2	n.a.	n.a.	n.a.	n.a	0.28/0.07	0.01	n.a.	n.a.	n.a.	n.a.
	ME	n.a.	n.a.	n.a.	n.a	0.00	−282	n.a.	n.a.	n.a.	n.a.

n.a. not available

Fluxes

At all sites dynamics in R_{eco} fluxes were simulated considerably better than GPP (Table 5). Performances for NEE were worse as simulation errors in GPP and R_{eco} are summed up. In respect to R_{eco} and GPP the selected single runs represent a parameter configuration close to the best ones possible in the tested range: their R^2 value did not differ more than 0.05 from the best result achieved in the multiple calibration, while ME values were smaller $|0.1|$ g C m^{-2} day^{-1}. Clearly lower R^2 and higher ME values in single runs for biomass and LAI simulation, indicates that none of the runs could give best results for all variables at the same time. E.g., best values for GPP can only be achieved if poorer performance would have been accepted for other parameters like winter R_{eco} or LAI (cf. selected criteria in Table A1.8 in the appendix).

The ME values in Table 5 show a clear overestimation of winter fluxes by 3.21 and 2.11 g C m^{-2} day^{-1} for the single runs at FsA and FsB, respectively, and a weaker overestimation for the accepted runs. The overestimation was less pronounced at Amo (0.13 g C m^{-2} day^{-1}) and Lom (0.01 g C m^{-2} day^{-1}). At Hor winter fluxes were underestimated with a ME of -0.26 g C m^{-2} day^{-1}. This was reflected in the accumulated NEE (Fig. 8) leading to a much higher CO_2 loss compared to the CO_2 balance estimated by the empirical model approach at FsA and FsB. At Lom higher accumulated NEE due to the overestimation of winter R_{eco} was visible in the first months of each year. It was nearly compensated due to the underestimated spring R_{eco}, or overcompensated due to GPP overestimation, as e.g. in summer 2006, which was very dry.
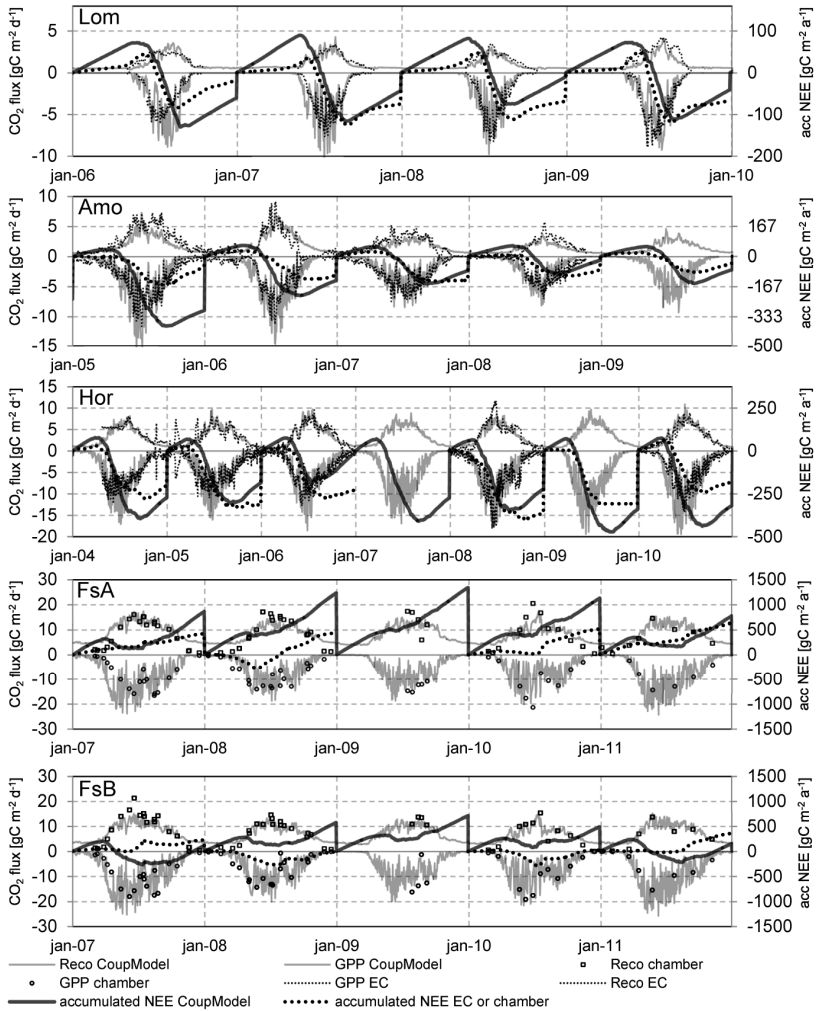
Figure 8. Simulated and measured Reco (positive) and GPP (negative) fluxes and accumulated NEE for one selected set of parameter values (C1) common between all sites. Note the different scales.

Explanatory variables

Of all variables, the highest R^2 values were achieved for soil temperature at all sites. Temperatures in deeper soil layers (−50 or −60 cm) had better fits than in upper layers with R^2 values close to 0.9 or higher and maximum mean deviation of 0.15 °C. The fit of modelled vs. measured snow depth, which was only available at Lom, had a R^2 value of 0.75 with a mean error of less than 10 cm.

Simulation of LAI represented the measurements quite well with R^2 values between 0.53 and 0.76 and mean error of maximum 0.12 m^2 m^{-2}. An exception was Hor, where LAI was underestimated by ME of −0.61 and −1.49 m^2 m^{-2} in the accepted 75 runs and in the selected single run C1, respectively. At Hor, root biomass was underestimated in the single run by ME of −281 g C m^{-2} and living leaf biomass by −122 g C m^{-2}.

In most of the runs of the basic calibration at Hor, either GPP was overestimated or leaf biomass and LAI was underestimated. Therefore, beside the common configuration C1, a different configuration was tested where plant respiration and litter fall parameters for Hor were set to much lower values than in the tested range to fit to GPP and LAI at the same time. However, this reduced performance for R_{eco} R^2 to 0.66 compared to 0.75 in C1 and led to an overestimation of winter R_{eco} with a ME of 0.75 g C m^{-2} day^{-1}.

3.1.2 Parameter constraint

Site-specific calibration was needed for the speed at which the maximum surface cover is reached (p_{ck}), the mean value in the analytical air temperature function (T_{amean}), temperature sum for reaching plant maturity ($T_{MatureSum}$), coefficient for determining allocation to mobile internal storage pool (m_{retain}), decomposition rate of the fast SOC pools (k_l) and radiation use efficiency (ε_L). A description of the used parameter symbols can be found in the appendix, Table A1.4-1.7.

Activity under saturated conditions ($p_{\theta Satact}$), threshold temperature for plant dormancy (T_{DormTh}), response to a 10 °C soil temperature change on the microbial activity (t_{Q10}) and base temperature for the microbial activity (t_{Q10bas}) covaried with performance indices but showed different patterns for different validation variables and for different sites.

Most of the parameters did not show any influence on performance indices within the tested range (Fig. A2.1 in the appendix), demonstrating that either the relatively low effect of the parameter was overcompensated by

the effect of more sensitive parameters, or the range used for calibration is sufficiently constraining. Each of these parameters did not reduce model performance indicated by R^2 by more than 0.05 for GPP or R_{eco} after setting them to a common value.

3.1.3 Correlations between parameters

In the basic calibration, the following parameters were identified to interact with other parameters: p_{ck} covaried with the extinction coefficient in the Beer law (k_{rn}) which is used to calculate the partitioning of net radiation between canopy and soil surface. Strong linear negative correlation between coefficients for growth (k_{gresp}) and maintenance respiration ($k_{mrespleaf}$) was detected.

The effect of the different parameter in the water response function $p_{\theta Satact}$, $p_{\theta Upp}$ and $p_{\theta p}$ compensated each other. They could not be constrained without a very high measurement resolution of fluxes and water table combined with high water table fluctuation at the same time. Therefore, $p_{\theta Upp}$ and $p_{\theta p}$ were set to default values and $p_{\theta Satact}$ constrained by additional multiple runs together with k_l. Differences between sites in k_l are reduced with higher $p_{\theta Satact}$ (Fig. 9), however, higher $p_{\theta Satact}$ increased overestimation of winter R_{eco} at FsA and FsB (Fig. 10 and Fig. 11d). A wider range of $p_{\theta Satact}$ was acceptable for summer R_{eco} (Fig. 10).

Beside moisture response, decomposition rate (k_l) and temperature response (t_{Q10}, t_{Q10bas}) controlled soil respiration. The effect on R_{eco} was confounded by plant respiration. Different patterns for different sites and variables for each of the parameters were even more pronounced when only k_l, t_{Q10} and $k_{mrespleaf}$ were in calibration (Fig. 10).

Single runs with different configurations (Fig. 10) revealed that higher plant respiration as well as steeper temperature response can lead to less overestimation of respiration in winter (Fig. 10d) but lead to reduced performance (Fig. 10c). In all single runs, despite the different configurations, FsA always showed the highest k_l while Amo had the lowest (Fig. 10a). A higher saturation activity reduces the difference in k_l values, but leads to higher overestimation of winter fluxes.
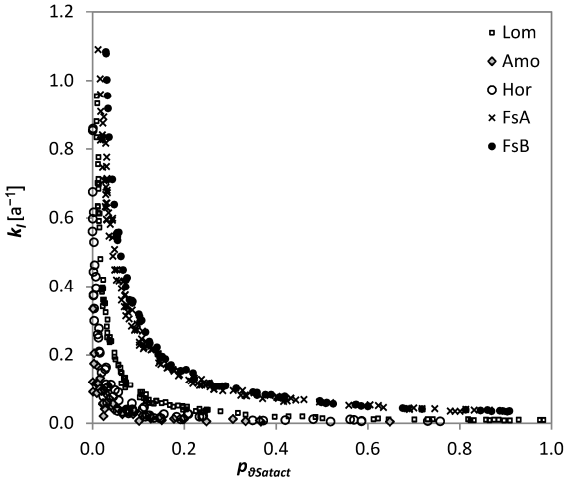
Figure 9. Dependencies between the parameters for decomposition rate and saturation activity for the different sites, based on additional multiple runs.
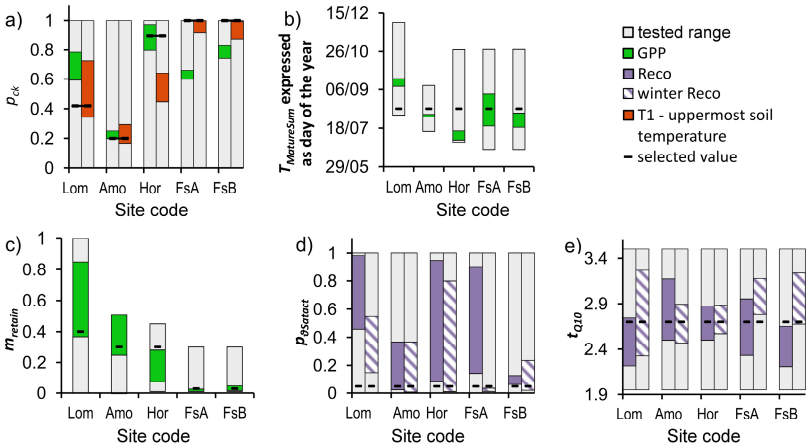
Figure 10. Obtained distributions of parameter values as constrained by additional multiple runs (calibration step III). Ranges for k_{II} and ε_L are not shown due to their interactions with several parameters. Coloured bars show the range of the 10 runs with the best performance for each validation variable. Prior ranges are indicated by the frame around the bar. Black dash is the value chosen for the common configuration C1.
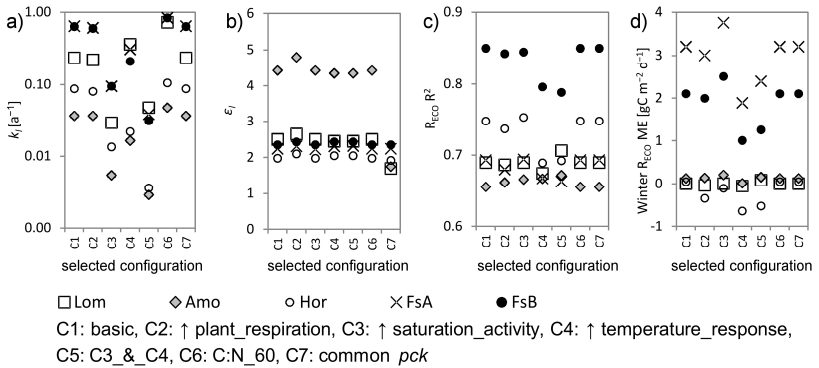
Figure 11. Values for the parameters decomposition rate (a) and light use efficiency (b) and resulting model performance (c, d) when applying various single value representations of parameters (C1-C7, see Table A1.9 in the appendix).

3.2   Discussion of site comparison (study I)

The aim of this study was to find out whether CO_2 fluxes, measured at different sites, can be explained by common processes and parameters or to what extend a site-specific configuration is needed. A site-independent configuration means that differences in the measured fluxes could be explained solely by model input data: water table, meteorological data, management and soil inventory data. This was true for most of the parameters, but not for example for the rate coefficients for heterotrophic respiration, which are connected to soil C pools. Measured soil C stocks were applied to the model pools without using a initialisation routine, as most of the sites were disturbed and therefore not expected to be in steady state (Section 3.2.1). Observed differences in model performance indices between sites and variables do not necessarily describe the models ability to describe certain phenomena, but depend also on measurement methods, resolution and site heterogeneity (Section 3.2.2). Specific parameter values for the timing of plant leafing-out and senescence, the photosynthesis response to temperature, litter fall and plant respiration rates, leaf morphology and allocation fractions of new assimilates, were not needed, even though the gradient in site latitude ranged from 48°N (South Germany) to 68°N (North Finland) and sites differed largely in their vegetation and management. This was also true for common parameters defining the moisture and temperature response for decomposition, leading to the conclusion, that a site-specific interpretation of these processes is not necessary. However, in several processes, the response to the input data differed, making a site-specific configuration necessary. If the model should

be used for predictions, these information need to be measured or estimated from available proxies: For the parameter defining the annual mean of the lower boundary of the soil temperature profile, snow cover might be important (Section 3.2.3). The coverage of vascular plants and mosses would help to configure a site-specific parameter which interacts with the photosynthetic efficiency and defines the upper boundary of the soil temperature profile (Section 3.2.4). Start of senescence for grasses and herbs might be stronger related to the day of the year, instead of temperature sums (Section 3.2.5). The proportion of C stored during litterfall for regrowth in spring as well as the photosynthetic efficiency could be fitted if a time series of biomass or LAI measurements were available (Sections 3.2.6 and 3.2.7). Temperature response parameter differed not only between sites, but also between seasons, which might be resolved by using a more sophisticated temperature response function (Section 3.2.8). Redox potential and coverage of plants containing aerenchyma might help finding explainations for the differences in soil moisture response (Section 3.2.9). Substrate quality is an important factor influencing heterotrophic respiration rates, but still a lot of research is needed to find clear connections and measurable variables (Section 3.2.10).

The parameters found to be sensitive and site-specific in the present study are important candidates for future calibration of peatland CO_2 models, whereas the remaining candidates might be less important and negligible in order to save computing time. However, one need to be aware, that also these parameters might become sensitive under different conditions and wider value ranges. The proxies and measurement variables which might be helpful in estimating the sensitive and site-specific parameters should be included in future measurement setups.

3.2.1 Model initialisation

Many models use spin-up routines of many years until SOC pools reach a steady state (e.g. Dimitrov et al., 2010; Smith et al., 2010; Thornton and Rosenbloom, 2005). In study I, measured C:N values were used to partition the SOC between pools, while ranges for parameter values were chosen in a way, that the amount of carbon in the soil pools did not change very drastically. However, no further effort was made to force the pools to be in equilibrium. It was assumed that this might not be the case in the real world either: Drainage ditches at FsA and FsB are still maintained, leading to high carbon losses and changes in substrate quality. Land use at Hor was quite recently changed from a fertilized and deeply drained crop land to a nature reserve with restored water table. Also Amo used to be more intensively

managed and drained, but the drainage system was not maintained. Land-use history was not known and SOC measurements were available from only one date per site. The measured carbon fluxes were therefore the only indication about carbon loss or addition to the complete system, while changes in relative pool sizes were not known. The partitioning of the SOC has implications on the parameter distribution for the rate coefficient for decomposition, which is discussed in Section 3.2.10.

3.2.2 Model performance

The best achieved performance highly differed between the different validation variables and between the different sites. This was not only caused by the models ability to simulate the different output parameters but also due to measurement quality, measurement uncertainty, measurement methods (temporal and spatial resolution) and heterogeneity of the sites.

GPP was simulated markedly poorer as compared to R_{eco} at all sites and not only in the single runs, but also in the complete set of performed multiple runs. An explanation might be that in the model the whole plant community consisting of different individuals, species and even functional types, with different life cycles and adaptations to light availability and temperature was simplified to only one plant. Especially mosses differ largely from vascular plants in respect to their ecology and response to water, temperature and light conditions (Gaberščik and Martinčič, 1987; Harley et al., 1989; Murray et al., 1993; Turetsky, 2003), which might be important at the moss rich Lom and Amo. The vegetation at Hor consists of species with very different strategies and requirements for nutrient and water. At FsB, reed, which is known for a late emerge, was well present in some of the years while it did hardly appear in other years. FsA is relatively species rich and several of these species are abundant only during parts of the vegetation period. Also, using a more complex photosynthesis model like e.g. Farquhar et al. (1980 and 2001) and testing a wider range of parameters might lead to a better fit. Including plant stress due to high water levels and nutrient limitation might improve the performance on some sites. E.g. Sagerfors et al. (2008) found photosynthesis to be limited also by too high water levels, so that the McGill wetland model assumes reduced photosynthesis outside a water level range of −10 to −20 cm (Wu et al., 2013). Furthermore, GPP cannot be measured directly neither by the chamber nor the EC method. Instead it was derived from NEE and R_{eco} or night time NEE, including the uncertainty of two different measurements and empirical modelling.

Heterogeneity of vegetation was very distinct at Hor, which might explain the difficulties to simulate the right amounts of GPP and biomass at the same time. The biomass and LAI taken into account for the present study might not be fully representative of the whole EC fetch for all wind directions. Hor is also a site which deviates strongly with respect to other sites, with recent large changes in management. It is in successional transition from intensively used dairy farming meadow (approximately 20 years ago) towards reed fen with willow thickets. Soil and vegetation still show the imprint of high nutrient level derived from manuring practices (e.g. patches with abundant *Urtica dioca*). This likely still affects GPP. These features could be a better explanation of the deviating GPP than the additionally tested configuration with strongly reduced litter fall and plant respiration rates.

Even though the winter fluxes are small compared to the summer fluxes they have a marked role in the annual NEE balances (Fig. 8). Overestimation of winter R_{eco} in combination with slightly underestimated winter GPP lead to high overestimation of annual accumulated NEE, emphasising the importance of winter flux dynamics in the annual balances. At all sites except Hor, winter R_{eco} was overestimated in the selected single run. For FsB and especially FsA, this was also true for all multiple runs. As R_{eco} at Lom and Amo are typically relative low, the effect was less pronounced.

Several different reasons for the winter R_{eco} overestimation are possible: explanations due to model setup and parameterisation are discussed in the sections 3.2.8, 3.2.9 and 3.2.10. Additionally, gases might be trapped within the snow and under the ice (Bubier et al., 2002; Maljanen et al., 2010) and therefore be seen by the measurement instruments only in spring time, when they are released. A gastight ice cover was not realised in the current model setup. Frozen or ice covered soils are quite common at the boreal Lom, but also at FsA and FsB which have a more continental climate than the other sites.

The ability of the model in simulating soil moisture could not be evaluated, as this variable was measured only at Lom, where the soil was close to saturation throughout the year. Therefore, and as ground water level was used as input, hydraulic properties could not be constrained. Further, swelling, shrinking and hysteresis effect which are important factors in hydraulic characteristics of peat soils (e.g. Kellner and Halldin, 2002) were not accounted for. This could have an effect on model performance and parameter values, especially those related to the soil moisture response.

3.2.3   Soil temperature dynamics

Due to the insulating impact of the snow cover (e.g. Zhang, 2005), the value of mean annual soil temperature (T_{amean}) was expected to be slightly higher than the mean annual air temperature. Constrained values of soil temperature were 1.5 to 5 °C higher than the mean annual air temperature at all sites. If the model was run under different conditions without further fitting, factors causing differences between mean annual soil temperatures and corresponding air temperature need to be considered.

3.2.4   The role of soil temperature and GPP to constrain the plant cover

Accepted fits for soil temperature in the uppermost measured soil layer led to p_{ck} values, close to the measured coverage of vascular plants for each site. Therefore, the measured coverage could directly be used in the configuration C1 (Fig. 10a). Setting p_{ck} to a common value of 100% reduced the differences in ε_L between the sites C7 (Fig. 10e), but led to underestimation of soil temperature in the uppermost soil layer by at most −0.45 °C in ME at Amo. An explanation could be that mosses are contributing to the plant coverage in respect to GPP but not to temperature, especially at sites where they are the main peat forming material.

3.2.5   Start of senescence

Site-specific calibration was needed for the temperature sum initiating the start of senescence ($T_{MatureSum}$). However, if the resulting day of the year was plotted instead, the differences between sites became small (Fig. 10) and setting it to the mean value of all sites did not reduce model performance in GPP R^2 by more than 0.05. Induction of senescence with graminoids is known to depend on both, temperature and day length (Nuttonson, 1958; Proebsting et al., 1976; Thomas and Stoddart, 1980; Davidson and Campbell, 1983). However, the differences between the sites in the present study could be explained solely by the relative day length.

3.2.6   Seasonal and management control of mobile plant pool for regrowth

The proportion of C in the plant which does not become litter, but instead is stored for leafing-out in the next year (m_{retain}), differed largely between sites. At Lom, a value of at least 40% led to accepted performance while a maximum of 3% was found for FsA and FsB; a mean value of 20% would reduce R^2 of GPP by at least 0.04 for these sites. At Amo and Hor neither a value of 3% nor 40% reduced R^2 of GPP by more than 0.01. An explanation

for low m_{retain} at FsA and FsB could be that the same pool is used for regrowth after cut and therefore not available for leafing-out anymore, as the regrowth rate in both early spring and after cut depend on carbohydrate reserve (White, 1973; Davies, 1988; Klimeš and Klimešová, 2002). Steele et al. (1984) conclude that defoliation late in the year will affect spring regrowth.

At Lom, high m_{retain} might be an adaption to the short vegetation period (Kistritz et al., 1983). Evergreen parts of the vegetation like dwarf shrubs, lower leaf parts of graminoides and mosses were not accounted for, which also affects regrowth in spring. Saarinen (1998) found that 60-70% of shoots and 20% of green biomass in a *Carex rostrata* fen survived the winter and hypothesised based on comparison with other studies that the proportion increase with increasing latitude.

The storage pool is an important parameter needing site-specific calibration but can be fitted if several measurements during spring and early summer of either GPP, biomass or LAI are available.

3.2.7 Radiation use efficiency

As plants were not nutrient limited in the model setup, lowest values for ε_L were expected under the most nutrient poor conditions (e.g. Longstreth and Nobel, 1980; Reich et al., 1994; Haxeltine and Prentice, 1996; Gamon et al., 1997). The opposite was true if site-specific values were used for p_{ck}. However, a common value for p_{ck} reduced the differences in ε_L and led to low ε_L at the ombrotrophic Amo site, but to an even lower value at the minerotrophic Lom. Nutrient status of the soil can therefore not explain the differences in ε_L. The assumption of plants being well-adapted to nutrient and water stress might not be true for the restored Hor site, where parts of the vegetation still consists of species which are not typical for wetlands. This might explain the low productivity at that site, but could only be covered by a model, if site-specific plant responses to high water levels would be applied. Additionally, ε_L is known to be species specific (Sinclair and Horie, 1989; Reich et al., 1998; Wohlfahrt et al., 1999).

Radiation use efficiency is an important parameter needing site-specific calibration. If common values were used for ε_L, p_{ck} and m_{retain}, mean GPP would be underestimated by a factor of 2.4 (FsB) or overestimated by a factor of 3 (Lom). If site-specific values were used for p_{ck} and m_{retain} the discrepancy would be even higher. However, ε_L can easily be fitted if either GPP, biomass, or LAI is known.

3.2.8 The control of decomposition and plant respiration by soil temperature

The whole year R_{eco}, which was dominated by summer R_{eco} could be described by a single temperature response function at all sites. However, it was not possible to find an equal good fit to both summer and winter R_{eco}, using the same t_{Q10} value. Higher t_{Q10} would decrease overestimation of winter R_{eco} especially at the southern sites FsA and FsB, but also reduce model performance for whole year R_{eco}. Different temperature responses for different sites (e.g. Jacobs et al., 2007), seasons (e.g. Lipson et al., 2002) and temperature ranges (e.g. Lloyd and Taylor, 1994; Paul, 2001; Atkin et al., 2003) are reported in the literature. This is partly explained by multiplicative effects of several temperature sensitive processes (Davidson et al., 2006; Kirschbaum, 2006) but still, a constant t_{Q10} might be a wrong assumption (Atkin et al., 2005).

More sophisticated temperature responses like the Ratkowsky-function (Ratkowsky et al., 1982) might improve the performance for individual sites. This might also be true for separate temperature response functions for plant and soil, as summer R_{eco} includes autotrophic and heterotrophic respiration, while winter R_{eco} is strongly dominated by heterotrophic respiration.

3.2.9 The control of decomposition by soil moisture

The activity under saturated conditions in respect to unsaturated conditions is described by $p_{\theta Satact}$ and was strongly negative correlated with decomposition rate k_l. Patterns for $p_{\theta Satact}$ differed between sites and variables. At all sites a minimum value of around 5% led to acceptable performance in whole year R_{eco}, while also quite high values did not reduce the performance except at FsB. At Lom only winter R_{eco} was considered, as conditions were always saturated during summer. For acceptable winter R_{eco}, $p_{\theta Satact}$ needed to be very low. This was not true for Lom, where water in the upper soil layer partly froze in the model and led to high winter respiration.

As the soil at FsA and FsB was saturated during winter, a common lower value for $p_{\theta Satact}$ would decrease overestimation of winter fluxes. However, it would also reduce model performance at all sites and increase the site-specific differences in k_l (Fig. 11).

Permanently saturated soils contain less O_2 than temporally saturated ones (e.g. Kettunen et al., 1999), which effects decomposition (e.g. Reddy and Patrick, 1975; DeLaune et al., 1981; Holden et al., 2004). Therefore, lower

$p_{\theta Satact}$ would be justified for wetter sites. If k_l was constant between sites and instead $p_{\theta Satact}$ fitted, this would lead to the value of $p_{\theta Satact}$ to decrease in the order FsB > FsA > Lom > Hor > Amo (Fig. 5) which cannot be justified by the differences in water levels which increase in FsA < FsB << Amo < Hor << Lom. Therefore, a different $p_{\theta Satact}$ cannot explain differences in soil respiration between sites. However, amount of aerenchymous plants, leading to soil aeration (e.g. Armstrong, 1980) were not taken into account. They reach the highest coverage at FsB (90%), followed by FsA (62%), Hor (50%), Lom (around 10%) and Amo (around 6%). Modelling water response depending on soil O_2 and redox potential, including O_2 conductance from plants, might help to analyse the differences in decomposition rate and reduce winter overestimation. E.g. in the Wetland-DNDC model, the water response function depends on redox potential: decomposition under saturated condition is reduced by a factor of 0.6 if redox potential is high, but by a factor of 0.2 if redox potential is low (Zhang et al., 2002).

3.2.10 The control of decomposition by substrate

The largest differences of parameters between sites appeared for the maximum decay rate of the fast C pools k_l. Setting it to a common value would lead to an underestimation of mean R_{eco} by a factor of 2.8 at FsB or an overestimation by a factor of 4 at Amo.

Despite different temperature and water response curves being tested, k_l values at FsA and FsB are substantially higher than at Amo (Fig. 9 and Fig. 11). Higher t_{Q10} values lead to two groups of k_l values: similar high ones for Lom, FsA and FsB and substantially lower ones for Hor and Amo (Fig. 11).

The partitioning into SOC pools strongly effects the differences, as can be shown by calculating decomposition rates for the total SOC (k_{tot}) based on k_l, k_h and SOC in the pools of the upper 30 cm as used in the C1 scenario (Fig. 12). However, FsB and FsA still have much higher rates than Amo. Resulted values and ranges of k_{tot} (0.02-0.16 a^{-1}) are comparable with reported values from laboratory incubation studies of peat cores (0.03-1.66 a^{-1}, Moore and Dalva, 1997; 0.01-0.35 a^{-1}, Glatzel et al., 2004; 0.008 a^{-1}, Kechavarzi et al., 2010; a SOC content of 30% was assumed for conversion from dry mass).
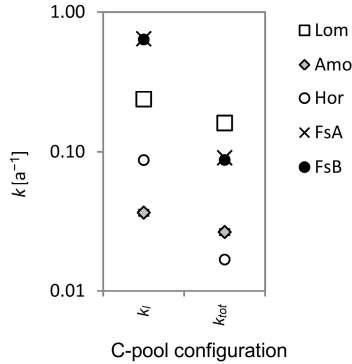
Figure 12. Decomposition rates of fast pools (kl) and calculated rates of total organic matter decomposition if only one pool was used (ktot) for each site and each layer.

Lower decomposability is often associated with higher C:N ratios (e.g. Zeitz and Velty, 2002; Limpens and Berendse, 2003; Bragazza et al., 2006), which might be important especially for the moss rich Amo and Lom. Assuming a C:N ratio of 60 for the fast pools (Fig. 11, C6) leads to a decomposition rate at Lom which is close to those at FsA and FsB, while those of Hor and Amo remain substantially lower.

Low pH might be one reason for the low k_l at Amo (e.g. DeLaune et al., 1981; Bergman et al., 1999). Despite being nutrient rich and having a high pH and high biomass production, leading to large amounts of labile carbon added to the soil, k_l values at Hor were very low. This might be connected to land-use history and the origin of the peat from partly clayey-lake sediment. Most of the labile C in the parent peat in the upper, formerly drained soil layers might have been decomposed before and therefore stabilised.

In the current setup the slow pools were almost inert. A higher decay rate for the slow pools would result in a lower k_l for sites with high C stock in the slow pools (cf Table A1.1 in the appendix). This would decrease the differences between FsA and FsB compared to Lom and Amo, but increase the differences between FsA compared to FsB and compared to Hor.

Substrate quality is known to effect decomposition rates (e.g. Raich and Schleisinger, 1992; Yeloff and Mauquoy, 2006). Therefore, many other SOC models use several different SOC pools (e.g. Franko et al., 1997; Smith et al., 1997; Cui et al., 2005; Del Grosso et al., 2005; van Huissteden et al., 2006) to account for differences in substrate quality. This leads to the

problem of partitioning total SOC into the pools (e.g. Helfrich et al., 2007; Zimmermann et al., 2007). In some models, the various SOC pools differ also in their response functions (e.g. Smith et. al, 2010).

The highest decomposition rates occurred at sites with highest biomass production. A correlation of productivity with soil respiration was found in several comparison studies (e.g. Janssens et al., 2001; Reichstein et al., 2003). Fresh material provided by the plants might lead to higher microbial activity and priming effect (e.g. Kuzyakov, 2002; Fontaine et al., 2007). Higher plant to soil respiration ratio reduced the differences in k_l between the sites and lowered winter R_{eco}, especially at the highly productive FsA and FsB, but also reduced the model performance at all sites except Amo.

Vegetation at Amo and Lom consist largely of mosses which are more resistant to decomposition then vascular plants (Rudolph and Samland, 1985; Verhoeven and Toth, 1995; Moore et al., 2007) and might further explain the low k_l value at Amo. Despite the lower biomass production, higher moss cover and higher C:N ratio compared to Hor, FsA or FsB, Lom has a relative high decomposition rate. This can be explained by the very low dry bulk density, resulting in low amount of C in the upper soil layers (Table A1.1 in the appendix) which are most exposed to decomposition (e.g. Fang and Moncrieff, 2005). Also, a low dry bulk density accompanies with low degree of degradation and therefore high amounts of labile carbon (e.g. Grosse-Brauckmann, 1990).

Despite the large differences in accumulated NEE (Fig. 2) between FsA and FsB, they almost do not differ in their decomposition rates. This confirms the expectations that the differences in NEE between FsA and FsB can be fully explained by the differences in water table, biomass and carbon stocks.

3.2.11 Conclusions of site comparison (study I)

Differences between sites in respect to CO_2 fluxes could be explained if beside air temperature, water table and soil C- & N- stocks, also site-specific plant productivity and decomposition rates were taken into account. Differences in nutrients availability and soil wetness could not explain the differences in plant productivity between the sites. Substrate quality, litter input, as well as pH values were likely explanations for the differences in decomposition rates. A site-specific interpretation was not needed for processes related to plant phenology, their response to temperature, allocation of new assimilates and plant respiration and litter fall rates.

The model parameters which strongly affected model performance were successfully constrained by the available long term measurement data on

NEE, partitioned into GPP and R_{eco}, LAI and biomass, including rooting depth and root biomass at one site, water table, soil temperature and soil C and N stocks as well as meteorological data and snow data at one site. It would have been useful if additional information was available about root biomass at all sites, root litter fall and soil water content to validate the model performance in the corresponding processes. A second measurement of C and N stocks, several years after the first, as well as information about the degree of decomposition on all sites would have been very helpful to constrain decomposition rates and partitioning between SOM pools.

Some improvements in the model and its configuration were identified to obtain a better performance for simulations of GHG fluxes from treeless peatlands. Examples include separate temperature responses for plant and soil heterotrophic respiration. The static response to water saturated conditions needs to be replaced by a function that considers the change of O_2 in the soil.

3.3 Results of process interactions (study II)

Interactions between the different biotic and abiotic processes that are related to the carbon cycle were investigated in the second study. Processes as well as parameters were found to be strongly interacting, which was reflected in sensitivities of each variable to several different modules, correlations between the performance in different variables, and in equifinalities between parameters of different modules.

About half of the parameters were sensitive to model performance in one or more variables, but only very few had a distinct range (Section 3.3.1). Instead they affected several processes, causing trade-offs in model performance between the different measurement variables, but also several supporting effects could be identified (Section 3.3.2). A lot of equifinalities were identified between parameters. Parameters were correlated with up to seven other parameters, often from different modules. Therefore, a good performance often requires certain combinations of parameter values, rather than specific parameter values (Section 3.3.3).

Each of the available measurement variables (NEE, LAI, sensible and latent heat fluxes, net radiation, soil temperatures, water table depth and snow depth) constrained several parameters, without any variable being redundant (Section 3.3.4). Nevertheless, large uncertainty remained in especially the unsaturated water distribution in the soil (Fig. 13), which affected all considered processes and hindered further parameter constrain. This might be solved by additional measurements of i.e. soil hydraulic properties. Other important parameters that could not be constrained define aerodynamic resistance, radiation interception (in particular moss albedo), timing of snow melt, and in case of NEE mostly the leaf litter fall rate of vascular plants during the growing season (Fig. 13).

A detailed description of the key parameters for each process and the detected interactions can be found in the appendix, section 3.1. Results for model fits to the different variables can be found in Fig. A3.4.1 in the appendix.
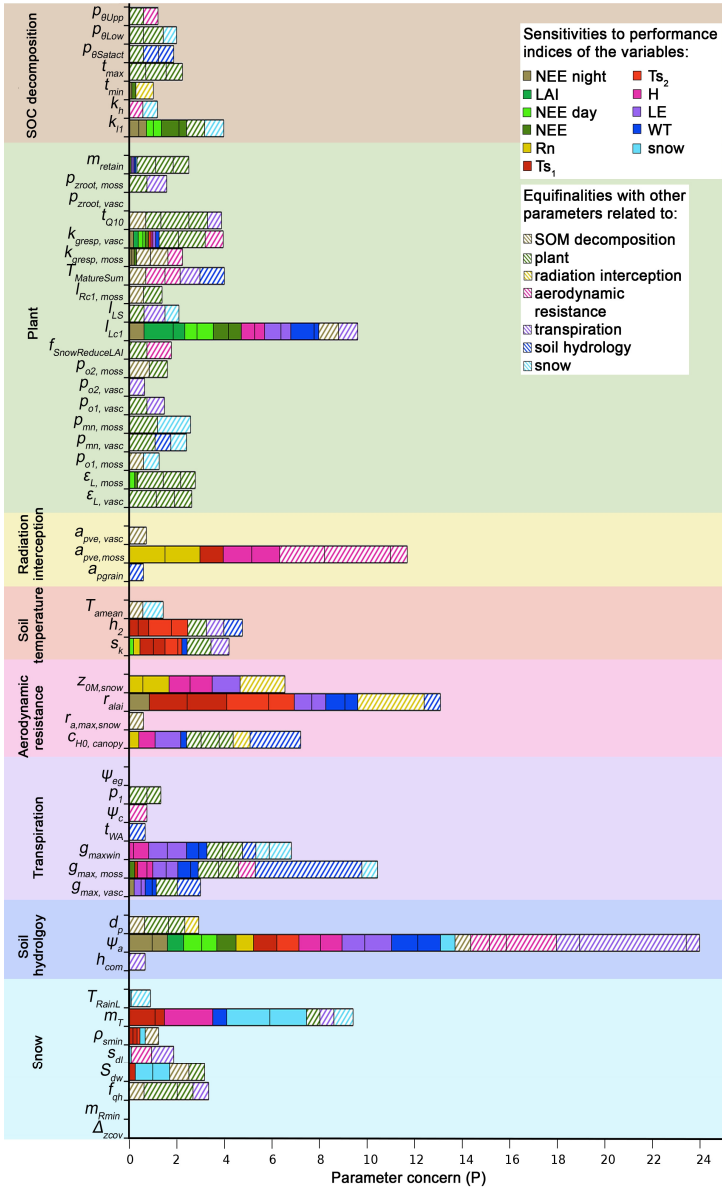
Figure 13. Parameter concern is shown on the y axis as sum of equifinalities (hatched) and sensitivities that could not be constrained unambiguously (solid). The x-axis shows the parameters, which belong to the module of the background colour.

3.3.1 Parameter sensitivity

Most of the 27 sensitive parameters were sensitive to performance in more than one variable but resulting value ranges differed depending on both, the variable and the performance index (Fig. A3.4.2 in the appendix).

Performance in Ts and WT was determined by 12 key parameters belonging to seven and six different modules, respectively (Fig. 14). In contrast, snow depth and LAI depended mainly on parameters from their own modules.

Large differences in resulting accepted ranges depended on the selected performance index and the considered sub-period: On average, accepted value ranges overlapped with 35% between different performance indices and between different sub periods of the same variable and with 6% if additionally the differences between different variables were considered (Fig. 15). Radiation and LAI were the simplest processes in respect to number of connected parameters (Fig. 14). However, radiation was, together with snow depth, the process with the strongest average disagreement in parameter value ranges between the different selection criteria for this variable (Fig. 15).

In case of eleven parameters, the accepted ranges did not overlap at all (Fig. A3.4.2 in the appendix). Four parameters were sensitive to at least half of the considered processes (Fig. 13): The parameter defining the water retention curve and unsaturated soil hydraulic conductivity (ψ_a) affected model performance in variables of all eight considered processes. Moss transpiration coefficient ($g_{max,moss}$), vascular plant respiration coefficient ($k_{gresp,vasc}$) and litter fall rate (l_{Lc1}) were important parameters for not only LAI and NEE, but also H, LE and WT, $g_{max,moss}$ and $k_{gresp,vasc}$, additional for Ts.

The sensitivity of the single parameters is described in more detail in section A3.1 in the appendix. The full table of the correlation coefficients between parameters and performance can be found in the appendix (Table A3.3.1).
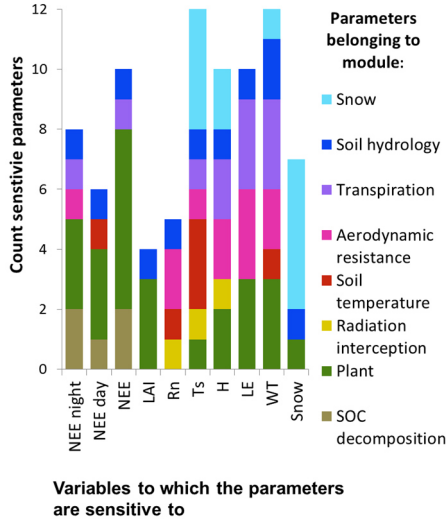
Figure 14. Connections between processes and parameters of different modules. The y-axis shows the count of parameters from the different modules (colours) that are sensitive to model performance in the various variables (x-axis).
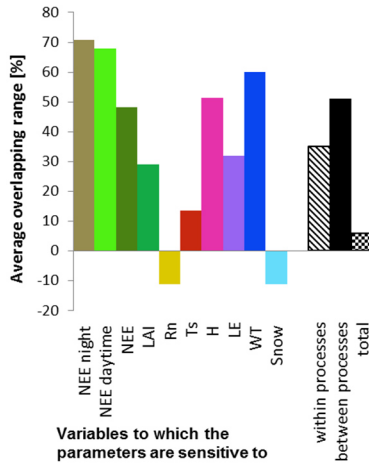
Figure 15. Average overlap of accepted ranges per parameter within each process and between processes, i.e. how unambigously the parameters could be constrained. Negative values indicate the distance between accepted ranges when ranges did not overlap at all.

3.3.2 Confounding and supporting effects of interacting processes

The performances of several variables were connected in supporting and confounding ways (Fig 16 and 17). Especially ME of LE and WT were strongly connected, but also ME of LAI had an impact on the performance in many other variables. Trade-offs existed not only between the performances of different variables, but also within a variable, depending on chosen performance index or seasonality.

The magnitude of vascular plant LAI was strongly correlated with the magnitude of LE, WT, H and NEE, especially if daytime and night time values were considered (Fig. 16). Thereby, the lowest ME in day and night time NEE, as well as ME and dynamics of H, went along with a slight underestimation, and for LE and WT with a slight overestimation of vascular plant LAI. Best performance for WT dynamics was reached if the magnitude of vascular plant LAI was correct (Fig. 17). A noticeable existence of the vascular plants (LAI ME > -0.4) increased the fit in NEE R^2 to at least 0.2, but this was not a necessary precondition for good NEE performance (Fig. 6). Highest performance in dynamics of WT, H and Ts in the upper layer coincided with a good fit in NEE magnitude (Fig. 17). This relationship was even stronger if these variables were compared to ME in NEE night time and NEE daytime.

A correct representation of WT dynamics and depth coincided with high performance in H dynamics and a correct or slightly underestimated H (Fig. 16 and 17). A small ME in H correlated with high performance in WT dynamics. Performances in soil temperatures of different layers were strongly correlated with each other in both, dynamics and magnitude.

Underestimation of LE was connected to an overestimation of H, but also to better dynamics in H (Fig. 16). ME in Net radiation was positively correlated with ME in H. A good fit between modelled and observed snow depth did not correlate with the performance in any other variable. The only exception was a negative correlation between the dynamics in snow depth and H, if exclusively performance during spring time was considered (Fig. A3.4.3 in the appendix).

Trade-offs existed not only between different variables but also between different performance indices of the same variable. Especially for snow, Rn, and in case of some parameters also for Ts, accepted ranges were contradictory depending on whether R^2 or ME was chosen. In case of moss albedo ($a_{pve,moss}$) and aerodynamic resistance dependency on LAI (r_{alai}), the ranges also strongly depended on the season during which the variable was

considered. For two aerodynamic resistance and one soil parameter ($z_{0M,snow}$, $c_{H0,canopy}$, s_k) ranges differed between R^2 of actual values and R^2 of accumulated values.

Additional to the uncertainty from unambiguous parameter ranges, further uncertainty results from equifinalities between parameters.
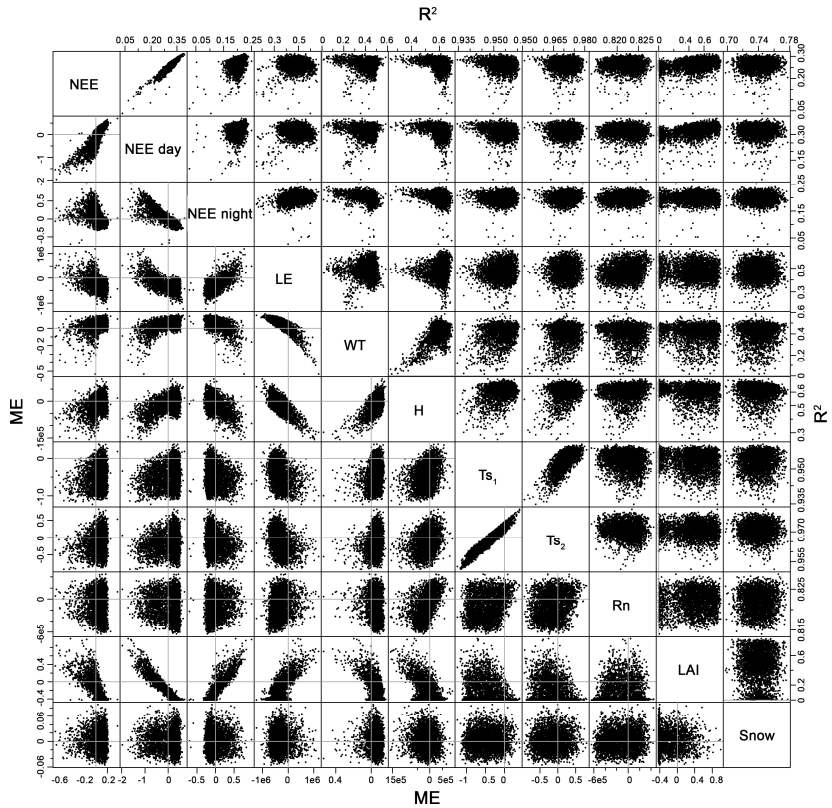
Figure 16. Correlations between performance indices in the prior distribution (3200 random runs): R^2 versus R^2 (upper panel); ME versus ME (lower panel). Each of the dots represents a parameter set. Grey lines indicate the axes through zero.
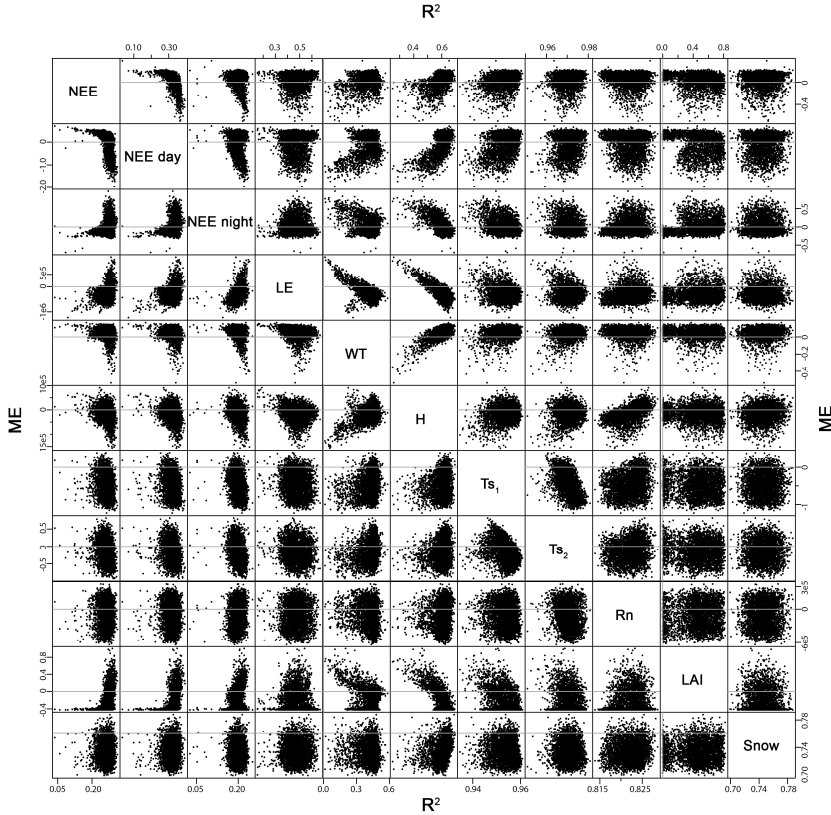
Figure 17. Correlations between performance indices in the prior distribution (3200 random runs): R^2 (columns) versus ME (rows). Each of the dots represents a parameter set. Grey lines indicate the axes through zero.

3.3.3 Equifinalities

Parameters were strongly inter-correlated, often with several parameters, and often from different modules. Equifinalities can hinder the identification of sensitivities, which was especially true for the basic selection: Despite reducing the number of runs by 97.48%, posterior and prior ranges differed hardly (Table A3.3.2 in the appendix). Instead certain value triples for photosynthetic efficiency ($\varepsilon_{L,vasc}$) with the respiration coefficient ($k_{gresp,vasc}$) and with the storage fraction for plant regrowth in spring (m_{retain}) were crucial for the survival of the vascular plant layer. Certain value pairs for the moss transpiration coefficient ($g_{max,moss}$) with the

shape parameter of soil water retention (ψ_a) were crucial for a reasonable water table depth.

Equifinalities existed not only between parameters of the same modules, but even more often between parameters of different modules (Fig. 18). Parameters defining radiation interception, soil temperature, aerodynamic resistance, transpiration, and soil hydrology correlated with exclusively parameter from different modules. Parameters defining radiation interception were mostly correlated with parameters defining aerodynamic resistance. Only in case of plant and SOC decomposition parameters, equifinalities existed mainly between parameters of the same modules.

All sensitive parameters, except ρ_{smin}, and further other parameters were detected to correlate with up to five other parameters in the final selections, ψ_a correlated with even seven others (Fig. 13). Two parameters had very strong correlations ($R^2 \geq 0.3$) with two other parameters each, which belong to different modules (ψ_a with $c_{H0,canopy}$ and $g_{max,moss}$ and $a_{pve,moss}$ with $z_{0M,snow}$ and r_{alai}) (Table A3.3.3 in the appendix).
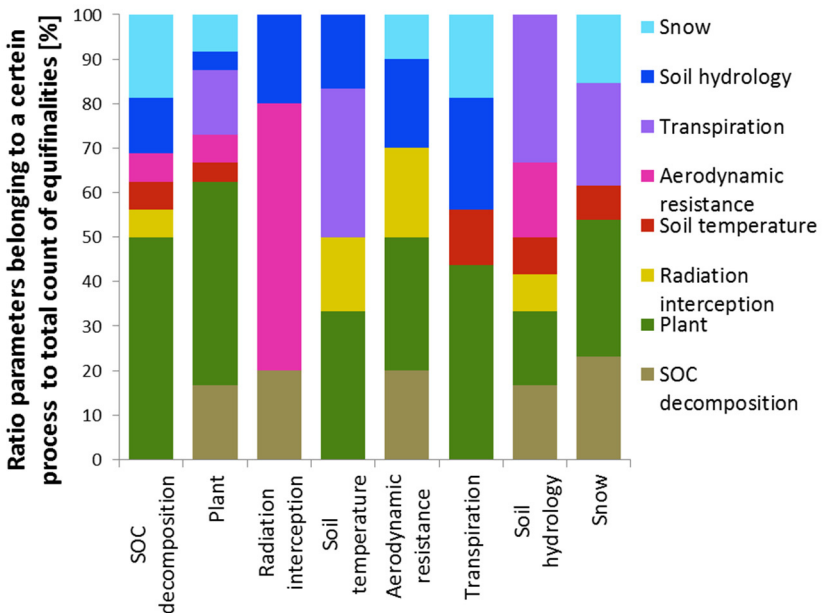
Figure 18. Module belongings of parameters that correlated with parameters of a certain module.

3.3.4   Usefulness of measurement variables

All available measured variables (NEE, LAI, LE, H, Rn, Ts, WT and snow depth) were helpful in constraining parameter ranges (Fig. 13). None of the supporting effects was strong enough, to make one variable fully replaceable by another. Even for the strongest correlation between soil temperatures of the different layers, the remaining uncertainty in one temperature when knowing the other would be in the magnitude of 0.5°C, which corresponds to more than 25% of the total uncertainty resulting from the tested parameter ranges (Fig. 16).

13 parameters could be unambiguously constrained to a more narrow range, as their resulting ranges were well overlapping (Fig. A3.4.2 in the appendix). The performance on each variable was correlated with many parameters from different processes (Fig. 14). The highest number of correlations was detected for the performance in WT and Ts, which constrained 12 parameters from different modules. Also the available data for LE, H, and NEE constrained many parameters.

Still, large uncertainty remained due to equifinalities and differences in accepted ranges: The largest uncertainty was caused by a parameter defining the shape of the water retention curve (air entry, ψ_a). As this was the only calibrated parameter of the water retention curve, it determined the unsaturated hydraulic conductivity of the soil. ψ_a was sensitive to all considered processes and had many strong interactions with other parameters, while it was not possible to constrain it to an unambiguous value range (Fig. A3.4.2 in the appendix). Therefore, it would be of great value to be able to deduce such parameters from additional measurements. This applies also to following parameters, which could not be constrained unambiguously: Leaf litter fall rate of vascular plants during the growing season (l_{Lc1}) was the second most sensitive parameter, affecting the performance in NEE, H, LE and WT. Moss albedo ($a_{pve,moss}$), aerodynamic resistance dependency on LAI (r_{alai}) and transpiration coefficients ($g_{max,vasc}$, $g_{max,moss}$, g_{maxwin}) had similar importance, due to their equifinalities to other parameters. Plant respiration ($k_{gresp,vasc}$) had strong sensitivity, but could be constrained unambiguously by the available data.

3.4   Discussion of process interactions (study II)

Unlike many previous CO_2 modelling studies that usually focus on NEE as only calibration variable, the present study considered several abiotic and biotic measurements to investigate the interactions between different

processes in a peatland ecosystem. Many connections between parameters of to the same, but also of different modules were identified, revealing the dependency of constrained parameter ranges to model structure and calibration setup.

The gained knowledge on parameter sensitivities can help to simplify future calibrations. The identified interactions and equifinalities between different processes are relevant for modellers in their decisions on the criteria for selecting accepted runs and on the processes and parameters that need be included in the calibration. Especially if only few parameters and processes are calibrated, resulting constrained ranges might not be comparable and transferable between models differing in their structure or constant parameter values. While parameter ranges and the exact shape of the connections are model and site-specific, the existence of the interactions between the processes and their parameters is supposed to be independent of these factors and therefore also relevant for other models and similar ecosystems. Beside parameter uncertainty, also uncertainty in model structure and in measured input and calibration data contribute to model uncertainty (Thorsen et al., 2001; Beven and Freer, 2001), but go beyond the scope of this study.

Experimentalist are recommended to provide beside the model input data (meteorological and SOC data) also ancillary data for their variable of interest, because of the strong interactions between the different processes. Measurements of NEE, LAI, LE, H, Rn, Ts, WT and snow were all found to be valuable for constraining parameters from several different modules and can therefore reduce uncertainty in model predictions. Further constraint would be possible, if especially additional water content or soil hydraulic properties were measured.

A detailed discussion of the detected sensitivities and interactions per process can be found in the appendix, Section A3.2.

3.4.1   Parameter sensitivity

The most influential parameters from various modules (SOC decomposition, plant growth related processes, radiation interception, soil temperature, aerodynamic resistance, transpiration, soil hydrology and snow) were identified in their sensitivity on model performance in multiple variables (NEE, LAI, Rn, Ts, H, LE, WT and snow depth) at a boreal open peatland. This will help future model users to minimize calibration effort and computing time, by calibrating only key parameters and modules for their variable of interest.

Especially abiotic processes were strongly inter-linked, but also biotic variables showed sensitivities to parameters from up to seven different modules, suggesting that parameter sensitivities and model performance of a certain process depend on which other modules are considered in the model and in the calibration. The knowledge on these dependencies can help modellers to select an appropriate model including the processes and modules which need to be considered together, depending on their variable of interest.

The parameter ranges that could be constrained in this study to a narrower range should be compared with studies on other sites, to find out if they are site-independent or to what extent they can be related to site conditions and therefore used for predictions and upscaling. The key parameters that could not be constrained, reveal needs for further investigations including additional measurement data (Section 3.4.4).

One or more of the following parameters that we identified as key parameters were also key parameters in other studies using other models on different ecosystems: The respiration rate coefficients, radiation use efficiency, transpiration coefficients or the soil water capacity were among the most sensitive parameters in e.g. the GUESS-ROMUL model on peatland (Yurova et al., 2007), the EPIC model on cropland (Wang et al., 2005), the ACASA model on spruce forest (Staudt et al., 2010), the FORUG model on beech forest (Verbeeck et al., 2006) or the BIOME-BGC model for different tree species (Tatarinov and Cienciala, 2006). These sensitivities seem to be therefore quite independent of model structure, included processes and parameters used for calibration. However, resulting constrained ranges are connected to the environmental scenario and the chosen prior distributions of the parameters. Further, the results of the present study have shown that parameter ranges depend on model structure, on the selection of parameters for calibration and on the selected acceptance criteria.

3.4.2   Confounding and supporting effects of interacting processes

Criteria selection is a subjective choice of the modeller if multiple output variables are available. The identified supporting effects and trade-offs between the performances in different variables allow modellers to assess the implications of a certain criteria on model performance and parameter ranges and to choose criteria according to the processes of interest.

Usually, LE is assumed to be closely connected to NEE due to the coupling of transpiration and carbon assimilation in vascular plants. The present study reveals much stronger relations between parameters defining H and NEE, than between LE and NEE. Trade-offs between performance in LE and NEE were also found by Staudt et al. (2010) and Prihodko et al. (2008). However, only the effect of parameters, not the effect of input variables on these processes, was analysed.

Trade-offs existed not only between different variables but also within the same variable, depending on whether ME, R^2 of actual or R^2 of accumulated values was chosen and which season was considered. This implies that the problems of a subjective criteria selection also exist if only one time series variable is considered.

Also several supporting effects were detected, indicating that some measurement variables can partly compensate absence or low resolution of a connected variable, even though they were not strong enough to make one variable fully redundant. For example, LAI measurements could reduce uncertainty in model predictions of the magnitudes of NEE, LE, H and WT on locations where these variables are not available. If H fluxes are available, the model is constrainable to produce improved WT dynamics, even if WT measurements were missing. High resolution of soil temperature measurements in one layer are sufficient to model good temperatures if just the magnitude of soil temperature in an upper and a lower layer is known, e.g. due to short time or low resolution measurements.

The knowledge on supporting effects helps modellers in their site selection and in uncertainty estimation of model predictions depending on available ancillary data. It further can help experimentalists in their decisions which variables should and which need to be measured if the site should be usable for model constraint.

3.4.3 Equifinalities

The fit of model output to measured data in complex models is often not driven by a particular parameter but instead by interactions among parameters (e.g. Beven and Freer, 2001; Verbeeck et al., 2006), which was also the case for several parameters in the present study, hindering the constraint to a more narrow range.

The knowledge on equifinalities is needed for a better parameter constraint in future calibrations as it allows calibration of the connected parameters in dependency of each other. Another way to respond to identified

equifinalities is to calibrate only one of the connected parameters. However, the resulting range will then not be transferable to other models using different values for connected, constant parameters.

Many equifinalities were identified, not only between parameters from the same module, but also from different modules. This implies that the problem of limited transferability also applies, if parameters from only one module are calibrated (which is often the case), or if models differ in the structures and implementations of their modules.

Some equifinalities included several parameters, making their visualisation impossible and simple regression as insufficient tool for fully detecting and describing them. These equifinalities need to be further investigated in additional calibrations which incorporate those parameter interactions and constrained ranges which were unambiguous, to achieve a higher number of acceptable runs. This is needed, because the numbers of accepted runs in the final selections (50) did not allow a much more detailed analysis in such a complex model, as was apparent in comparison with the basic selection: An R^2 threshold value of 0.1 was sufficient to identify equifinalities in the basic selection of 1286 accepted runs, but with just 50 accepted runs in the final selections, this threshold value could easily be exceeded by a random distribution, even that a higher threshold value of 0.15 was used. A threshold of 0.15 was on the other hand already too high, to detect for example the strong relationships between the plant parameters which were only clearly visible in the basic selection. Nevertheless the six equifinalities with R^2 of higher than 0.30 are unambiguous and those with lower values are still very useful to design future calibrations to further investigate and describe these equifinalities.

3.4.4 Usefulness of measurement variables

Each of the available measurement variables (NEE, LAI, LE, H, Rn, Ts, WT and snow depth) contributed to parameter constraint and therefore helped for model improvement and uncertainty reduction. Thereby none of the variables could be fully replaced by another. Due to the strong interactions and as parameters of each module were constrained by several different variables, ancillary variables are valuable even if only one certain process is of interest. In case of snow, the results suggest that data on snow cover might be sufficient, if snow depth is not available.

In a forest site simulation with the ORCHIDEE model, H and Rn were found to be redundant for constraining energy balance parameters if NEE and LE were available (Santaren et al., 2007). In contrast, some energy

balance related parameters in the present study were constrained by Rn and H only, or additionally by LE but with different resulting ranges. This reveals the usefulness of Rn and H measurements for model constraints and shows that variables which might have been identified as redundant in one study could be of high importance on another ecosystem or for another model calibrating a different parameter selection.

Several influential parameters could not be unambiguously constrained or showed equifinalities and need additional measurements to be further investigated. This includes soil water content or soil water retention properties, as well as canopy albedo and leaf litter fall during the growing season. Except for water retention properties these variables are needed as time series throughout the year. A more detailed discussion of the benefit of such measurements can be found in the appendix, section A3.2.

3.4.5   Conclusions for process interactions (study II)

CO_2 models are usually calibrated on NEE as only measurement variable. The present study investigated the interactions between different abiotic and biotic processes and their parameters, as well as the implications and usefulness of data on not only NEE, but also LAI, sensible and latent heat fluxes, radiation, water table depth, soil temperatures and snow depth for model calibration on a boreal peatland. Different processes and their parameters as well as model performance between different observation variables were strongly interlinked. This needs to be taken into account in model calibrations and when transferring calibrations results between models differing in their structure or in their constant parameters.

Key parameters were identified for each calibration variable, helping future model users to design model calibrations: Selecting only the most influential parameters for the variable of interest and using a narrower range for the constrained parameters means a simpler calibration and faster computation. This in turn, allows the inclusion of a more detailed investigation of a process of certain interest. On the other hand, the results revealed the strong dependence of constrained parameter ranges to other parameters and to the chosen criteria. This means, that a study aiming to understand and interpret parameter values need to calibrate processes and parameters of many different modules, using a wide range and multiple criteria on various observation variables. Parameter interactions were found to be more important than parameter value ranges, revealing the need for accounting for equifinalities: Either by calibrating correlated parameters in dependence of each other or by calibrating only one of the correlated

parameters. The latter will lead to a narrower constrained range, but this range might not be transferable to other sites and other models.

The gained knowledge on trade-offs will be useful to avoid modelling studies with too many purposes and helps model users assessing the implications of their criteria choice. The validity of calibrated models is always restricted and robustness of obtained parameters should be questioned. The identified supporting effects between some variables indicated that some measurement variables can partly compensate absence or low resolution of the connected variable. This information tells experimentalists which measurement variables are helpful and which are obligatory if a certain process should be understood from the underlying regulating principles. It further helps modellers to decide if a site has enough available data for model calibration and to estimate uncertainties in model predictions depending on available ancillary data.

All observed calibration variables (NEE, LAI, sensible and latent heat fluxes, net radiation, soil temperatures, water table depth and snow depth) helped for model constraint and interpretation. They should therefore be measured on sites used for calibration of complex process-oriented models. Additional measurements of in particular soil hydraulic properties or water content would largely reduce uncertainty and help for a better parameter constraint.

3.5   Results of vegetation indices as proxies (study III)

The potential of using optical vegetation indices as proxies for vegetation characteristics like biomass and photosynthesis was investigated on several grasslands with different management intensity in the Freisinger Moos. The usability of vegetation indices as a proxy for biophysical vegetation characteristics varied greatly for the different relationships: Pearson correlation coefficients ranged from 0.06 for NDVI as a proxy for biomass, up to 0.60 for NDVI as a proxy for green-ratio (Table 6). Relationships were in mean stronger when intensive and extensive meadows were considered separately, except the relationship between NDVI and PP.

Table 6. Correlation matrix for the investigated relationships between vegetation indices and characteristics, showing R2 values for all, intensive and extensive meadows.

	PAI			NDVI		
	All	intensive	extensive	All	intensive	extensive
NDVI	0.24	0.33	0.27	–	–	–
PP	0.36	0.48	0.30	0.53	0.34	0.56
Biomass	0.30	0.25	0.42	0.06	0.08	0.13
Green-ratio	–	–	–	0.60	0.59	0.63

3.5.1   Seasonal patterns of NDVI and PAI

NDVI values at intensive meadows saturated earlier than those at extensive meadows, but both reached similar maxima, close to 1 (Fig. 19a). Faster spring growth at intensive meadows was also reflected in PAI values (Fig. 19b). The first cuttings on intensive meadows took place before PAI saturation. During winter, intensively managed parcels exhibited a high NDVI (around 0.75), while it was considerably lower on extensive meadows (around 0.6). PAI values decreased towards end of the year and were lower at intensive meadows compared with extensive meadows during winter.
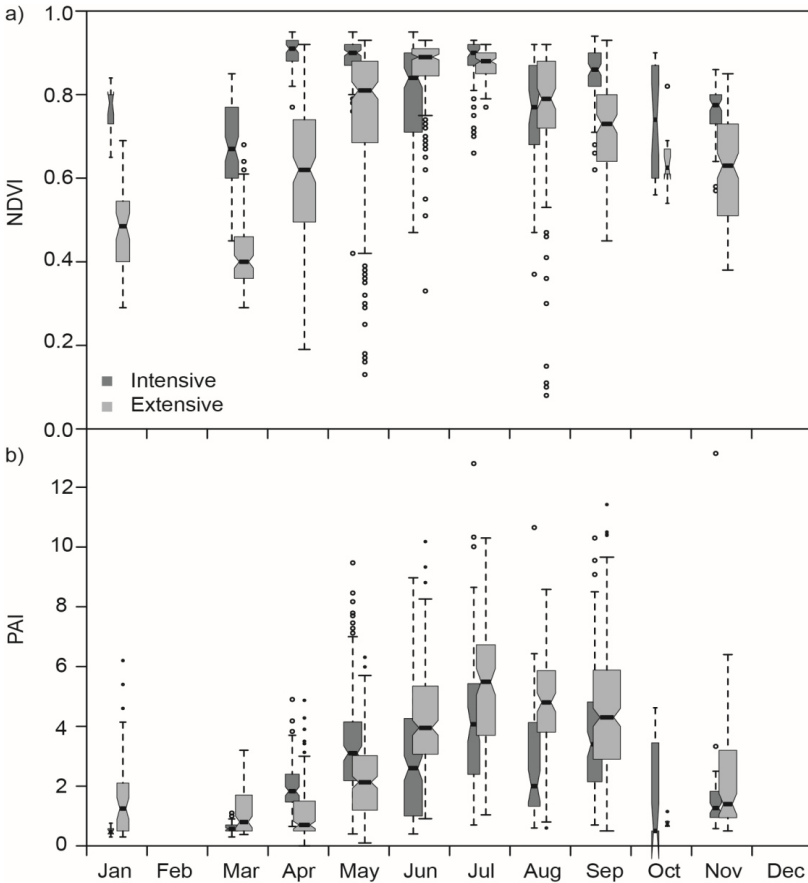
Figure 19. Ground NDVI (a) and plant area index (b) values in the course of the year for the whole dataset from end of April 2010 to beginning of July 2011. The width of the boxes indicates the number of observations in each category. The maximum width corresponds to 2670 data points, the minimum to 128. Boxplots for intensive meadows are shifted to the left for better visibility.

3.5.2   NDVI as proxy for green-ratio

The relationship between NDVI and green-ratio was similar between management intensities, but the distribution within the relationship was not (Fig. 20): only two samples from intensive meadows had NDVI values lower than 0.7, while more than half had values greater than 0.9. The lowest

value for green-ratio at intensive meadows was 0.16, with an NDVI value of 0.77, while 53% of the observations showed a green-ratio higher than 0.7. In contrast, 28% of the samples from extensive meadows had NDVI values lower than 0.7, and 21% a green ratio larger than 0.7. Large scatter occurred for low values, especially at extensive meadows where samples with 20 – 40% brown biomass span a NDVI range from 0.44 to 0.92.
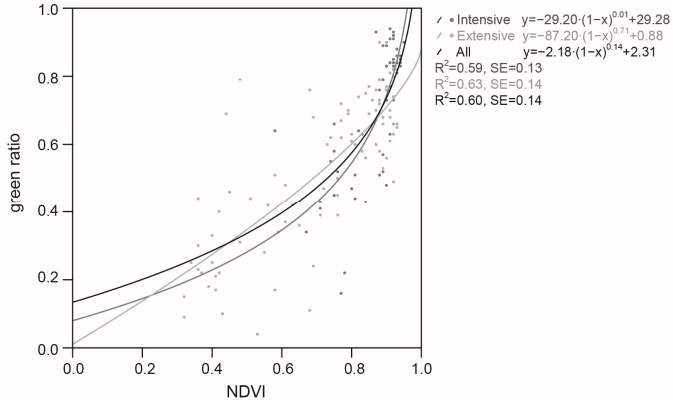
Figure 20. Ground NDVI from the intensive, the extensive and the intensive and extensive meadows together, measured on several dates throughout the year, plotted against green-ratio, determined at the same spots.

3.5.3 NDVI as proxy for LAI

At both intensive and extensive meadows, NDVI was saturated with high PAI values (Fig. 21, a). The relationships showed considerable noise, especially at extensive meadows for low and high NDVI values. Intensive meadows showed a similarly large scatter only for NDVI values larger than 0.7.

Extensive meadows had considerably higher mean PAI values compared with intensive meadows for NDVI values smaller than 0.9 (Fig. 21b). This was also true when GAI values were compared with NDVI values (Fig. 21c). However, GAI values on intensive meadows were higher in the NDVI interval between 0.9 and 1.
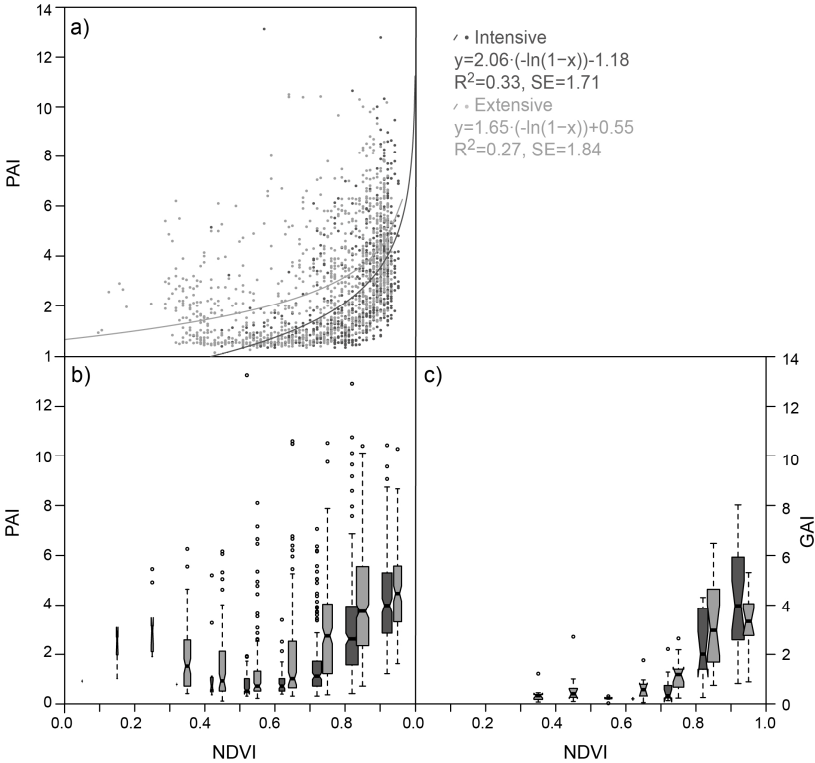
Figure 21. Ground NDVI plotted against plant area indexAI (a, b) and green area index (c) determined a at intensive and extensive meadows on several days throughout the year. The width of the boxes indicates the number of observations in each category. The maximum width corresponds to 374 (b) and 27 (c) data points. Boxplots for intensive meadows are shifted to the left for better visibility.

3.5.4 PAI and NDVI as proxies for biomass

Plants from intensive meadows tended to have a higher SPA compared with those from extensive ones, but the scatter was enormous (Fig. 22) and therefore PAI was a poor predictor. NDVI was an even worse predictor for biomass than PAI: a linear correlation for all observations resulted in an R^2 value of 0.06 (Fig. A4.2. in the appendix).
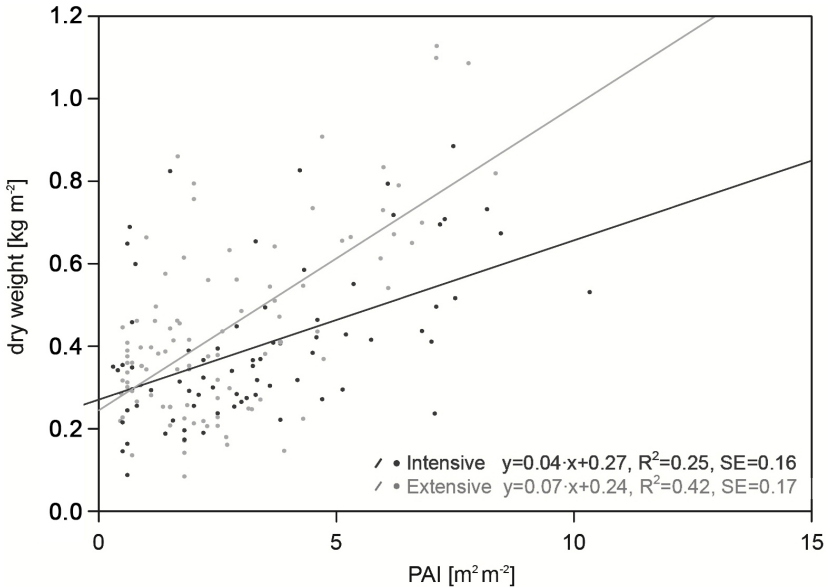
Figure 22. Plant area index plotted against total biomass from intensive and extensive meadows, measured on several dates throughout the year.

3.5.5   NDVI and PAI as proxies for PP

The relationship between PP and NDVI was linear for both satellite- and ground-measured NDVI values, with only small differences between management intensities (Fig. 23a). The relationship between PP versus GAI showed strong saturation effects for GAI values larger than 1 (Fig. 23b). Differences were observed not only between intensive and extensive meadows, but also between different parcels. Intensive meadows had higher PP values at the same GAI values than extensive meadows. Among the extensive meadows, the protected biotope E2 had higher values than the hay meadow E3, while the natural monument E1 had the lowest values.
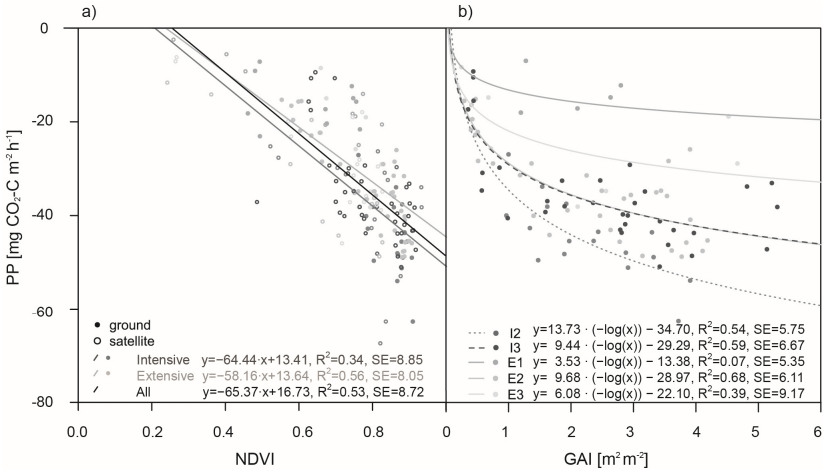
Figure 23. Potential photosynthesis derived from chamber flux measurements, plotted against NDVI (a) and green area index (b). NDVI data was used from both sources: ground measurements and satellite images. As the relationships between photosynthesis potential and green area index (b) showed clear site specific patterns, they were plotted for each meadow, whereas I2 and I3 are intensive and E1, E2 and E3 extensive meadows (cf. Table 4).

3.6 Discussion of vegetation indices as proxies (study III)

Managed grassland fens are the land cover type with the second highest net climate effect in Europe, just after arable fens; their CO_2 emissions are especially high in Germany, where they are often intensively managed (Drösler et al., 2008). Due to the relevance of vegetation parameters for carbon-related processes, the results of the present study have strong implications for e.g. CO_2 models using vegetation indices as input, but also for biomass estimations from remote sensing data and non-destructive methods. The productivity of fens is of interest for management decisions, as they are of high conservation value due to their significance for e.g. biodiversity and endangered species preservation, flood mitigation and water quality improvement (Mitsch and Gosselink, 2000), especially if management intensity is low. In general, the observed relationships between NDVI or LAI with vegetation characteristics on the temperate fen meadows in the Freisinger Moos were poorer and showed higher scatter compared with relationships that have been reported for other ecosystems. In particular, the widely used LAI was shown to be a poor predictor for biomass and PP, and could only poorly be estimated from NDVI. Further, the shapes of the underlying relationships depended on management

intensity. Therefore, the application of LAI as model input or biomass proxy on these meadows will result in high uncertainty. NDVI was found to be a better predictor for PP and should thus replace LAI in photosynthesis models. This study further revealed the need for ecosystem-specific validation studies for commonly used relationships between vegetation indices and vegetation characteristics. The results for each relationship are discussed in more detail in the following sections. Uncertainty in the data, resulting from the optical measurement methods, is treated in the last part of the discussion.

3.6.1 Seasonal patterns of NDVI and PAI

Extensive and intensive meadows differed largely in their seasonal patterns of both NDVI and LAI. A higher proportion and different distribution of standing brown biomass might be the main reason for the higher winter PAI and lower winter, spring, and autumn NDVI values on extensive meadows compared with intensive meadows, where standing litter was removed by the more frequent cuttings. Also, species-specific reflection might be important: The extensive meadows investigated hosted a larger number of species including some sedge species and reed (*Phragmites australis*), which differed visibly from the grass species on intensive meadows by a more grey-blue leaf colour, especially in the spring. Grey-green and yellow-green leaf colours can lead to lower NDVI values compared with green vegetation (Satterwhite and Ponder Henley, 1987), and different reflectance properties were reported for different wetland species (Anderson, 1995). High correlations between NDVI, visible colour, chlorophyll content, and leaf nitrogen content have been reported for several grass species (Bell et al., 2004). The close connections between chlorophyll content and red spectrum (e.g. Tucker, 1979) used in NDVI calculations, and between leaf chlorophyll and nitrogen content (e.g. Gáborčík, 2003) are well-established concepts and might serve as explanations for differences between the fertilised intensive and non-fertilised extensive meadows.

Mapping studies have shown that peatlands can be distinguished from similar ecosystems on mineral soils by a significantly lower maximum NDVI that is reached at a later date (e.g. Gardi et al., 2009). In the present study, the extensive meadows were wetter and consisted of a more peatland-typical vegetation than intensive meadows. Therefore, lower maximum NDVI values, reached at a later date were expected at extensive meadows. However, the results confirmed these differences only with respect to the timing, but not with respect to the magnitude of maximum NDVI values.

A trend of increasing spring time NDVI with management intensity can also be found, when satellite NDVI is compared with cutting frequency as surveyed by Drösler et al. (2013a) at 62 land parcels in the Freisinger Moos (Fig. A4.3 in the appendix). This hints to a possible application of spring time NDVI as proxy for management intensity, and should be further investigated on further fen peatlands, whereas the phonological spring needs to be considered for exact timing of NDVI collection.

3.6.2   NDVI as proxy for green-ratio

A potentially useful aspect of the relationship between NDVI and green-ratio would be the correction of ceptometer-derived PAI to derive GAI, when destructive sampling is not possible or is too time-consuming. NDVI was reported to be a reliable predictor of green-ratio, showing a linear relationship without any saturation for several grasslands in the Italian Alps and in New Zealand (Gianelle and Vescovo, 2007). In contrast, the data from the Freisinger Moos showed large scatter, a curved relationship and a rather different distribution within the relationship depending on management intensity. This might be explained by a very heterogeneous litter distribution: During the seasonal growth of gramnoids in particular, leaves are developed on top of the canopy, while lower leaves are shadowed and die (Robson, 1973). Hence, brown biomass is located under green leaves and cannot be detected by reflectance measured from above, resulting in a lower green-ratio at high NDVI values. This was especially pronounced at the quite productive site I3, before the first cut took place, and might explain that the curvature of the relationship was bent towards higher NDVI values. In contrast, sedges started yellowing at the leaf ends, leading to brown biomass covering green parts. Basal plant parts remained green during winter, which was also observed by Saarinen (1998) in a *Carex rostrata* fen. Furthermore, at extensive meadows without a cut in late autumn, a considerable amount of brown standing biomass was still present in spring, when new green leaves emerged under their shadow.

3.6.3   NDVI as proxy for LAI

The relationship between NDVI and PAI is especially relevant for the estimation of LAI from remotely sensed data. In the present study, the relationship showed larger scatter compared with previous studies (e.g. Gamon et al., 1995; Darvishzadeh et al., 2008), and this was especially pronounced at extensive meadows. This might be explained by the different seasonal patterns of NDVI and PAI, mainly due to large amounts of brown standing biomass.

Higher mean PAI values at extensive compared with intensive meadows for NDVI values smaller than 0.9 cannot be fully explained by their higher amount of brown biomass, as the pattern was similar when GAI was compared with NDVI (Fig. 3c). Instead, leaf colour might be an important factor. The opposite case in which NDVI values are larger than 0.9 might result from higher maximum GAI reached at intensive meadows.

Usually, the relationship between NDVI and LAI is described as a hyperbolic or exponential function, where NDVI saturates at LAI values around 2 or 3 $m^2 m^{-2}$ (e.g. Sellers, 1985; Gamon et al., 1995; Gianelle et al., 2009). For crops, this saturation might be reached at LAI values above 5 $m^2 m^{-2}$ (Viña et al., 2011). A linear relationship is reported for low canopies (e.g. Fan et al., 2009; Rocha and Shaver, 2009 with LAI < 0.8 and < 2, respectively). In contrast, some samples in the present study had reached maximum NDVI values already at PAI values smaller than 1 $m^2 m^{-2}$. This occurred at intensive meadows, particularly after harvest, if they had been cut before lower parts of the vegetation started senescence. The use of spectral indices, which include other wavebands like those in the red-edge (Huete, 1988; Viña et al., 2011), or green spectrum (Gianelle et al., 2009), or a the use of a weighting factor (Gitelson, 2004), might help to overcome the saturation problem, but not the problem of high amounts of brown biomass, which was especially pronounced at extensively managed fen meadows. The resulting high uncertainty has to be considered when using LAI estimated from satellite data, especially on ecosystems with high amounts of standing litter.

3.6.4 PAI and NDVI as proxies for biomass

Optical measurement methods are important alternatives to destructive biomass sampling and provide a possibility to achieve yield estimates from remote sensing. Large scatter in the relationship between PAI and biomass results from different SPA due to different leaf thicknesses and densities, and different amounts and densities of stems: Data from leaf area meter (Li-3100, LI-COR, Lincoln, USA) measurements at the studied sites showed considerably higher mean SPA values for plants from intensive (170 $cm^2 g^{-1}$) meadows compared with plants from extensive meadows (101 $cm^2 g^{-1}$) (Fig. A4.4 in the appendix). Species-specific differences ranged from 33 (*Schoenus ferrugineus*) to 204 $cm^2 g^{-1}$ (*Plantago lanceolata*) (Fig. A4.5 in the appendix). The higher SPA values for intensive meadows are in accordance with the larger slope of the regression between PAI and dry weight (Fig. 22). Based on dependencies between nutrient conditions in plant habitats, relative growth rate and leaf nitrogen, it was postulated that

nutrient-rich environments host species with high specific leaf area, while low specific leaf area species are found in nutrient-poor environments (Poorter and Jong, 1999). Similarly, increasing specific leaf area rates were found with increasing nutrient availability (Meziane and Shipley, 1999). Specific leaf area has further been shown to vary depending on seasonality (Pierce et al., 1994). Additional destructive biomass sampling throughout all seasons of at least one year is therefore strongly recommended to identify site-specific correction factors.

In contrast to the results of the present study, a strong linear relationship between NDVI and biomass was found in a wetland around a Chinese lake (Rendong and Jiyuan, 2002). Good correlations were also reported for wet tundra vegetation (Boelman et al., 2003; Doiron et al., 2013), but their maximum biomass values were much lower compared with ours. Many studies investigating grasslands on mineral soils reported a poor relationship between NDVI and biomass (e.g. Gamon et al., 1995). To overcome saturation effects at high biomass values modified indices were introduced that include the blue waveband (Huete et al., 2002) or the near-infrared shoulder (Vescovo et al., 2012) or which are based on narrow bandwidths (Thenkabail et al., 2002) or band depth analysis (Mutanga and Skidmore, 2004). In future research, it should be tested, if such modified indices can reduce the uncertainty in biomass estimation from satellite data.

3.6.5   NDVI and PAI as proxies for PP

The estimation of PP from NDVI or PAI is of high interest, as more direct photosynthesis measurement methods are cost- and effort-intensive and not possible on a global scale. The results showed a management-independent, nearly linear relationship between NDVI and PP. Some studies have reported a strong saturation effect at high rates of photosynthesis when using NDVI based on red and NIR bands (e.g. in a mountain grassland, Gianelle et al., 2009; in a pine forest, Wang et al., 2004) and, therefore, suggest the use of green instead of red wavebands (Gianelle et al., 2009) or additionally including blue wavebands (Schubert et al., 2010). Such saturation effects were not distinct in the present study, but might depend on the ecosystem. A linear relationship between PP and NDVI was supported by findings in tundra (McMichael, 1999), grasslands (Gamon et al., 1995; Wu, 2012) and four northern peatlands (Kross et al., 2013).

GAI was a comparably inferior predictor for PP, due to being site- and management-dependent and due to saturation at larger GAI values. Saturation between photosynthesis and LAI has been reported by many other studies (e.g. Sellers, 1985) and indicates a strong self-shading effect of

upper leaves shading lower leaves. In a wet *Senecioni-Brometum* grassland, 50% of the light was found to be intercepted by fewer than 10% of the leaves (Fliervoet and Werger, 1984). Site-specific differences might be explained by different vegetation on the different sites: Species- and plant functional type-specific differences in the relationship between LAI and photosynthesis were previously reported for boreal mires (Wilson et al., 2007; Leppälä et al., 2008), ranging from a linear to an exponential relationship. Further uncertainty in the relationship between GAI and PP results from the derivation of GAI from PAI values by applying the poor relationship between green-ratio to NDVI. A destructive sampling for a more direct determination of green-ratio or GAI was, however, not possible at the chamber plots.

Many ecosystem models use LAI to calculate photosynthesis. The present study has shown that NDVI is a better proxy for PP and should therefore be incorporated in carbon models.

3.6.6   Uncertainty in NDVI

Some scatter in the studied relationships could also be caused by uncertainty in the optical measurements. However, the comparison between NDVI from satellite data and ground measurements was generally in good agreement without bias (Fig. A4.6 in the appendix), indicating that the uncertainty in NDVI values is relatively low. With an R^2 of 0.58, the relationship was slightly stronger and showed similar noise compared with the findings of Hmimina et al. (2013) for savannah ($R^2 = 0.45$) and crops ($R^2 = 0.56$) when comparing ground with MODIS NDVI, while they found a R^2 of 0.91 for deciduous forest. Despite using high-resolution (5 x 5 m^2) satellite images in the present study, the SE of 0.08 indicates considerable noise at both intensive and extensive meadows. This can partly be explained due to heterogeneity in the vegetation patches: ground-measured NDVI varied within a vegetation patch each day, on average, by a standard deviation of 0.03 (Table 7). Further uncertainty results from time gaps between ground and satellite measurements. Noise resulting from sensors, sensor angle and elevation, sun angle, background reflection and atmosphere are discussed elsewhere (e.g. Adam et al., 2010 and references therein).

Table 7. Standard deviations from mean values measured at sites and vegetation patches.

	Average	Max
Ground LAI at vegetation patches and sites	0.51	2.98
Ground NDVI at vegetation patches and sites	0.03	0.18
Satellite NDVI at vegetation patches	0.02	0.12
PP at sites [mg CO_2-C m^{-2} h^{-1}]	1.47	8.09
Biomass at vegetation patches [kg m^{-2}]	0.83	2.39
Green:brown ratio at vegetation patches	0.08	0.34

3.6.7 Uncertainty in PAI

When vegetation height and density was low, the PAI probe was not fully covered with vegetation. Therefore, measurement results strongly differ according to the quantity of leaves shadowing the ceptometer, which depends on solar zenith angle and plant architecture. During spring emergence and especially after harvest, the assumption of a random spherical distribution of leaves might have led to underestimated PAI values. Further, leaf angle and plant architecture can vary considerably between different wet grassland communities (Fliervoet and Werger, 1984). Heterogeneity within the vegetation patches deviated in PAI, on average, by 0.51 m^2 m^{-2} (Table 7). If tussock sedges were present, the soil surface was especially uneven, which could lead to considerable underestimation of PAI if the probe rested on a high point. The uncertainty resulting from the optical measurement method due to clumping, leaf orientation, plant architecture, leaf size and sun angle (e.g. Breda, 2003) is reflected in the noise when ceptometer-based PAI is compared with the more direct method of scanning leaf area (data not shown), which resulted in a rather high SE of 1.65 m^2 m^{-2} and an R^2 value of 0.46.

3.6.8 Conclusions of vegetation indices as proxies (study III)

Almost all investigated relationships differed depending on land-use intensity and they showed large scatter. Thus, on temperate grassland fens, the application of NDVI as a proxy for LAI, biomass, or green-ratio as well as PAI and GAI as proxies for biomass or PP is characterised by high uncertainty and should be performed under consideration of management

intensity. This is especially true for less frequently harvested meadows containing high amounts of brown plant material. Still, optical indices are non-destructive measurement methods that can be automated and are available from satellite images on a global scale. Due to the discovered high uncertainty, it is strongly recommended to perform additional direct measurements of the variable of interest to correct and validate the estimations, especially on extensively managed grasslands and throughout the year. The relationship between NDVI and photosynthesis potential was management-independent and showed hardly any saturation effects. Therefore, assimilation models using LAI as an input parameter might consider incorporating NDVI instead.

4 General discussion

The overall aim of this thesis was to increase understanding in carbon related processes for model improvements and reduced uncertainty in model predictions on peatlands. Thereby, the suggested model improvements did not only include the implementation of new or changed functionalities and the usage of different underlying model equations, but also model configuration, parameter constraint and the identification of sensitive parameters, their equifinalities and their possible dependencies on measurable factors. Further, they include the identification of valuable available and additional required observation variables, that will allow better parameter constrain and resolving equifinalities and thereby contribute to better process understanding. LAI, an especially influential variable, also for empiric modelling (Reichstein et al., 2003), was tested together with other vegetation characteristics to be estimated from remote sensing and optical measurements. The investigated relationships are not only interesting for modelling CO_2, but also for e.g. estimations of yield or productivity in a non-destructive way.

Some of the model improvements suggested in study I were already incorporated and tested in study II. Most of the parameter constraints from study II confirmed the results from study I and several of the suggested model advancements as well as parameter dependencies to measureable factors were also supported by the results of study II. This encourages future applications of the constrained model to many further sites, to be able to establish dependency curves between parameter values and their identified possible proxies. The suggested model improvements are relevant for also other CO_2 models applied to peatlands, as they are often based on the same or similar underlying equations. The most important parameters for different processes were identified, whereby not only the direct sensitivity of a parameter on model performance was accounted for, but also how well a parameter can be constrained by the available data, whether the constraint is site-specific, and the existence and intensity of parameter interactions. Knowing the key parameters for a certain process is valuable information for the setup of future model calibrations, as a limited number of parameters mean lower requirements on the number of calibration runs and fewer equifinalities, allowing faster computation and simpler analysis methods. In addition, this information describes where the largest uncertainties are located when using a model for predictions. For experimentalists, the identified key parameters point out needs for further research and additional measurements.

4.1   Soil temperature, temperature response

Several results in respect to soil temperature simulation and temperature response of study I, were confirmed by study II. As hypothesised in study I, the inclusion of a separate moss layer in study II largely improved soil temperature dynamics of the upper soil layers, while the effect on photosynthesis dynamics was minor. The calibrated mean temperature defining soil temperature at the lower soil profile boundary of study II was at the higher end of the range reported in study I, supporting the supposed connection to snow cover at this high latitude site.

The seasonal dependence of temperature response parameter was suspected to be resolvable by using a more sophisticated temperature response function than the simple Q10 approach. This was confirmed by study II where the Ratkowsky function (Ratkowsky et al., 1982) was used for heterotrophic respiration, independently of the temperature response for the plant, which improved model performance in NEE. Temperature response interacted with the highly influential respiration coefficients of SOC pools. Large uncertainty was remaining in valid parameter ranges, due to many equifinalities, limited information about the soil and lacking process understanding. The usage of the best temperature response curve is controversial discussed (Kirschbaum, 2006) as well as the usage of different temperature responses for different SOC pools (Fang et al., 2005).

4.2   SOC pools and decomposition rates

The partitioning of SOC between pools, which is directly connected to respiration rate coefficients, is still an open issue. Despite the availability of detailed and long term CO_2 flux data as well as SOC and C:N in the different soil horizons, site-specific differences, equifinalities and many interactions with other biotic and abiotic processes, as identified in study I and II, hindered the constrain of pool sizes and decomposition rates. Various different fractionating and partitioning methods have been developed for mineral soils, but do not correspond to specific stabilisation mechanisms and hence do not describe functional SOC pools (Lützow et al., 2007). Further, their applicability to peat soils is questionable, as at least the physical methods are based on complexes between mineral and organic compounds. The site-specific differences found in study I and confirmed by study II need to be related to proxies like land-use history, vegetation or soil data that is available on a global scale. Therefore, further model applications to many more sites are required.

A number of open issues for future experimental and modelling research are remaining in the context of decomposition rates, SOC pools as well as the response to soil temperature and soil moisture.

4.3 Winter and spring fluxes

The problems of accurately simulating the spring CO_2 emission peak at Lom in study I was repeated at Deg in study II and is therefore independent of whether the Q10 or the Ratkowsky function was used as temperature response. Instead, as already assumed in study I, snow and ice coverage might play an important role. Such spring time emission peaks can be seen in NEE time series plots at other treeless wetlands in northern latitudes (Aurela, 2004; Oechel et al., 2000), while they are lacking at sites in the temperate region (Chojnicki et al., 2012; Carroll and Crill, 1997). Despite that spring and winter emissions make only a relatively small proportion of the annual balance, these periods are of special interest as they are expected to be highly affected by climate change. Therefore, further research of this phenomenon is needed. This requires model ability of correctly representing of winter fluxes, which was also not given on sites with only short snow cover as shown in study I. It need to be tested, if an implementation of redox potential dependencies can reduce the overestimation of winter fluxes on the sites with low snow cover which had a continuously high water table during winter. The ECOSSE model has incorporated such a dependency by including the duration of saturated conditions in the soil moisture response (Smith et al., 2010), which should be tested for the CoupModel as well. Due to the relatively small NEE values during winter time the dynamics and corresponding processes are often hardly visible in indices of model performance. It is therefore recommended to include exclusively winter time fluxes as additional calibration and validation variable in future CO_2 modelling studies.

4.4 Plant C balance, C storage and litter fall

Results in respect to plant carbon household related parameters disagreed between study I and II, indicating the requirement of model calibration and validation at many more sites.

Especially, storing C reserves during litter fall and the initiation of senescence need to be further investigated by experiments and modelling. The parameterisation for C uptake versus losses in study II strongly derivate from the common configuration applicable in study I, indicating that the plants at the very nutrient poor site in study II were much more efficient in building biomass and storing C with relatively little assimilates compared to

plants from the more nutrient rich sites in study I. This was the case, despite the latitudes of the sites in study I ranged from 48°N (South Germany) to 68°N (North Finland) and the vegetation differed largely. It means that a common parameterisation giving good results at five different open peatland sites, still might need site specific adaption at another open peatland site, implying that model applications at many more sites are required. The total number of performed peatland modelling studies might be high; however, many different models, modified models, different calibration setup and different performance measures were used. As shown in study II, model results are only partly transferable if the models derivate in these factors. This implies the need for using the same model in the same configuration and calibration setup at many sites and comparing the results between the sites. In a second step, comparisons should be done with other models which might have been run on the same sites.

The site-specific differences found in study I in the proportion of C stored during litterfall for regrowth in spring was expected to be caused by cutting, species specific adaptations to growing season length and green overwintering plant parts. The very high value found for Deg in study II supports these explanations, as *Eriophorum vaginatum*, the dominating vascular plant at Deg has highly efficient remobilization from senescing leaves (Jonasson and Chapin III, 1985; Shaver and Laundre, 1997) and evergreen mosses play an important role at this site which is also characterized by a short vegetation period length and not harvested. Thus, further model applications to different vegetation communities and to further sites dominated by *Eriophorum vaginatum* and mosses are needed to confirm this hypothesis.

Data on litter fall in combination with LAI or biomass could be helpful in resolving equifinalities and further constrain of C household related parameters and for investigating dependencies on the vegetation community. Litter fall of above-ground biomass is often measured on forest sites, but usually not on treeless sites, where dead plant material might remain attached to the living plant until it is decomposed.

In study I and II, initiation of leaf senescence and therefore initiation of increased litter fall rates were found to be stronger related to the day of the year than to temperature sums or thresholds. However, a combination of these factors might lead to even better dynamics and explanations for site and year specific deviations. As supported by study III, high resolution NDVI time series have a high potential to further investigate leaf senescence patters between different latitudes and different vegetation types. A coupling of NDVI with process-oriented modelling will probably help in parameter constrain and resolving equifinalities.

4.5   Regrowth after cut

At the sites FsA and FsB, preparatory study results showed a delay in regrowth and reach measured LAI and C uptake values after cut. Wu and McGechan (1997) reported difficulties in a previous version of the model in reaching measured biomass values after cut. Therefore, a new option was implemented, resetting of the growth stage after cut to a lower value, to avoid immediate litter fall of the new developed leaves (e.g. Thomas and Stoddart, 1980) and reallocating C from the root pool to leaves like reported in laboratory results for e.g. *Festuca pratensis* (Johansson, 1992 and 1993). To calibrate this function, measurements shortly before and after the cutting event is required. This data was not available at the tested manual chamber sites. Best would be a time series of high resolution measurements as offered by automatic chambers or the EC method. However, many of the existing EC sites on mown grasslands span over several parcels with different cutting dates or are mixed with grassing management and are therefore less suitable for this purpose. Further, calibration on fertile and frequently cut mineral soils might not lead to a good estimate for the corresponding parameters on peat meadows, as species are known to largely differ in their mowing tolerance and ability to regrow after cut (Briemle and Ellenberg, 1994). Additional experimental data is required to accurately calibrate this functionality and further research is needed to investigate the connection with the C storage used for regrowth in spring. High resolution time series of LAI or biomass can provide valuable information for further investigations on both, regrowth after cut and during leafing-out in spring.

4.6   LAI and modelling

In study I, the proportion for remobilization during litter fall for regrowth in the next spring as well as for the photosynthetic efficiency could be fitted to measured LAI or biomass time series. Therefore, it would be of high interest for upscaling issues to derive these parameters from satellite data. Unfortunately the results from using NDVI as proxy for LAI or biomass and LAI as proxy for biomass or photosynthesis were not satisfactory in the Freisinger Moos due to the high amount of standing brown biomass. This will probably hinder such derivations on other peatlands as well, especially if biomass quantities are high. In contrast to LAI, NDVI showed stronger and simpler connections to photosynthesis. The incorporation of NDVI as input to process-oriented models is therefore promising and should be tested in future research. This might be also true for other vegetation indices that can be directly calculated from satellite data like the enhanced vegetation index (EVI, Schubert et al., 2010) or the MERIS terrestrial chlorophyll index (MTCI, Harris and Dash, 2011).

For the site Deg in study II, fitting the photosynthetic efficiency parameter to LAI by using the common parameters from the sites of study I, would lead to much overestimated photosynthesis, even if a high value for the remobilization fraction would be chosen. This was probably related to its vegetation community: the dominating vegetation at the poor fen Deg consisted of mosses, which are evergreen and *Eriophorum vaginatum* which is highly efficient in retaining C (Jonasson and Chapin III, 1985; Shaver and Laundre, 1997). The vegetation of the sites of study I consisted mainly of sedges, grasses, dwarf-shrubs and herbs in different proportions. These plants seem therefore less efficient in building biomass with only little amount of assimilates. This implies that derivation of photosynthetic efficiency from LAI can only work, if further information about the vegetation community would be available and considered. Much more model applications to sites with different vegetation communities need to be performed and compared to find reliable connections and derivate corresponding parameter sets for each community. Further it would be interesting to test if using NDVI instead of LAI for fitting photosynthetic efficiency is less dependent on the vegetation community. Leaf area index is not only important for photosynthesis, but also for temperature insulation and transpiration. This information might be estimated from e.g. vegetation type which can be derived from satellite data time series (Gardi et al., 2009; Joosten and Couwenberg, 2009).

4.7   Scope and limitations

Carbondioxid is an important GHG, emitted from peatlands. Further, emissions of methane (CH_4) and nitrous oxide (N_2O) need to be considered in management practices and restoration practices, especially on sites with high water level (CH_4) or fertilisation management and water table fluctuations (N_2O). However, the investigation of these gases and related processes lay outside the scope of this thesis. Even that they are 28 (CH_4) and 265 (N_2O) times more harmful than CO_2 (Myhre et al., 2013) the global warming potential from peatlands is strongly correlated to their net C balance (Drösler et al., 2008) and on drained peatlands clearly dominated by CO_2 fluxes (Drösler et al., 2013b). Especially CH_4 emissions are closely linked to CO_2 (Bellisario, L. M. et al., 1999; Panikov and Dedysh, 2000). Therefore, a reasonable representation of CO_2 is a precondition for CH_4 modelling which can be investigated in the second step.

4.8   Conclusions

Using process-oriented modelling was shown to be a useful tool to identify and explain differences in measured CO_2 balances between different peatland sites, which leads to increased process understanding and is a precondition for predictive modelling. By applying the model, several phenomena could be explained, many open issues for further research were identified and several model improvements suggested.

Especially in study I, several parameters could be constrained to a more narrow range and several interactions and equifinalities were identified and described in study I and II, which will be helpful information for designing future calibrations. Study II revealed that resulting parameter ranges do not only depend on the tested range, but also on the calibration variables, performance indices, model components, processes and parameters accounted for in a calibration. This implies that parameter ranges are only partly transferable between models differing in their structure or calibration setup.

A number of processes and their parameters were tested for sensitivity and site dependence and several possible proxies for site-specific parameters were proposed. This is valuable information for up scaling and model predictions. Future research should investigate the proposed connections between parameters and proxies at many more sites to develop reliable relationships and test the generality of the results for peatland CO_2 modelling.

NDVI, which is derivable from satellite images, was tested as proxy for LAI and LAI as proxy for biomass and photosynthesis on productive temperate fen meadows. However, such applications were shown to go along with high uncertainty due to the high amount of standing brown biomass. The results suggested that incorporating NDVI instead of LAI as either input or calibration variable is much more promising for modelling CO_2 fluxes on peatlands.

All available measurement variables were shown to be helpful in model constrain and further additional information was identified which was not available at the tested sites, but would be highly useful for better model constrain and reducing uncertainty in model predictions.

The results of this thesis contain therefore valuable information for peatland modellers and experimentalists, regarding the design of model calibrations, further model development, improved parameterisation, up scaling requirements and limitations as well as measurement setup.

5 Acknowledgements

Further I would like to thank the co-authors of paper I and II for providing me all the data which I used for running and evaluating the model and the support I got from my coauthors in technical understanding of the data and measurement methods, showing me the sites, replying to all my site-specific questions and giving helpful comments to the manuscript. I would also like to thank my colleague Christoph Förster who helped me a lot in interpreting the data from the Freisinger Moos used in paper I.

Many thanks to the co-authors of paper III, who provided me the GPP_{2000} values and gave helpful comments to the manuscript. I like to thank many students, in particular Janna Feigen, Silvia Burgmeier and Barbara Dennerlein whom I supervised in their project work in the frame of the TUM-Kolleg respectively their master programme at TUM. They helped me a lot with the data sampling and partly with the data processing.

I am grateful for my colleagues and fellow PhD students at TUM, HSWT and KTH for fruitful discussions, sharing "ups" and "downs" during our doctoral programmes, a nice working atmosphere and friendship. Last but not least, I would like to thank my husband and my mother for their patience during all my absences, first in Freising, later in Stockholm.

6   References

Abdalla, M., Hastings, A., Bell, M. J., Smith, J. U., Richards, M., Nilsson, M. B., Peichl, M., Löfvenius, M. O., Lund, M., Helfter, C., Nemitz, E., Sutton, M. A., Aurela, M., Lohila, A., Laurila, T., Dolman, A. J., Belelli-Marchesini, L., Pogson, M., Jones, E., Drewer, J., Drosler, M., and Smith, P.: Simulation of CO2 and Attribution Analysis at Six European Peatland Sites Using the ECOSSE Model, Water Air Soil Pollut, 225, 1–14, doi:10.1007/s11270-014-2182-8, 2014.

Adam, E., Mutanga, O., and Rugege, D.: Multispectral and hyperspectral remote sensing for identification and mapping of wetland vegetation: A review, Wetlands Ecology and Management, 18, 281–296, doi:10.1007/s11273-009-9169-z, 2010.

Aerts, R. and Toet, S.: Nutritional controls on carbon dioxide and methane emission from Carex-dominated peat soils, Soil Biology and Biochemistry, 29, 1683–1690, doi:10.1016/S0038-0717(97)00073-4, 1997.

Anderson, J. E.: Spectral Signatures Of Wetlands Plants, Technical report, U.S. Army Corps of Engineers Topographic Engineering Center, Alexandria, Virgina, U.S. 6 pp., 1995.

Armstrong, W.: Aeration in Higher Plants, Advances in Botanical Research, 7, 225–332, doi:10.1016/s0065-2296(08)60089-0, 1980.

Atkin, O. K., Bruhn, D., Hurry, V. M., and Tjoelker, M. G.: Evans Review No. 2: The hot and the cold: unravelling the variable response of plant respiration to temperature, Functional Plant Biology, 32, 87–105, doi:10.1071/FP03176, 2005.

Atkin, O. K., Tjoelker, M. G., and Atkin, O.: Thermal acclimation and the dynamic response of plant respiration to temperature, Trends in Plant Science, 8, 343–351, doi:10.1016/s1360-1385(03)00136-5, 2003.

Aurela, M.: The timing of snow melt controls the annual CO 2 balance in a subarctic fen, Geophys. Res. Lett., 31, doi:10.1029/2004GL020315, 2004.

Aurela, M., Lohila, A., Tuovinen, J.-P., Hatakka, Juha Riutta Terhi, and Laurila, T.: Carbon dioxide exchange on a northern boreal fen, Boreal environment research, 14, 699–710, 2009.

Baldocchi, D. D., Hincks, B. B., and Meyers, T. P.: Measuring Biosphere-Atmosphere Exchanges of Biologically Related Gases with Micrometeorological Methods, Ecology, 69, 1331, doi:10.2307/1941631, 1988.

Bauer, D. F.: Constructing Confidence Sets Using Rank Statistics, Journal of the American Statistical Association, 67, 687–690, doi:10.2307/2284469, 1972.

References

Bazin, M. J. and Prosser, J. I.: Physiological models in microbiology, CRC series in mathematical models in microbiology, CRC Press, Boca Raton, Fla., 2 volumes, 1988.

Bell, G. E., Howell, B. M., Johnson, G. V., Raun, W. R., Solie, J. B., and Stone, M. L.: Optical Sensing of Turfgrass Chlorophyll Content and Tissue Nitrogen, HortScience, 39, 1130–1132, 2004.

Bellisario, L. M., Bubier, J. L., Moore, T. R., and Chanton, J. P.: Controls on CH4 emissions from a northern peatland, Global Biogeochem. Cycles, 13, 81–91, 1999.

Bergman, I., Lundberg, P., and Nilsson, M.: Microbial carbon mineralisation in an acid surface peat: effects of environmental factors in laboratory incubations, Soil Biology and Biochemistry, 31, 1867–1877, doi:10.1016/s0038-0717(99)00117-0, 1999.

Beven, K. and Freer, J.: Equifinality, data assimilation, and uncertainty estimation in mechanistic modelling of complex environmental systems using the GLUE methodology, Journal of Hydrology, 249, 11–29, doi:10.1016/s0022-1694(01)00421-8, 2001.

BMUB, Nationale Klimapolitik des Bundesministeriums für Umwelt, Naturschutz, Bau und Reaktorsicherheit, http://www.bmub.bund.de/themen/klima-energie/klimaschutz/nationale-klimapolitik/, last access: 17 December 2015

Boelman, N., Stieglitz, M., Rueth, H., Sommerkorn, M., Griffin, K., Shaver, G., and Gamon, J. A.: Response of NDVI, biomass, and ecosystem gas exchange to long-term warming and fertilization in wet sedge tundra, Oecologia, 135, 414–421, doi:10.1007/s00442-003-1198-3, 2003.

Bonan, G. B.: Importance of leaf area index and forest type when estimating photosynthesis in boreal forests, Remote Sensing of Environment, 43, 303–314, doi:10.1016/0034-4257(93)90072-6, 1993.

Bragazza, L., Freeman, C., Jones, T., Rydin, H., Limpens, J., Fenner, N., Ellis, T., Gerdol, R., Hájek, M., Tomáš, H., Lacumin, P., Kutnar, L., Tahvanainen, T., and Toberman, H.: Atmospheric nitrogen deposition promotes carbon loss from peat bogs, PNAS, 103, 19386–19389, 2006.

Breda, N. J. J.: Ground-based measurements of leaf area index: A review of methods, instruments and current controversies, Journal of Experimental Botany, 54, 2403–2417, doi:10.1093/jxb/erg263, 2003.

Briemle, G. and Ellenberg, H.: Zur Mahdverträglichkeit von Grünlandpflanzen. – Natur und Landschaft 69. Jg. H.4: 139-147, Natur und Landschaft, 69, 139–147, 1994.

Brooks, R. H. and Corey, A. T.: Hydraulic Properties of Porous Media, Colorado State University, Fort Collins, Colorado, US, Hydrology Paper No. 3, 03, 27 pp.

Bubier, J., Crill, P., and Mosedale, A.: Net ecosystem CO2 exchange measured by autochambers during the snow-covered season at a temperate peatland, Hydrological processes, 16, 3667–3682, 2002.

Byrne, K. A., Chojnicki, B., Christensen, T. R., Drösler, M., Freibauer, A., Friborg, T., Frolking, S., Lindroth, A., Mailhammer, J., and Malmer, N.: EU peatlands: Current carbon stocks and trace gas fluxes, Concerted Action–Synthesis of the European Greenhouse Gas Budget, Report, 1–58, 2004.

Carroll, P. and Crill, P.: Carbon balance of a temperate poor fen, Global Biogeochemical Cycles, 11, 349–356, 1997.

Carvalhais, N., Reichstein, M., Ciais, P., Collatz, G. James, Mahecha, M. D., Montagnani, L., Papale, D., Rambal, S., and Seixas, J.: Identification of vegetation and soil carbon pools out of equilibrium in a process model via eddy covariance and biometric constraints, Glob Change Biol, 16, 2813–2829, doi:10.1111/j.1365-2486.2010.02173.x, 2010.

Chojnicki, B. H., Michalak, M., Acosta, M., Juszczak, R., Augustin, J., Drösler, M., and Olejnik, J.: Measurements of Carbon Dioxide Fluxes by Chamber Method at the Rzecin Wetland Ecosystem, Poland, Polish J. of Environ. Stud., 19, 283–291, 2010.

Chojnicki, B. H., Michalak, M., Konieczna, N., and Olejnik, J.: Sedge community (Caricetum elatae) carbon dioxide exchange seasonal parameters in a wetland, Polish Journal of Environmental Studies, 21, 579–587, 2012.

Clymo, R. S.: The Growth of Sphagnum: Some Effects of Environment, Journal of Ecology, 61, 849–869, doi:10.2307/2258654, 1973.

Clymo, R. S.: The Limits to Peat Bog Growth, Royal Society Publishing, 303, 605–654, 1984.

Clymo, R. S. and Hayward, P. M.: The Ecology of Sphagnum, in: Bryophyte Ecology, Smith, A. J. E. (Ed.), Springer Netherlands, 229–289, 1982.

Conant, R. T., Drijber, R. A., Haddix, M. L., Parton, W. J., Paul, E. A., Plante, A. F., Six, J., and Steinweg, J. M.: Sensitivity of organic matter decomposition to warming varies with its quality, Glob Change Biol, 14, 868–877, doi:10.1111/j.1365-2486.2008.01541.x, 2008.

Cowling, S. A. and Field, C. B.: Environmental control of leaf area production: Implications for vegetation and land-surface modeling, Global Biogeochem. Cycles, 17, 7-1–7-14, doi:10.1029/2002gb001915, 2003.

CoupModel, Current version of COUP model for download, available at the model homepage: "http://www.coupmodel.com", last accessed: 20 October 2015

Cramer, W., Bondeau, A., Woodward, I. F., Prentice, C. I., Betts, R. A., Brovkin, V., Cox, P. M., Fisher, V., Foley, J. A., Friend, A. D., Kucharik,

References

C., Lomas, M., Ramankutty, N., Sitch, S., Smith, B., White, A., and Young-Molling, C.: Global response of terrestrial ecosystem structure and function to CO2 and climate change: results from six dynamic global vegetation models, Glob Change Biol, 7, 357–373, 2001.

Cui, J., Li, C., and Trettin, C. C.: Analyzing the ecosystem carbon and hydrologic characteristics of forested wetland using a biogeochemical process model, Glob Change Biol, 11, 278–289, doi:10.1111/j.1365-2486.2005.00900.x, 2005.

Darvishzadeh, R., Skidmore, A., Atzberger, C., and van Wieren, S.: Estimation of vegetation LAI from hyperspectral reflectance data: Effects of soil type and plant architecture, International Journal of Applied Earth Observation and Geoinformation, 10, 358–373, doi:10.1016/j.jag.2008.02.005, 2008.

Davidson, E. A., Janssens, I. A., and Luo, Y.: On the variability of respiration in terrestrial ecosystems: moving beyond Q10, Glob Change Biol, 12, 154–164, doi:10.1111/j.1365-2486.2005.01065.x, 2006.

Davidson, H. R. and Campbell, C. A.: The effect of temperature, moisture and nitrogen on the rate of development of spring wheat as measured by degree days, Canadian journal of plant science, 63, 833–846, 1983.

Davies, A.: The Regrowth of Grass Swards, in: The Grass Crop, Jones, M. B., Lazenby, A. (Eds.), The Grass Crop, Chapman and Hall, London, UK, 85–127, 1988.

De Vries, F. W. T. P.: The Cost of Maintenance Processes in Plant Cells, Annals of Botany, 39, 77–92, 1975.

Del Grosso, S. J, Mosier, A. R., Parton, W. J., and Ojima, D. S.: DAYCENT model analysis of past and contemporary soil NO and net greenhouse gas flux for major crops in the USA, Soil and Tillage Research, 83, 9–24, doi:10.1016/j.still.2005.02.007, 2005.

DeLaune, R. D., Reddy, C. N., and Patrick Jr, W. H.: Organic matter decomposition in soil as influenced by pH and redox conditions, Soil Biology and Biochemistry, 13, 533–534, 1981.

Dettmann, U., Bechtold, M., Frahm, E., and Tiemeyer, B.: On the applicability of unimodal and bimodal van Genuchten–Mualem based models to peat and other organic soils under evaporation conditions, Journal of Hydrology, 515, 103–115, doi:10.1016/j.jhydrol.2014.04.047, 2014.

Dimitrov, D. D., Grant, R. F., Lafleur, P. M., and Humphreys, E. R.: Modeling the effects of hydrology on ecosystem respiration at Mer Bleue bog, Journal of Geophysical Research: Planets, 115, 2010.

Dinsmore, K. J., Billett, M. F., Skiba, U. M., Rees, R. M., Drewer, J., and Helfter, C.: Role of the aquatic pathway in the carbon and greenhouse gas

budgets of a peatland catchment, Glob Change Biol, 16, 2750–2762, doi:10.1111/j.1365-2486.2009.02119.x, 2010.

Doiron, M., Legagneux, P., Gauthier, G., Lévesque, E., and Henebry, G.: Broad-scale satellite Normalized Difference Vegetation Index data predict plant biomass and peak date of nitrogen concentration in Arctic tundra vegetation, Applied Vegetation Science, 16, 343–351, doi:10.1111/j.1654-109X.2012.01219.x, 2013.

Drewer, J., Lohila, A., Aurela, M., Laurila, T., Minkkinen, K., Penttilä, T., Dinsmore, K. J., McKenzie, R. M., Helfter, C., Flechard, C., Sutton, M. A., and Skiba, U. M.: Comparison of greenhouse gas fluxes and nitrogen budgets from an ombotrophic bog in Scotland and a minerotrophic sedge fen in Finland, European Journal of Soil Science, 61, 640–650, doi:10.1111/j.1365-2389.2010.01267.x, 2010.

Drösler, M., Adelmann, W., Augustin, J., Bergman, L., Beyer, C., Chojnicki, B. H., Förster, C., Freibauer, A., Giebels, M., Görlitz, S., Höper, H., Kantelhardt, J., Liebersbach, H., Hahn-Schöfl, M., Minke, M., Petschow, U., Pfadenhauer, J., Schaller, L., Schägner, P., Sommer, M., Thuille, A., and Wehrhan, M.: Klimaschutz durch Moorschutz. Schlussbericht des BMBF-Vorhabens: Klimaschutz-Moornutzungsstrategien 2006-2010, TIB/UB-Hannover, Hannover, Germany, 201 pp., 2013a.

Drösler, M., Freibauer, A., Christensen, T. R., and Friborg, T.: Observations and Status of Peatland Greenhouse Gas Emissions in Europe, in: The continental-scale greenhouse gas balance of Europe, Dolman, A. J., Freibauer, A., Valentini, R. (Eds.), Ecological studies, 203, Springer, New York, 243–261, 2008.

Drösler, M., Verchot, L. V., Freibauer, A., Pan, G., Evans, C. D., Bourbonniere, R. A., Alm, J. P., Page, S., Agus, F., Hergoualch, K., Couwenberg, J., Jauhiainen, J., Sabiham, S., Wang, C., Srivastava, N., Borgeau-Chavez, L., Hooijer, A., Minkkinen, K., French, N., Strand, T., Sirin, A., Mickler, R., Tansey, K., and Larkin, N.: Drained Inland Organic Soils (chapter 2), in: 2013 Supplement to the 2006 IPCC Guidelines for National Greenhouse Gas Inventories: Wetlands, Methodological Guidance on Lands with Wet and Drained Soils, and Constructed Wetlands for Wastewater Treatment, Hiraishi, T., Krug, T., Tanabe, K., Srivastava, N., Jamsranjav, B., Fukuda, M., Troxler, T. (Eds.), IPCC, Switzerland, 2.1-2.76, 2013b.

Eickenscheidt, T., Heinichen, J., and Drösler, M.: The greenhouse gas balance of a drained fen peatland is mainly controlled by land-use rather than soil organic carbon content, Biogeosciences, 12, 5161–5184, doi:10.5194/bg-12-5161-2015, 2015.

Elatawneh, A., Rappl, A., Rehush, N., Schneider, T., and Knoke, T.: Forest tree species communities identification using multi phenological stages

References

RapidEye data: Case study in the forest of Freising, in: From the Basics to the Service, Borg, E. Daedelow, H., Johnson, R. (Ed.), GITO Verlag, Berlin, Germany, 21–38, 2013.

Falge, E., Baldocchi, D., Olson, R., Anthoni, P., Aubinet, M., Bernhofer, C., Burba, G., Ceulemans, R., Clement, R., Dolman, H., Granier, A., Gross, P., Grünwald, T., Hollinger, D. Y., Jensen, N.-O., Katul, G., Keronen, P., Kowalski, A., Lai, C. T., Law, B. E., Meyers, T., Moncrieff, J., Moors, E., Munger, W. J., Pilegaard, K., Rannik, Ü., Rebmann, C., Suyker, A., Tenhunen, J., Tu, K., Verma, S., Vesala, T., Wilson, K., and Wofsy, S.: Gap filling strategies for defensible annual sums of net ecosystem exchange, Agricultural and Forest Meteorology, 107, 43–69, doi:10.1016/s0168-1923(00)00225-2, 2001.

Fan, L., Gao, Y., Brück, H., and Bernhofer, C.: Investigating the relationship between NDVI and LAI in semi-arid grassland in Inner Mongolia using in-situ measurements, Theor Appl Climatol, 95, 151–156, doi:10.1007/s00704-007-0369-2, 2009.

Fang, C. and Moncrieff, J. B.: The variation of soil microbial respiration with depth in relation to soil carbon composition, Plant Soil, 268, 243–253, doi:10.1007/s11104-004-0278-4, 2005.

Fang, C., Smith, P., Moncrieff, J. B., and Smith, J. U.: Similar response of labile and resistant soil organic matter pools to changes in temperature, Nature, 433, 57–59, doi:10.1038/nature03138, 2005.

Farquhar, G. D., Caemmerer, S. v., and Berry, J. A.: Models of photosynthesis, Plant Physiology, 125, 42–45, 2001.

Farquhar, G. D., von Caemmerer, S. v., and Berry, J. A.: A biochemical model of photosynthetic CO2 assimilation in leaves of C3 species, Planta, 149, 78–90, 1980.

Feng, L., Rui, S., Tinglong, Z., Bo, H., and Tang, Y.: Simulation of carbon dioxide fluxes in agroecosystems based on BIOME-BGC model, Vancouver, BC; Canada, IEEE, 3327–3329, 2011.

Fliervoet, L. M. and Werger, M. J. A.: Canopy structure and microclimate of two wet grassland communities, New Phytologist, 96, 115–130, doi:10.1111/j.1469-8137.1984.tb03548.x, 1984.

Fontaine, S., Barot, S., Barré, P., Bdioui, N., Mary, B., and Rumpel, C.: Stability of organic carbon in deep soil layers controlled by fresh carbon supply, Nature, 450, 277–280, doi:10.1038/nature06275, 2007.

Franko, U., Crocker, G. J., Grace, P. R., Klír, J., Körschens, M., Poulton, P. R., and Richter, D. D.: Simulating trends in soil organic carbon in long-term experiments using the CANDY model, Geoderma, 81, 109–120, doi:10.1016/s0016-7061(97)00084-0, 1997.

Frolking, S. E., Roulet, N. T., Moore, T. R., Richard, P. J. H., Lavoie, M., and Muller, S. D.: Modeling Northern Peatland Decomposition and Peat

Accumulation, Ecosystems, 4, 479–498, doi:10.1007/s10021-001-0105-1, 2001.

Frolking, S. E., Roulet, N. T., Moore, T. R., Lafleur, P. M., Bubier, J. L., and Crill, P. M.: Modeling seasonal to annual carbon balance of Mer Bleue Bog, Ontario, Canada, Global Biogeochem. Cycles, 16, 4-1–4-21, doi:10.1029/2001gb001457, 2002.

Frolking, S. E., Roulet, N. T., Tuittila, E., Bubier, J. L., Quillet, A., Talbot, J., and Richard, Pierre J. H.: A new model of Holocene peatland net primary production, decomposition, water balance, and peat accumulation, Earth System Dynamics, 1, 1–21, doi:10.5194/esd-1-1-2010, 2010.

Fulkerson, W. J. and Donaghy, D. J.: Plant-soluble carbohydrate reserves and senescence-key criteria for developing an effective grazing management system for ryegrass-based pastures: A review, Animal Production Science, 41, 261–275, 2001.

Gaberščik, A. and Martinčič, A.: Seasonal Dynamics of Net Photosynthesis and Productivity of Sphagnum papillosum, Lindbergia, 13, 105–110, doi:10.2307/20149626, 1987.

Gáborčík, N.: Relationship between Contents of Chlorophyll (a+b) (SPAD values) and Nitrogen of Some Temperate Grasses, Photosynthetica, 41, 285–287, doi:10.1023/B:PHOT.0000011963.43628.15, 2003.

Gamon, J. A., Field, C. B., Goulden, M. L., Griffin, K. L., Hartley, A. E., Joel, G., Penuelas, J., and Valentini, R.: Relationships between NDVI, canopy structure, and photosynthesis in three Californian vegetation types, Ecological Applications, 5, 28–41, 1995.

Gamon, J. A., Serrano, L., and Surfus, J. S.: The photochemical reflectance index: an optical indicator of photosynthetic radiation use efficiency across species, functional types, and nutrient levels: An optical indicator of photosynthetic radiation use efficiency across species, functional types, and nutrient levels, Oecologia, 112, 492–501, 1997.

Gardi, C., Sommer, S., Seep, K., and Montanarella, L.: Estimate of Peatland Distributuion in Estonia Using an Integrated GIS/RS Approach, in: Proceedings of the 33rd International Symposium on Remote Sensing of Environment, Stresa, Italy, 2009.

Gianelle, D. and Vescovo, L.: Determination of green herbage ratio in grasslands using spectral reflectance. Methods and ground measurements, International Journal of Remote Sensing, 28, 931–942, doi:10.1080/01431160500196398, 2007.

Gianelle, D., Vescovo, L., Marcolla, B., Manca, G., and Cescatti, A.: Ecosystem carbon fluxes and canopy spectral reflectance of a mountain meadow, International Journal of Remote Sensing, 30, 435–449, doi:10.1080/01431160802314855, 2009.

References

Gitelson, A. A.: Wide Dynamic Range Vegetation Index for Remote Quantification of Biophysical Characteristics of Vegetation, Journal of Plant Physiology, 161, 165–173, doi:10.1078/0176-1617-01176, 2004.

Glatzel, S., Stephan, Basiliko, N., and Moore, T. R.: Carbon dioxide and methane production protentials of peats from natural, harvested and restored sites, Easten Québec, Canada, Wetlands, 24, 261–267, 2004.

Gong, J., Kellomäki, S., Wang, K., Zhang, C., Shurpali, N., and Martikainen, P. J.: Modeling CO_2 and CH_4 flux changes in pristine peatlands of Finland under changing climate conditions, Ecological Modelling, 263, 64–80, doi:10.1016/j.ecolmodel.2013.04.018, 2013.

Gorham, E.: Northern Peatlands: Role in the Carbon Cycle and Probable Responses to Climatic Warming, Ecological Applications, 1, 182–195, 1991.

Granberg, G., Grip, H., Löfvenius, M. O., Sundh, I., Svensson, B. H., and Nilsson, M.: A simple model for simulation of water content, soil frost, and soil temperatures in boreal mixed mires, Water Resour. Res., 35, 3771–3782, doi:10.1029/1999WR900216, 1999.

Grant, R. F., Desai, A. R., and Sulman, B. N.: Modelling contrasting responses of wetland productivity to changes in water table depth, Biogeosciences, 9, 4215–4231, 2012.

Grosse-Brauckmann, G.: Ablagerungen der Moore, in: Moor-und Torfkunde, 3rd ed., Gottlich, K. (Ed.), Schweizerbart'sche Verlagsbuchhandlung, Stuttgart, 17–236, 1990.

Harley, P. C., Tenhunen, J. D., Murray, K. J., and Beyers, J.: Irradiance and temperature effects on photosynthesis of tussock tundra Sphagnum mosses from the foothills of the Philip Smith Mountains, Alaska, Oecologia, 79, 251–259, doi:10.1007/BF00388485, 1989.

Harris, A. and Dash, J.: A new approach for estimating northern peatland gross primary productivity using a satellite-sensor-derived chlorophyll index, Journal of geohysical research, 116, G04002, doi:10.1029/2011jg001662, 2011.

Haxeltine, A. and Prentice, C. I.: A General Model for the Light-Use Efficiency of Primary Production, Funcional Ecology, 10, 551–561, 1996.

Heinsch, F. A., Zhao, M., Running, S. W., Kimball, J. S., Nemani, R. R., Davis, K. J., Bolstad, P. V., Cook, B. D., Desai, A. R., Ricciuto, D. M., Law, B. E., Oechel, W. C., Kwon, H., Luo, H., Wofsy, S. C., Dunn, A. L., Munger, J. W., Baldocchi, D. D., Xu, L., Hollinger, D. Y., Richardson, A. D., Stoy, P. C., Siqueira, M. B. S., Monson, R. K., Burns, S. P., and Flanagan, L. B.: Evaluation of remote sensing based terrestrial productivity from MODIS using regional tower eddy flux network observations, IEEE Transactions on Geoscience and Remote Sensing, 44, 1908–1925, doi:10.1109/tgrs.2005.853936, 2006.

Helfrich, M., Flessa, H., Mikutta, R., Dreves, A., and Ludwig, B.: Comparison of chemical fractionation methods for isolating stable soil organic carbon pools, European Journal of Soil Science, 58, 1316–1329, doi:10.1111/j.1365-2389.2007.00926.x, 2007.

Hendriks, D., van Huissteden, J., Dolman, A. J., and van der Molen, M. K.: The full greenhouse gas balance of an abandoned peat meadow, Biogeosciences, 4, 411–424, 2007.

Hmimina, G., Dufrêne, E., Pontailler, J. Y., Delpierre, N., Aubinet, M., Caquet, B., Grandcourt, A. de, Burban, B., Flechard, C., Granier, A., Gross, P., Heinesch, B., Longdoz, B., Moureaux, C., Ourcival, J. M., Rambal, S., Saint André, L., and Soudani, K.: Evaluation of the potential of MODIS satellite data to predict vegetation phenology in different biomes: An investigation using ground-based NDVI measurements, Remote Sensing of Environment, 132, 145–158, doi:10.1016/j.rse.2013.01.010, 2013.

Holden, J., Chapman, P. J., and Labadz, J. C.: Artificial drainage of peatlands: Hydrological and hydrochemical process and wetland restoration, Progress in Physical Geography, 28, 95–123, doi:10.1191/0309133304pp403ra, 2004.

Huete, A. R.: A soil-adjusted vegetation index (SAVI), Remote Sensing of Environment, 25, 295–309, doi:10.1016/0034-4257(88)90106-X, 1988.

Huete, A. R., Didan, K., Miura, T., Rodriguez, E. P., Gao, X., and Ferreira, L. G.: Overview of the radiometric and biophysical performance of the MODIS vegetation indices, Remote Sensing of Environment, 83, 195–213, doi:10.1016/s0034-4257(02)00096-2, 2002.

Humphreys, E. R., Lafleur, P. M., Flanagan, L. B., Hedstrom, N., Syed, K. H., Glenn, A. J., and Granger, R.: Summer carbon dioxide and water vapor fluxes across a range of northern peatlands, Journal of Geophysical Research: Planets, 111, G04011, doi:10.1029/2005JG000111, 2006.

Impens, I. and Lemeur, R.: Extinction of net radiation in different crop canopies, Arch. Met. Geoph. Biokl. B., 17, 403-412, doi:10.1007/BF02243377, 1969.

IPCC: Summary for Policymakers., in: Climate Change 2013: The Physical Science Basis. Contribution of Working Group I to the Fifth Assessment Report of the Intergovernmental Panel on Climate Change, Stocker, T. F., Quin, D., Plattner, G.-K., Tignor, M., Allen, S. K., Boschung, J., Nauels, A., Xia, Y., Bex, V., Midgley, P. M. (Eds.), Cambridge University Press, Cambridge, United Kingdom and New York, NY, USA, 2013.

Jacobs, C. M. J., Jacobs, A. F. G., Bosveld, F. C., Hendriks, D., Hensen, A., Kroon, P. S., Moors, E. J., Nol, L., Schrier-Uijl, A., and Veenendaal, E. M.: Variability of annual CO2 exchange from Dutch grasslands, Biogeosciences Discuss., 4, 803–816, 2007.

References

Janssens, I. A., Lankreijer, H., Matteucci, G., Kowalski, A. S., Buchmann, N., Epron, D., Pilegaard, K., Kutsch, W., Longdoz, B., Grünwald, T., Montagnani, L., Dore, S., Rebmann, C., Moors, E. J., Grelle, A., Rannik, Ü., Morgenstern, K., Oltchev, S., Clement, R., Guðmundsson, J., Minerbi, S., Berbigier, P., Ibrom, A., Moncrieff, J., Aubinet, M., Bernhofer, C., Jensen, N. O., Vesala, T., Granier, A., Schulze, E. D., Lindroth, A., Dolman, A. J., Jarvis, P. G., Ceulemans, R., and Valentini, R.: Productivity overshadows temperature in determining soil and ecosystem respiration across European forests, Glob Change Biol, 7, 269–278, doi:10.1046/j.1365-2486.2001.00412.x, 2001.

Jansson, P.-E.: CoupModel: Model use, Calibration, and Validation, Transactions of the ASABE, 55, 1335–1344, 2012.

Jansson, P.-E. and Halldin, S.: Model for the annual water and energy flow in a layered soil, Comparison of forest and energy exchange models. Society for Ecological Modelling, Copenhagen, 145–163, 1979.

Jansson, P.-E. and Karlberg, L.: Coupled heat and mass transfer model for soil–plant–atmosphere systems. Royal Institute of Technology, Stockholm, 484 pp., accessed: 17 November 2015 https://drive.google.com/file/d/0B0-WJKp0fmYCZ0JVeVgzRWFIbUk/view?pli=1, 2010.

Johansson, G.: Release of organic C from growing roots of meadow fescue (Festuca pratensis L.), Soil Biology and Biochemistry, 24, 427–433, doi:10.1016/0038-0717(92)90205-c, 1992.

Johansson, G.: Carbon distribution in grass (Festuca pratensis L.) during regrowth after cutting—utilization of stored and newly assimilated carbon, Plant Soil, 151, 11–20, 1993.

Jonasson, S. and Chapin III, F. S.: Significance of sequential leaf development for nutrient balance of the cotton sedge, Eriophorum vaginatum L, Oecologia, 67, 511–518, doi:10.1007/BF00790022, 1985.

Jonckheere, I., Fleck, S., Nackaerts, K., Muys, B., Coppin, P., Weiss, M., and Baret, F.: Review of methods for in situ leaf area index determination, Agricultural and Forest Meteorology, 121, 19–35, doi:10.1016/j.agrformet.2003.08.027, 2004.

Joosten, H. and Couwenberg, J.: Are emission reductions from peatlands MRV-able, Wetlands International, Ede, 15, 2009.

Ju, W. and Chen, J. M.: Distribution of soil carbon stocks in Canada's forests and wetlands simulated based on drainage class, topography and remotely sensed vegetation parameters, Hydrological processes, 19, 77–94, doi:10.1002/hyp.5775, 2005.

Kätterer, T. and Andrén, O.: Predicting daily soil temperature profiles in arable soils in cold temperate regions from air temperature and leaf area

index, Acta Agriculturae Scandinavica, Section B - Plant Soil Science, 59, 77–86, doi:10.1080/09064710801920321, 2009.

Kechavarzi, C., Dawson, Q., Bartlett, M., and Leeds-Harrison, P. B.: The role of soil moisture, temperature and nutrient amendment on CO2 efflux from agricultural peat soil microcosms, Geoderma, 154, 203–210, doi:10.1016/j.geoderma.2009.02.018, 2010.

Keddy, P. A.: Assembly and response rules: Two goals for predictive community ecology, Journal of Vegetation Science, 3, 157–164, doi:10.2307/3235676, 1992.

Keller, J. K., White, J. R., Bridgham, S. D., and Pastor, J.: Climate change effects on carbon and nitrogen mineralization in peatlands through changes in soil quality, Global Change Biology, 10, 1053–1064, doi:10.1111/j.1529-8817.2003.00785.x, 2004.

Kellner, E. and Halldin, S.: Water budget and surface-layer water storage in a Sphagnum bog in central Sweden, Hydrological processes, 16, 87–103, 2002.

Kettunen, A., Kaitala, V., Lehtinen, A., Lohila, A., Alm, J., Silvola, J., and Martikainen, P. J.: Methane production and oxidation potentials in relation to water table fluctuations in two boreal mires, Soil Biology and Biochemistry, 31, 1741–1749, doi:10.1016/s0038-0717(99)00093-0, 1999.

Kirschbaum, M.: The temperature dependence of organic-matter decomposition—still a topic of debate, Soil Biology and Biochemistry, 38, 2510–2518, doi:10.1016/j.soilbio.2006.01.030, 2006.

Kistritz, R. U., Hall, K. J., and Yesaki, I.: Productivity, detritus flux, and nutrient cycling in a Carex lyngbyei tidal marsh, Estuaries, 6, 227–236, 1983.

Klemedtsson, L., Arnold, K. v., Weslien, P., and Gundersen, P.: Soil CN ratio as a scalar parameter to predict nitrous oxide emissions, Global Change Biol, 11, 1142–1147, doi:10.1111/j.1365-2486.2005.00973.x, 2005.

Klemedtsson, L., Jansson, P.-E., Gustafsson, D., Karlberg, L., Weslien, P., Arnold, K., Ernfors, M., Langvall, O., and Anders, L.: Bayesian calibration method used to elucidate carbon turnover in forest on drained organic soil, Biogeochemistry, 89, 61–79, doi:10.1007/s10533-007-9169-0, 2008.

Klimeš, L. and Klimešová, J.: The effects of mowing and fertilization on carbohydrate reserves and regrowth of grasses: do they promote plant coexistence in species-rich meadows? Evolutionary Ecology, 363–382, doi:10.1007/978-94-017-1345-0_8, 2002.

Kross, A., Seaquist, J. W., Roulet, N. T., Fernandes, R., and Sonnentag, O.: Estimating carbon dioxide exchange rates at contrasting northern

peatlands using MODIS satellite data, Remote Sensing of Environment, 137, 234–243, doi:10.1016/j.rse.2013.06.014, 2013.

Kuzyakov, Y.: Review: factors affecting rhizosphere priming effects, Journal of Plant Nutrition and Soil Science, 165, 382, 2002.

Kuzyakov, Y., Friedel, J. K., and Stahr, K.: Review of mechanisms and quantification of priming effects, Soil Biology and Biochemistry, 32, 1485–1498, doi:10.1016/s0038-0717(00)00084-5, 2000.

Lafleur, P. M., Moore, T. R., Roulet, N. T., and Frolking, S. E.: Ecosystem Respiration in a Cool Temperate Bog Depends on Peat Temperature But Not Water Table, Ecosystems, 8, 619–629, doi:10.1007/s10021-003-0131-2, 2005.

Laine, A. M., Bubier, J., Riutta, T., Nilsson, M. B., Moore, T. R., Vasander, H., and Tuittila, E.-S.: Abundance and composition of plant biomass as potential controls for mire net ecosytem CO_2 exchange, Botany, 90, 63–74, doi:10.1139/b11-068, 2012.

Lappalainen, E.: Global peat resources, 4, International Peat Society, Jyskä, Finland, 359 pp., 1996.

Leppälä, M., Kukko-Oja, K., Laine, J., and Tuittila, E.-S.: Seasonal dynamics of CO2 exchange during primary succession of boreal mires as controlled by phenology of plants, Ecoscience, 15, 460–471, doi:10.2980/15-4-3142, 2008.

Leuning, R., Zhang, Y. Q., Rajaud, A., Cleugh, H., and Tu, K.: A simple surface conductance model to estimate regional evaporation using MODIS leaf area index and the Penman-Monteith equation, Water Resources Research, 44, W10419, doi:10.1029/2007WR006562, 2008.

Lilliefors, H. W.: On the Kolmogorov-Smirnov Test for Normality with Mean and Variance Unknown, Journal of the American Statistical Association, 62, 399–402, doi:10.2307/2283970, 1967.

Limpens, J. and Berendse, F.: How litter quality affects mass loss and N loss from decomposing Sphagnum, Oikos, 103, 537–547, 2003.

Lindroth, A., Lagergren, F., Aurela, M., Bjarnadottir, B., Christensen, T., Dellwik, E., Grelle, A., Ibrom, A., Johansson, T., Lankreijer, H., Launiainen, S., Laurila, T., Mölder, M., Nikinmaa, E., Pilegaard, K. I. M., Sigurdsson, B. D., and Vesala, T.: Leaf area index is the principal scaling parameter for both gross photosynthesis and ecosystem respiration of Northern deciduous and coniferous forests, Tellus B, 60, 129–142, doi:10.1111/j.1600-0889.2007.00330.x, 2008.

Lindroth, A., Lund, M., Nilsson, M., Aurela, M., Christensen, T. R., Laurila, T., Rinne, J., Riutta, T., Sagerfors, J., Ström, L., Tuovinen, J.-P., and Vesala, T.: Environmental controls on the CO2 exchange in north European mires, Tellus B, 59, 812–825, doi:10.1111/j.1600-0889.2007.00310.x, 2007.

Lipson, D. A., Schadt, C. W., and Schmidt, S. K.: Changes in Soil Microbial Community Structure and Function in an Alpine Dry Meadow Following Spring Snow Melt, Microbial Ecology, 43, 307–314, doi:10.1007/s00248-001-1057-x, 2002.

Lloyd, J. and Taylor, J. A.: On the Temperature Dependence of Soil Respiration, Functional Ecology, 8, 315–323, 1994.

Lohila, A., Aurela, M., Hatakka, J., Pihlatie, M., Minkkinen, K., Penttilä, T., and Laurila, T.: Responses of N2O fluxes to temperature, water table and N deposition in a northern boreal fen, European Journal of Soil Science, 61, 651–661, doi:10.1111/j.1365-2389.2010.01265.x, 2010.

Longstreth, D. J. and Nobel, P. S.: Nutrient Influences on Leaf Photosynthesis: Effects of nitrogen, phosphorus and potassium for Gossypium hirsutum L, Plant Physiology, 65, 541–543, 1980.

Lund, M., Lafleur, P. M., Roulet, N. T., Anders, L., Christensen, T. R., Aurela, M., Chojnicki, B. H., Lawrence, F. B., Humphreys, E. R., Laurila, T., Oechel, W. C., Olejnik, J., Rinne, J., Schubert, P. E. R., and Nilsson, M. B.: Variability in exchange of CO2 across 12 northern peatland and tundra sites, Glob Change Biol, 2436–2448, doi:10.1111/j.1365-2486.2009.02104.x, 2009.

Lundmark, A.: Monitoring transport and fate of de-icing salt in the roadside environment: Modelling and field measurements, PhD thesis, Royal Institute of Technology (KTH), Stockholm, 2008.

Lützow, M. v., Kögel-Knabner, I., Ekschmitt, K., Flessa, H., Guggenberger, G., Matzner, E., and Marschner, B.: SOM fractionation methods: Relevance to functional pools and to stabilization mechanisms: Relevance to functional pools and to stabilization mechanisms, Soil Biology and Biochemistry, 39, 2183–2207, doi:10.1016/j.soilbio.2007.03.007, 2007.

Maljanen, M., Sigurdsson, B. D., Guðmundsson, J., Óskarsson, H., Huttunen, J. T., and Martikainen, P. J.: Greenhouse gas balances of managed peatlands in the Nordic countries – present knowledge and gaps, Biogeosciences, 7, 2711–2738, doi:10.5194/bg-7-2711-2010, 2010.

McGill, R., Tukey, J. W., and Larsen, W. A.: Variations of Box Plots, The American Statistician, 32, 12–16, doi:10.2307/2683468, 1978.

McMichael, C. E.: Estimating CO2 exchange at two sites in Arctic tundra ecosystems during the growing season using a spectral vegetation index, International Journal of Remote Sensing, 20, 683–698, doi:10.1080/014311699213136, 1999.

Meziane, D. and Shipley, B.: Interacting determinants of specific leaf area in 22 herbaceous species: Effects of irradiance and nutrient availability, Plant, Cell & Environment, 22, 447–459, 1999.

Mitsch, W. J. and Gosselink, J. G.: The value of wetlands: importance of scale and landscape setting, Ecological Economics, 35, 25–33, 2000.

References

Monteith, J. L.: Solar radiation and productivity in tropical ecosystems, Journal of Applied Ecology, 9, 747–766, 1972.

Moore, T. R., Bubier, J. L., and Bledzki, L.: Litter Decomposition in Temperate Peatland Ecosystems: The Effect of Substrate and Site, 10, 949–963, doi:10.1007/s10021-007-9064-5, 2007.

Moore, T. R. and Dalva, M.: Methane and carbon dioxide exchange potentials of peat soils in aerobic and anaerobic laboratory incubations, Soil Biology and Biochemistry, 29, 1157–1164, doi:10.1016/s0038-0717(97)00037-0, 1997.

Moriasi, D. N., Arnold, J. G., Van Liew, M. W., Binger, R. L., Harmel, R. D., and Veith, T. L.: Model evaluation guidelines for systematic quantification of accuracy in watershed simulations, American Society of Agricultural and Biological Engineers, 50, 885–900, 2007.

Mualem, Y.: A new model for predicting the hydraulic conductivity of unsaturated porous media, Water Resources Research, 12, 513–522, doi:10.1029/WR012i003p00513, 1976.

Murray, K. J., Tenhunen, J. D., and Nowak, R. S.: Photoinhibition as a control on photosynthesis and production of Sphagnum mosses, Oecologia, 96, 200–207, doi:10.1007/BF00317733, 1993.

Mutanga, O. and Skidmore, A. K.: Hyperspectral band depth analysis for a better estimation of grass biomass (Cenchrus ciliaris) measured under controlled laboratory conditions, International Journal of Applied Earth Observation and Geoinformation, 5, 87–96, doi:10.1016/j.jag.2004.01.001, 2004.

Myhre, G., Shindell, D., Breon, F.-M., Collins, W., Fuglestvedt, J., Huang, J., Koch, D., Lamarque, J.-F., Lee, D., Mendoza, B., Nakajima, T., Robock, A., Stephens, G., Takemura T., and Zhang, H.: Anthropogenic and Natural Radiative Forcing., in: Climate Change 2013: The Physical Science Basis. Contribution of Working Group I to the Fifth Assessment Report of the Intergovernmental Panel on Climate Change, Stocker, T. F., Quin, D., Plattner, G.-K., Tignor, M., Allen, S. K., Boschung, J., Nauels, A., Xia, Y., Bex, V., Midgley, P. M. (Eds.), Cambridge University Press, Cambridge, United Kingdom and New York, NY, USA, 669–740, 2013.

Nash, J. E. and Sutcliffe, J. V.: River flow forecasting through conceptual models part I—A discussion of principles, Journal of Hydrology, 10, 282–290, 1970.

Norman, J., Jansson, P.-E., Farahbakhshazad, N., Butterbach-Bahl, K., Li, C., and Klemedtsson, L.: Simulation of NO and N2O emissions from a spruce forest during a freeze/thaw event using an N-flux submodel from the PnET-N-DNDC model integrated to CoupModel, Ecological Modelling, 216, 18–30, doi:10.1016/j.ecolmodel.2008.04.012, 2008.

Nuttonson, M. Y.: The role of bioclimatology in agriculture with special reference to the use of thermal and photo-thermal requirements of pure-line varieties of plants as a biological indicator in ascertaining climatic analogues (Homoclimes), International Journal of Biometeorology, 2, 129–148, 1958.

Oechel, W. C., Vourlitis, G. L., Hastings, S. J., Zulueta, R. C., Hinzman, L., and Kane, D.: Acclimation of ecosystem $CO2$ exchange in the Alaskan Arctic in response to decadal climate warming, Nature, 406, 978–981, doi:10.1038/35023137, 2000.

Päivänen, J.: Hydraulic conductivity and water retention in peat soils, Acta Forestalia Fennica, 129, 1973.

Panikov, N. S. and Dedysh, S. N.: Cold season $CH4$ and $CO2$ emission from boreal peat bogs (West Siberia): Winter fluxes and thaw activation dynamics, Global Biogeochem. Cycles, 14, 1071–1080, doi:10.1029/1999GB900097, 2000.

Papale, D., Reichstein, M., Aubinet, M., Canfora, E., Bernhofer, C., Longdoz, B., Kutsch, W., Rambal, S., Valentini, R., Vesala, T., and Yakir, D.: Towards a standardized processing of Net Ecosystem Exchange measured with eddy covariance technique: algorithms and uncertainty estimation, Biogeosciences, 3, 571--583, 2006.

Parish, F., A. Sirin, D. Charman, H. Joosten, T. Minaeva, and M. Silvius (Eds.): Assessment of peatlands, biodiversity and climate change: Main Report. Global Environment Centre, Kuala Lumpur, Malaysia, and Wetlands International, Wageningen, The Netherlands, 2008.

Paul, K.: Temperature and moisture effects on decomposition, Kirschbaum, M. U., Mueller, R. (Eds.), Net Ecosystem Exchange, Cooperative Research Centre for Greenhouse Accounting, 95–102, 2001.

Peacock, J. M.: Temperature and Leaf Growth in Lolium perenne. I. The Thermal Microclimate: Its Measurement and Relation to Crop Growth, Journal of Applied Ecology, 12, 99–114, doi:10.2307/2401720, 1975.

Peichl, M., Öquist, M., Löfvenius, M. O., Ilstedt, U., Sagerfors, J., Grelle, A., Lindroth, A., and Nilsson, M. B.: A 12-year record reveals pre-growing season temperature and water table level threshold effects on the net carbon dioxide exchange in a boreal fen, Environmental Research Letters, 9, 55006, 2014.

Peichl, M., Sonnentag, O., and Nilsson, M.: Bringing Color into the Picture: Using Digital Repeat Photography to Investigate Phenology Controls of the Carbon Dioxide Exchange in a Boreal Mire, Ecosystems, 18, 115-131, doi:10.1007/s10021-014-9815-z, 2015.

Petrescu, A. M. R., Lohila, A., Tuovinen, J.-P., Baldocchi, D. D., Desai, A. R., Roulet, N. T., Vesala, T., Dolman, A. J., Oechel, W. C., Marcolla, B., Friborg, T., Rinne, J., Matthes, J. H., Merbold, L., Meijide, A., Kiely, G.,

References

Sottocornola, M., Sachs, T., Zona, D., Varlagin, A., Lai, D. Y. F., Veenendaal, E., Parmentier, F.-J. W., Skiba, U., Lund, M., Hensen, A., van Huissteden, J., Flanagan, L. B., Shurpali, N. J., Grünwald, T., Humphreys, E. R., Jackowicz-Korczyński, M., Aurela, M. A., Laurila, T., Grüning, C., Corradi, C. A. R., Schrier-Uijl, A. P., Christensen, T. R., Tamstorf, M. P., Mastepanov, M., Martikainen, P. J., Verma, S. B., Bernhofer, C., and Cescatti, A.: The uncertain climate footprint of wetlands under human pressure, Proceedings of the National Academy of Sciences of the United States of America, 112, 4594–4599, doi:10.1073/pnas.1416267112, 2015.

Pierce, L. L., Running, S. W., and Walker, J.: Regional-scale relationships of leaf area index to specific leaf area and leaf nitrogen content, Ecological Applications, 4, 313–321, 1994.

Poorter, H. and Jong, R.: A comparison of specific leaf area, chemical composition and leaf construction costs of field plants from 15 habitats differing in productivity, New Phytologist, 143, 163–176, 1999.

Potter, C., Bubier, J., Crill, P. M., and Lafleur, P.: Ecosystem modeling of methane and carbon dioxide fluxes for boreal forest sites, Canadian Journal of Forest Research, 31, 208–223, doi:10.1139/x00-164, 2001.

Price, J. C.: How unique are spectral signatures?, Remote Sensing of Environment, 49, 181–186, 1994.

Prihodko, L., Denning, A. S., Hanan, N. P., Baker, I., and Davis, K.: Sensitivity, uncertainty and time dependence of parameters in a complex land surface model, Agricultural and Forest Meteorology, 148, 268–287, doi:10.1016/j.agrformet.2007.08.006, 2008.

Proebsting, W. M., Davies, P. J., and Marx, G. A.: Photoperiodic control of apical senescence in a genetic line of peas, Plant Physiology, 58, 800–802, 1976.

Pruim, R., Kaplan, D., and Horton, N. mosaic: Project MOSAIC (mosaic-web.org) statistics and mathematics teaching utilities. R package version 0.8-18. http://CRAN.R-project.org/package=mosaic, 2014

R Core Team. R: A language and environment for statistical computing. R Foundation for Statistical Computing, Vienna, Austria. URL http://www.R-project.org, 2014

Raich, J. W. and Schleisinger, W. H.: The global carbon dioxide flux in soil respiration and its relationship to vegetation and climate, Tellus, 44B, 81–99, 1992.

Ratkowsky, D. A., Olley, J., McMeekin, T. A., and Ball, A.: Relationship between temperature and growth rate of bacterial cultures, Journal of Bacteriology, 149, 1–5, 1982.

Ravina, M.: Modelling of methane emission from forest ecosystems. Implementation and test of submodel as part of the CoupModel, Master Thesis, KTH Royal Institute of Technology, 2007.

Reddy, K. R. and Patrick, W. H.: Effect of alternate aerobic and anaerobic conditions on redox potential, organic matter decomposition and nitrogen loss in a flooded soil, Soil Biology and Biochemistry, 7, 87–94, doi:10.1016/0038-0717(75)90004-8, 1975.

Reich, P. B., Ellsworth, D. S., and Walters, M. B.: Leaf structure (specific leaf area) modulates photosynthesis-nitrogen relations: evidence from within and across species and functional groups, Functional Ecology, 12, 948–958, 1998.

Reich, P. B., Walters, M. B., Ellsworth, D. S., and Uhl, C.: Photosynthesis-nitrogen relations in Amazonian tree species, Oecologia, 97, 62–72, 1994.

Reichstein, M., Falge, E., Baldocchi, D., Papale, D., Aubinet, M., Berbigier, P., Bernhofer, C., Buchmann, N., Gilmanov, T., Granier, A., Grünwald, T., Havránková, K., Ilvesniemi, H., Janous, D., Knohl, A., Laurila, T., Lohila, A., Loustau, D., Matteucci, G., Meyers, T., Miglietta, F., Ourcival, J.-M., Pumpanen, J., Rambal, S., Rotenberg, E., Sanz, M., Tenhunen, J., Seufert, G., Vaccari, F., Vesala, T., Yakir, D., and Valentini, R.: On the separation of net ecosystem exchange into assimilation and ecosystem respiration: review and improved algorithm, Glob Change Biol, 11, 1424–1439, doi:10.1111/j.1365-2486.2005.001002.x, 2005.

Reichstein, M., Rey, A., Freibauer, A., Tenhunen, J., Valentini, R., Banza, J., Casals, P., Cheng, Y., Grünzweig, J. M., Irvine, J., Joffre, R., Law, B. E., Loustau, D., Miglietta, F., Oechel, W., Ourcival, J.-M., Pereira, J. S., Peressotti, A., Ponti, F., Qi, Y., Rambal, S., Rayment, M., Romanya, J., Rossi, F., Tedeschi, V., Tirone, G., Xu, M., and Yakir, D.: Modeling temporal and large-scale spatial variability of soil respiration from soil water availability, temperature and vegetation productivity indices, Global Biogeochem. Cycles, 17, 1104, doi:10.1029/2003gb002035, 2003.

Rendong, L. and Jiyuan, L.: Wetland vegetation biomass estimation and mapping from Landsat ETM data: A case study of Poyang Lake, Journal of Geographical Sciences, 12, 35–41, 2002.

Richards, L. A.: Capillary conduction of liquids through porous mediums, Journal of Applied Physics, 1, 318–333, doi:10.1063/1.1745010, 1931.

Robson, M. J.: The Growth and Development of Simulated Swards of Perennial Ryegrass, Annals of Botany, 37, 487–500, 1973.

Rocha, A. V. and Shaver, G. R.: Advantages of a two band EVI calculated from solar and photosynthetically active radiation fluxes, Agricultural and Forest Meteorology, 149, 1560–1563, doi:10.1016/j.agrformet.2009.03.016, 2009.

References

Rossini, M., Cogliati, S., Meroni, M., Migliavacca, M., Galvagno, M., Busetto, L., Cremonese, E., Julitta, T., Siniscalco, C., Morra di Cella, U., and Colombo, R.: Remote sensing-based estimation of gross primary production in a subalpine grassland, Biogeosciences, 9, 2565–2584, doi:10.5194/bg-9-2565-2012, 2012.

Rudolph, H. and Samland, J.: Occurrence and metabolism of sphagnum acid in the cell walls of bryophytes, Phytochemistry, 24, 745–749, doi:10.1016/s0031-9422(00)84888-8, 1985.

Running, S. W. and Coughlan, J. C.: A general model of forest ecosystem processes for regional applications I. Hydrologic balance, canopy gas exchange and primary production processes, Ecological Modelling, 42, 125–154, doi:10.1016/0304-3800(88)90112-3, 1988.

Saarinen, T.: Demography of Carex rostrata in a boreal mesotrophic fen: Shoot dynamics and biomass development, Annales Botanici Fennici, 35, 203–209, 1998.

Sagerfors, J., Lindroth, A., Grelle, A., Klemedtsson, L., Weslien, P., and Nilsson, M.: Annual CO2 exchange between a nutrient-poor, minerotrophic, boreal mire and the atmosphere, J. Geophys. Res. Biogeosci., 113, G01001, doi:10.1029/2006JG000306, 2008.

Santaren, D., Peylin, P., Bacour, C., Ciais, P., and Longdoz, B.: Ecosystem model optimization using in situ flux observations: Benefit of Monte Carlo versus variational schemes and analyses of the year-to-year model performances, Biogeosciences, 11, 7137–7158, doi:10.5194/bg-11-7137-2014, 2014.

Santaren, D., Peylin, P., Viovy, N., and Ciais, P.: Optimizing a process-based ecosystem model with eddy-covariance flux measurements: A pine forest in southern France, Global Biogeochem. Cycles, 21, n/a, doi:10.1029/2006GB002834, 2007.

Satterwhite, M. B. and Ponder Henley, J.: Spectral characteristics of selected soils and vegetation in Northern Nevada and their discrimination using band ratio techniques, Remote Sensing of Environment, 23, 155–175, doi:10.1016/0034-4257(87)90035-6, 1987.

Schneider, R. R., Stelfox, J. B., Boutin, S., and Wasel, S.: Managing the cumulative impacts of land uses in the Western Canadian Sedimentary Basin: a modeling approach, Conservation Ecology, 7, 8, 2003.

Schubert, P., Eklundh, L., Lund, M., and Nilsson, M.: Estimating northern peatland CO2 exchange from MODIS time series data, Remote Sensing of Environment, 114, 1178–1189, doi:10.1016/j.rse.2010.01.005, 2010.

Schuldt, R. J., Brovkin, V., Kleinen, T., and Winderlich, J.: Modelling Holocene carbon accumulation and methane emissions of boreal wetlands – an Earth system model approach, Biogeosciences, 10, 1659–1674, doi:10.5194/bg-10-1659-2013, 2013.

Schulz, K. and Beven, K.: Data-supported robust parameterisations in land surface-atmosphere flux predictions: towards a top-down approach, Hydrol. Process., 17, 2259–2277, doi:10.1002/hyp.1331, 2003.

Sellers, P. J.: Canopy reflectance, photosynthesis and transpiration, International Journal of Remote Sensing, 6, 1335–1372, doi:10.1080/01431168508948283, 1985.

Shaver, G. R. and Laundre, J.: Exsertion, elongation, and senescence of leaves of Eriophorum vaginatum and Carex bigelowii in Northern Alaska, Glob Change Biol, 3, 146–157, doi:10.1111/j.1365-2486.1997.gcb141.x, 1997.

Sinclair, T. R. and Horie, T.: Leaf Nitrogen, Photosynthesis, and Crop Radiation Use Efficiency: A Review, Crop Science, 29, 90–98, doi:10.2135/cropsci1989.0011183X002900010023x, 1989.

Smith, J., Gottschalk, P., Bellarby, J., Chapman, S., Lilly, A., Towers, W., Bell, J., Coleman, K., Nayak, D., Richards, M., Hillier, J., Flynn, H., Wattenbach, M., Aitkenhead, M., Yeluripati, J., Farmer, J., Milne, R., Thomson, A., Evans, C., Whitmore, A., Falloon, P., and Smith, P.: Estimating changes in Scottish soil carbon stocks using ECOSSE. I. Model description and uncertainties, Clim. Res., 45, 179–192, doi:10.3354/cr00899, 2010.

Smith, P., Smith, J. U., Powlson, D. S., McGill, W. B., Arah, J. R. M, Chertov, O. G., Coleman, K., Franko, U., Frolking, S. E., Jenkinson, D. S., Jensen, L. S., Kelly, R. H., Klein-Gunnewiek, H., Komarov, A. S., Li, C., Molina, J. A. E., Mueller, T., Parton, W. J., Thornley, John H. M., and Whitmore, A. P.: A comparison of the performance of nine soil organic matter models using datasets from seven long-term experiments, Geoderma, 81, 153–225, doi:10.1016/s0016-7061(97)00087-6, 1997.

Sponagel, H.: Bodenkundliche Kartieranleitung: 5., verb. und erw. Aufl., Schweizerbart, Stuttgart, Germany, 438 S., 2005.

Staudt, K., Falge, E., Pyles, R. D., Paw, U. K. T., and Foken, T.: Sensitivity and predictive uncertainty of the ACASA model at a spruce forest site, Biogeosciences, 7, 3685–3705, doi:10.5194/bg-7-3685-2010, 2010.

Steed, J. E., DeWald, L. E., and Kolb, T. E.: Physiological and Growth Responses of Riparian Sedge Transplants to Groundwater Depth, International Journal of Plant Sciences, 163, 925–936, doi:10.1086/342634, 2002.

Steele, J. M., Ratliff, R. D., and Ritenour, G. L.: Seasonal variation in total nonstructural carbohydrate levels in Nebraska sedge, Journal of Range Management, 37, 465–467, 1984.

St-Hilaire, F., Wu, J., Roulet, N. T., Frolking, S. E., Lafleur, P. M., Humphreys, E. R., and Arora, V.: McGill wetland model: evaluation of a peatland carbon simulator developed for global assessments, Biogeosciences, 7, 3517–3530, doi:10.5194/bg-7-3517-2010, 2010.

References

Stocker, T. F., Quin, D., Plattner, G.-K., Tignor, M., Allen, S. K., Boschung, J., Nauels, A., Xia, Y., Bex, V., and Midgley, P. M. (Eds.): Climate Change 2013: The Physical Science Basis. Contribution of Working Group I to the Fifth Assessment Report of the Intergovernmental Panel on Climate Change, Cambridge University Press, Cambridge, United Kingdom and New York, NY, USA, 2013.

Strack, M. (Ed.): Peatlands and Climate Change, University of Calgary, Calgary, 223 pp., 2008.

Tatarinov, F. A. and Cienciala, E.: Application of BIOME-BGC model to managed forests, Forest Ecology and Management, 237, 267–279, doi:10.1016/j.foreco.2006.09.085, 2006.

Thenkabail, P. S., Smith, R. B., and Pauw, E.: Evaluation of narrowband and broadband vegetation indices for determining optimal hyperspectral wavebands for agricultural crop characterization, Photogrammetric Engineering and Remote Sensing, 68, 607–622, 2002.

Thomas, H. and Stoddart, J. L.: Leaf Senescence, Ann. Rev. Plant Physiol., 31, 83–111, 1980.

Thornton, P. E. and Rosenbloom, N. A.: Ecosystem model spin-up: Estimating steady state conditions in a coupled terrestrial carbon and nitrogen cycle model: Estimating steady state conditions in a coupled terrestrial carbon and nitrogen cycle model, Ecological Modelling, 189, 25–48, doi:10.1016/j.ecolmodel.2005.04.008, 2005.

Thorsen, M., Refsgaard, J. C., Hansen, S., Pebesma, E., Jensen, J. B., and Kleeschulte, S.: Assessment of uncertainty in simulation of nitrate leaching to aquifers at catchment scale, Journal of Hydrology, 242, 210–227, doi:10.1016/S0022-1694(00)00396-6, 2001.

Tucker, C. J.: Red and photographic infrared linear combinations for monitoring vegetation, Remote Sensing of Environment, 8, 127–150, doi:10.1016/0034-4257(79)90013-0, 1979.

Tuittila, E.-S., Komulainen, V.-M., Vasander, H., and Laine, J.: Restored cut-away peatland as a sink for atmospheric CO2, Oecologia, 120, 563-574, doi:10.1007/s004420050891, 1999.

Turetsky, M. R.: The Role of Bryophytes in Carbon and Nitrogen Cycling, The Bryologist, 106, 395–409, doi:10.2307/3244721, 2003.

UNEP year book: Emerging issues in our global environment 2012, United Nations Environment Programme, Nairobi, Kenya, vii, 68, 2012.

Updegraff, K., Pastor, J., Bridgham, S. D., and Johnston, C. A.: Environmental and substrate controls over carbon and nitrogen mineralization in northern wetlands, Ecological Applications, 5, 151–163, 1995.

van Huissteden, J., van den Bos, Remco, and Alvarez, I. Marticorena: Modelling the effect of water-table management on CO2 and CH4 fluxes from peat soils, Netherlands Journal of Geosciences, 85, 3–18, 2006.

Verbeeck, H., Samson, R., Verdonck, F., and Lemeur, R.: Parameter sensitivity and uncertainty of the forest carbon flux model FORUG: A Monte Carlo analysis, Tree Physiology, 26, 807–817, doi:10.1093/treephys/26.6.807, 2006.

Verhoeven, J. T. A. and Toth, E.: Decomposition of Carex and Sphagnum litter in fens: Effect of litter quality and inhibition by living tissue homogenates, Soil Biology and Biochemistry, 27, 271–275, doi:10.1016/0038-0717(94)00183-2, 1995.

Vescovo, L., Wohlfahrt, G., Balzarolo, M., Pilloni, S., Sottocornola, M., Rodeghiero, M., and Gianelle, D.: New spectral vegetation indices based on the near-infrared shoulder wavelengths for remote detection of grassland phytomass, International Journal of Remote Sensing, 33, 2178–2195, doi:10.1080/01431161.2011.607195, 2012.

Viña, A., Gitelson, A. A., Nguy-Robertson, A. L., and Peng, Y.: Comparison of different vegetation indices for the remote assessment of green leaf area index of crops, Remote Sensing of Environment, 115, 3468–3478, 2011.

Vuichard, N., Soussana, J.-F., Ciais, P., Viovy, N., Ammann, C., Calanca, P., Clifton-Brown, J., Fuhrer, J., Jones, M., and Martin, C.: Estimating the greenhouse gas fluxes of European grasslands with a process-based model: 1. Model evaluation from in situ measurements, Global Biogeochem. Cycles, 21, n/a, doi:10.1029/2005GB002611, 2007.

Waddington, J. M., Strack, M., and Greenwood, M. J.: Toward restoring the net carbon sink function of degraded peatlands: Short-term response in CO 2 exchange to ecosystem-scale restoration, J. Geophys. Res., 115, doi:10.1029/2009JG001090, 2010.

Wania, R., Ross, I., and Prentice, I. C.: Integrating peatlands and permafrost into a dynamic global vegetation model: 1. Evaluation and sensitivity of physical land surface processes, Global Biogeochem. Cycles, 23, n/a, doi:10.1029/2008GB003412, 2009a.

Wania, R., Ross, I., and Prentice, I. C.: Integrating peatlands and permafrost into a dynamic global vegetation model: 2. Evaluation and sensitivity of vegetation and carbon cycle processes, Global Biogeochem. Cycles, 23, n/a, doi:10.1029/2008GB003413, 2009b.

Wang, Q., Tenhunen, J., Dinh, N. Q., Reichstein, M., Vesala, T., and Keronen, P.: Similarities in ground- and satellite-based NDVI time series and their relationship to physiological activity of a Scots pine forest in Finland, Remote Sensing of Environment, 93, 225–237, doi:10.1016/j.rse.2004.07.006, 2004.

References

Wang, X., He, X., Williams, J. R., Izaurralde, R. C., and Atwood, J. D.: Sensitivity and uncertainty analyses of crop yields and soil organic carbon simulated with EPIC, American Society of Agricultural and Biological Engineers, 48, 1041–1054, 2005.

Ward, S. E., Ostle, N. J., Oakley, S., Quirk, H., Henrys, P. A., Bardgett, R. D., and van der Putten, W.: Warming effects on greenhouse gas fluxes in peatlands are modulated by vegetation composition, Ecology Letters, 16, 1285–1293, doi:10.1111/ele.12167, 2013.

Watson, D. J.: Comparative physiological studies on the growth of field crops: I. Variation in net assimilation rate and leaf area between species and varieties, and within and between years: I, Annals of Botany, 11, 41–76, 1947.

Webb, N., Nichol, C., Wood, J., and Potter, E.: User Manual for SunScan v2.0, Ltd, D.-T. D. (Ed.), Derbyshire, U.K, 83 pp, 2008.

Wedin, D. A.: Nutrient Cycling in grasslands: An Ecologist`s Perspective, in: Nutrient Cycling in Foragesystems, Joost, R. E., Roberts, C. A. (Eds.), Potash and Posphate Institute, Manhattan, KS, U.S, 29–44, 1996.

White, L. M.: Carbohydrate Reserves of Grasses: A Review, Journal of Range Management, 26, 13–18, 1973.

Wilson, D., Alm, J., Riutta, T., Laine, J., Byrne, K. A., Farrell, E. P., and Tuittila, E.-S.: A high resolution green area index for modelling the seasonal dynamics of CO_2 exchange in peatland vascular plant communities, Plant Ecology, 190, 37–51, doi:10.1007/s11258-006-9189-1, 2007.

Wingler, A.: The role of sugars in integrating environmental signals during the regulation of leaf senescence, Journal of Experimental Botany, 57, 391–399, doi:10.1093/jxb/eri279, 2005.

Wohlfahrt, G., Bahn, M., Haubner, E., Horak, I., Michaeler, W., Rottmar, K., Tappeiner, U., and Cernusca, A.: Inter-specific variation of the biochemical limitation to photosynthesis and related leaf traits of 30 species from mountain grassland ecosystems under different land use, Plant, Cell and Environment, 22, 1281–1296, 1999.

Wohlfahrt, G., Pilloni, S., Hörtnagl, L., and Hammerle, A.: Estimating carbon dioxide fluxes from temperate mountain grasslands using broad-band vegetation indices, Biogeosciences, 7, 683–694, 2010.

Wu, C.: Use of a vegetation index model to estimate gross primary production in open grassland, Journal of Applied Remote Sensing, 6, 63532, doi:10.1117/1.JRS.6.063532, 2012.

Wu, J., Roulet, N. T., Sagerfors, J., and Nilsson, M. B.: Simulation of six years of carbon fluxes for a sedge-dominated oligotrophic minerogenic peatland in Northern Sweden using the McGill Wetland Model (MWM),

J. Geophys. Res. Biogeosci., 118, 795–807, doi:10.1002/jgrg.20045, 2013.

Wu, L., McGechan, M. B., and Knight, A. C.: Simulation of allocation of accumulated biomass to leaf and stem in a grass growth model, Grass and Forage Science, 52, 445–448, 1997.

Wu, Y. and Blodau, C.: PEATBOG: a biogeochemical model for analyzing coupled carbon and nitrogen dynamics in northern peatlands, Geoscientific Model Development, 6, 1173–1207, doi:10.5194/gmd-6-1173-2013, 2013.

Yeloff, D. and Mauquoy, D.: The influence of vegetation composition on peat humification: Implications for palaeoclimatic studies, Boreas, 35, 662–673, doi:10.1080/03009480600690860, 2006.

Yu, Z. C.: Northern peatland carbon stocks and dynamics: A review, Biogeosciences, 9, 4071–4085, 2012.

Yurova, A., Wolf, A., Sagerfors, J., and Nilsson, M.: Variations in net ecosystem exchange of carbon dioxide in a boreal mire: Modeling mechanisms linked to water table position, J. Geophys. Res. Biogeosci., 112, G02025, doi:10.1029/2006JG000342, 2007.

Zeitz, J. and Velty, S.: Soil properties of drained and rewetted fen soils, Soil Science Society of America Journal, 165, 618–626, 2002.

Zhang, T.: Influence of the seasonal snow cover on the ground thermal regime: An overview, Reviews of Geophysics, 43, RG4002, doi:10.1029/2004RG000157, 2005.

Zhang, Y., Li, C., Trettin, C. C., Li, H., and Sun, G.: An integrated model of soil, hydrology, and vegetation for carbon dynamics in wetland ecosystems, Global Biogeochem. Cycles, 16, 9-1–9-17, doi:10.1029/2001gb001838, 2002.

Zimmermann, M., Leifeld, J., Schmidt, M. W. I., Smith, P., and Fuhrer, J.: Measured soil organic matter fractions can be related to pools in the RothC model, European Journal of Soil Science, 58, 658–667, doi:10.1111/j.1365-2389.2006.00855.x, 2007.

7   Appendix

Table of contents in the appendix

List of figures in the appendix

List of tables in the appendix

A1 Appendix to materials and methods

A1.1 Detailed description of the calibration procedure of study I.

A stepwise approach was used to calibrate model parameter: (I) Parameter ranges of 45 parameters were constrained by applying a Monte Carlo based calibration by multiple runs with randomized parameter values in a defined range, similar to the Generalized Likelihood Uncertainty Estimation by Beven and Binley (1992) and Beven (2006). Ranges were selected according to experiences from previous model runs, in most cases a certain range around the default values. The list of parameters and their tested ranges are displayed in Table A1.4. The output of these runs was compared with several different variables derived from measurements. A number of performance indicators were considered to define the behavioural models with an acceptable fit in step I a. Parameter ensembles of accepted behavioural models were further analysed to identify covariance between parameters and also to understand the importance and effect of multiple criteria (I b). 350'000 runs were executed for each site, except for Hor, for which 700'000 runs were performed. The higher amount of runs at Hor was motivated by the observed discrepancy in chamber versus EC derived R_{eco} values and a wider range for some parameters due to the relatively high ratio of biomass to GPP.

(I a) From these runs, around 75 behavioural models per site were selected according to an acceptable fit (Table A1.8) to measurement derived R_{eco} and GPP respectively in case of Hor NEE and plant biomass. Due to their relatively small amplitude, winter fluxes hardly affect performance indices of the whole year. However they have a high proportion of soil to plant respiration and are therefore of special interest. Hence, performance in modelling R_{eco} and GPP during winter, respectively late autumn in case of Lom were additionally taken into account. As the ability to constrain parameter values and the model performance depend on quality and frequency of the available measurement data, different criteria (Table A1.8) had to be applied for each site.

(I b) Performance (R^2, ME and NSE) of the 75 accepted runs on each variable was plotted against values for each parameter as well as values for each parameter against values for each other parameter. These plots were visually analysed to detect covariance between parameters which were further analysed in step III and between parameters and performance which were further analysed in step I c.

(I c) The best fit for one variable does not necessarily lead to the best fit for another variable. Therefore, a further constraint was achieved by selecting

each best 10 out of the 75 runs independently for each of the variables and each parameter as listed in Table A1.10. According the results from I b, different performance indices were used depending on the variable: R^2 was chosen in case of R_{eco} and GPP as effect on ME can be compensated by radiation use efficiency (ϵ_L) in case of GPP and decomposition rate for the fast SOC pools (k_l) in case of R_{eco}. Mean error was chosen in case of temperature, NSE for all other variables, including winter R_{eco} and winter GPP. This procedure leads to several ranges for each parameter producing the best performance depending on the variable and the site.

(I d) The ranges were merged together to a new range for each parameter, starting with the highest value of the lower ends of all ranges and lasts to the lowest of the upper ends. These ranges will be called "overlapping ranges" in the following, even though they did not overlap in some few cases.

(II) Parameters might interact with one or more other parameters and counteract or even compensate the effect of other parameters. Ranges for such parameters could be same or overlapping between the sites, but the application of a single set of parameter values might reveal that only site specific values for one or several of these parameters lead to acceptable performance. To test this, for each site one of the 75 runs with the highest performance in R^2 of R_{eco} selected and ϵ_L and k_l adjusted until ME in GPP and R_{eco} was smaller than $|0.1|$ g C m^{-2} day^{-1}. Afterwards, stepwise each parameter was set to the rounded mean value of the overlapping range from I d and again ϵ_L and k_l adjusted until ME in GPP and R_{eco} was smaller than $|0.1|$ g C m^{-2} day^{-1}. If then the performance in R^2 of R_{eco} and GPP was not reduced by more than 0.05 the modified parameter was kept at this value. Otherwise it was set back to the previous value and further investigated in III. This procedure was repeated for all parameters except ϵ_L and k_l.

(III) Parameters showing strong interactions or showing different valid ranges for the different sites or variables were investigated by further multiple calibrations with 2500 to 5000 runs. For each parameter only this particular parameter and very few other parameters which are directly related to it were calibrated, while all others were kept constant to the values from step II. Criteria for accepted runs were a mean error of max $|0.3|$ g C m^{-2} day^{-1} in R_{eco} and GPP, respectively in GPP and uppermost temperature case of p_{ck}, to accept 60 to 150 runs. Such additional multiple calibrations were also performed if the previous results indicated an optimal range outside the tested range. In this case the calibration range of the parameter was increased.

Then steps I c, d and II were repeated for these additional calibration. If the performance in R^2 of R_{eco} and GPP was reduced by more than 0.05 the parameter was considered to be site specific. Again, ϵ_L and k_l were adjusted until ME in GPP and R_{eco} was smaller than $|0.1|$ g C m^{-2} day^{-1}. This set of parameter values will be called common configuration (C1) in the following.

(IV) Different combination of parameter values might lead to similar good results, which is called equifinality (Beven, 2006). In those cases were step I to III indicated covariance between parameters, several different combinations of parameter values leading to similar good results (ME in GPP and R_{eco} smaller than $|0.1|$ g C m^{-2} day^{-1}) were tested. Such runs with a single set of parameter values are called single runs in the following and numbered with C1 to C7 (Table A1.9).

Table A1.8. Partitioning of measured SOC to the pools in study I. The data in the table is aggregated into 3 soil layers, however 12 layers were used in the model.

	depth [m]	Lom	Amo	Hor	FsA	FsB
Measured total C [kg m−3]	0-0.1	24	190	72	107	88
	0.1-0.3	30	187	79	104	90
	> 0.3	51	175	156	70	61
Measured C:N [kg m−3]	0-0.1	27	23	13	11	12
	0.1-0.3	20	22	13	14	13
	> 0.3	20	21	22	17	17
Estimated fraction of fast pool / total C	0-0.1	95%	72%	18%	3%	9%
	0.1-0.3	56%	73%	20%	20%	16%
	> 0.3	55%	68%	62%	35%	41%
Dry bulk density [g cm−3]	0-0.1	0.06[a]	0.39	0.35	0.59	0.33
	0.1-0.3	0.06	0.37	0.48	0.29	0.52
	> 0.3	0.10	0.37[b]	0.50	0.18	0.17

[a] no data available, value from lower layer used
[b] no data available, value from upper layer used

Table A1.9. Dynamic data for model calibrations and comparison – methods and instruments.

Site	Variable	Period	Resolution as used for calibration	Method	replicates	Described in	number of data points
Lom	NEE	mid 2006-10	hourly	EC	1	Aurela et al., 2009	34895
	R_{eco}	2007, 2009, 2010	hourly, summer only	automatic opaque chamber	2	Lohila et al., 2010	27853
	R_{eco}, GPP	mid 2006-10	hourly	empirical modelling from EC data	1	Aurela et al., 2009	15236
	winter R_{eco}	2006-2010	hourly	empirical modelling from night NEE EC data during Sept.-Nov.	1		6356
	soil temperature at −7 cm	mid 2006-10	hourly	automatic temperature sensors	1		34318
	soil temperature at −60 cm	mid 2006-10	hourly	automatic temperature sensors	1		34318
	LAI	2007-10	4-10 times each summer	optical canopy analyser	9-19		41
	Snow depth	mid 2006-10	hourly	automatic sensor	1		34316
Amo	NEE	mid 2006-10	hourly	EC	1	Drewer et al., 2010	38710
	R_{eco}	mid 2006-10	biweekly	manual opaque chamber	9	Dinsmore et al., 2010	57
	R_{eco}, GPP	mid 2006-10	hourly	empirical model from EC data	1	Drewer et al., 2010	43475
	winter R_{eco}	mid 2006-10	hourly	empirical modelling from night NEE EC data during Nov. - Apr.	1		5348
	soil temperature at −10 cm	mid 2006-10	hourly	automatic temperature sensors	1		35808
	soil temperature at −40 cm	mid 2006-10	hourly	automatic temperature sensors	1		35808
	LAI	2004	11 times	optical canopy analyser	2		11
Hor	NEE	2004-10,	hourly	EC	1	Hendriks et al.,	49611

Appendix to materials and methods

Site	Variable	Period	Resolution as used for calibration	Method	replicates	Described in	number of data points
		except 2007				2007	
	R_{eco}	2003-06	biweekly	manual opaque chamber	6		53
	R_{eco}, GPP	2004-10, except 07,09	hourly	empirical model from EC data	1	Reichstein et al., 2005; Papale et al., 2006	39420
	winter R_{eco}	2004-10, except 07,09	hourly	empirical modelling from night NEE EC data during Nov. - Apr.	1		3966
	soil temperature at −8 cm	mid 2004-mid 2011	hourly	automatic temperature sensors	1		48881
	soil temperature at −11 cm	mid 2004-mid 2011	hourly	automatic temperature sensors	1		48881
	LAI	2006-07	4 times a year	optical canopy analyser, weighted mean from 7 vegetation types	3	Hendriks, 2009	8
	above-ground biomass	2005-07	4 times a year	0.16 m^2 clipped, dead leaves removed, weighted mean from 7 vegetation types	3	Hendriks, 2009	12
	Root biomass	2006-07	4 times a year	sieved soil cores of $1.15 \cdot 10^{-4} \, m^3$, dead roots manually removed, weighted mean from 7 vegetation types	2	Hendriks, 2009	8
FsA and FsB	NEE	2007-2011	3-4 weekly several measurements per day	manual transparent chamber	3	Eickenscheidt et al., 2015	1161
	R_{eco}	2007-2011	3-4 weekly several measurements per day	manual opaque chamber	3	Eickenscheidt et al., 2015	1161
	GPP	2007-2011	3-4 weekly several measurements per day	empirical model from chamber data	3	Eickenscheidt et al., 2015	1161
	winter R_{eco}	2007-2011	3-4 weekly several measurements	manual opaque chamber during Nov.-Apr.	3		357

Site	Variable	Period	Resolution as used for calibration per day	Method	replicates	Described in	number of data points
	soil temperature at −2 cm	2007	hourly	automatic temperature sensors	1		36447
	soil temperature at −50 cm	2007	hourly	automatic temperature sensors	1		36447
	LAI	summer 2011-summer 2012	~3 weekly	optical canopy analyser	3		26
	Above-ground biomass	2007-2011	4 weekly	0.04 m², since 2011 0.16 m², clipped and sorted into living and dead	3		43
Deg	NEE	2001-2012	hourly	EC	1	Peichl et al., 2014 and references therein	86523
	LE & H	2001-2009	hourly		1		78872
	Net radiation	2001-2012	hourly		1		81717
	water table depth	2001-2009	daily		1		2981
	soil temperature at −2 cm	2001-2012	hourly	automatic temperature sensors	1		84258
	soil temperature at −42 cm	2001-2012	hourly	automatic temperature sensors	1		84154
	LAI	May-Sept 2012	biweekly	optical canopy analyser	7	Peichl et al., 2015	9
	Above-ground biomass	August 2008	once	clipping from one quarter of a circular 15 cm radius plot	32	Laine et al., 2012; Peichl et al., 2015	1
	Snow depth	mid 2006-10	hourly	automatic sensor	1		34316

Appendix to materials and methods

Table A1.10. List of main equations used in study I and II.

Equation	No.	Definition
Plant biotic processes		

$$C_{Atm \to a} = \varepsilon_L \cdot \eta \cdot f(T_l) \cdot f(E_{ta} / E_{tp}) \cdot R_{s,pl}$$

1.1 — Rate of photosynthesis g C m^{-2} day^{-1}

where ε_L is the radiation use efficiency and η is the conversion factor from biomass to carbon. $R_{s,pl}$ is the global radiation absorbed by canopy and $f(T_l)$,and $f(E_{ta} / E_{tp})$ limitations due to unfavourable temperature, nitrogen, and water conditions.

$$f(T_l) = \begin{cases} 0 & T_l < p_{mn} \\ (T_l - p_{mn})/(p_{o1} - p_{mn}) & p_{mn} \le T_l \le p_{o1} \\ 1 & p_{o1} < T_l < p_{o2} \\ 1 - (T_l - p_{o2})/(p_{mx} - p_{o2}) & p_{o2} \le T_l \le p_{mx} \\ 0 & T_l > p_{mx} \end{cases}$$

1.2 — Temperature response function for photosynthesis

where p_{mn}, p_{o1}, p_{o2} and p_{mx} are parameters and T_l the leaf temperature.

$$f(E_{ta} / E_{tp}) = \frac{E_{ta}}{E_{tp}}$$

1.3 — Response function for transpiration

where E_{ta} Eq. 29 and E_{tp} Eq. 23 are actual and potential transpiration.

$$C_{a \to Leaf} = l_{cl} \cdot C_a$$

1.4 — Allocation of new assimilates to the leaves

where l_{cl}, is a parameter and C_a the new assimilated carbon.

$$C_{a \to Root} = (1 - l_{cl}) \cdot C_a$$

1.5 — Allocation of new assimilates to the roots, respectively to below ground parts in case of mosses

where l_{cl}, is a parameter and C_a the new assimilated carbon.

$$C_{respleaf} = k_{mrespleaf} \cdot f(T) \cdot C_{leaf} + k_{gresp} \cdot C_{a \to Leaf}$$

1.6 — Plant growth and maintenance respiration g C m^{-2} day^{-1}

where $k_{mrespleaf}$ is the maintenance respiration coefficient for leaves, k_{gresp} is the growth respiration coefficient, and fT_a is the temperature. The equation calculates respiration from stem, roots, and grains by exchanging $k_{mrespleaf}$ to $k_{mrespstem}$, $k_{mresproot}$, $k_{mrespgrain}$, and using the corresponding storage pools. Respiration from the old carbon pools is estimated with the same maintenance respiration coefficients as for respiration from new carbon pools.

$$f(T) = t_{Q10}^{(T - t_{Q10bas})/10}$$

1.7 — Temperature response function for maintenance respiration –

where t_{Q10} and t_{Q10bas} are parameters.

$$C_{Leaf \to Stem} = l_{LS} \cdot C_{Leaf}$$

1.8 — Reallocation of C from leaf pool to stem pool – here used as pool for senescent leaves.

where l_{LS} is a parameter and C_{Leaf} the carbon in the leaf pool.

$$C_{Leaf \to LitterSurface} = f(T_{Sum}) \cdot f(A_l) \cdot s_{newleaf} \cdot C_{Leaf}$$

1.9 — Leaf C entering the surface litter pool is depending on the temperature sum and leaf area index.

where $s_{newleaf}$ is a scaling factor. Stem C is calculated analogously with $s_{newstem}$.

$$f(l_{Lc}) = l_{Lc1} + (l_{Lc2} - l_{Lc1}) \cdot \min\left(1, \frac{\max(0, T_{Sum} - t_{L1})}{\max(1, t_{L2} - t_{L1})}\right)$$

1.10 — Leaf litter fall dependence of temperature sum

where t_{L1}, t_{L2}, l_{Lc1} and l_{Lc2} are parameters and T_{Sum} is the so called "dorming" temperature sum, $T_{DormSum}$. $T_{DormSum}$ is calculated at the end to the growing season when the air temperature is below the threshold temperature $T_{DormTth}$, as the accumulated difference between $T_{DormTth}$ and Ta. $T_{DormTth}$ is a parameter.
The stem litter rate is calculated analogously with the parameters t_{S1}, t_{S2}, l_{Sc1} and l_{Sc2}, the root litter rate with the parameters l_{Lc2} to t_{R1}, t_{R2}, l_{Rc1} and l_{Rc2}.

Equation	No.	Definition

$$f(A_l) = e^{l_{LaiEnh} \cdot A_l}$$

1.11 — Litter fall dependency of LAI

where l_{LaiEnh} is a parameter and A_l the leaf area index

$$C_{Root \rightarrow Litter} = f(l_{Rc}) \cdot C_{Root} \cdot s_{newroot}$$

1.12 — Root C entering the soil litter pool of the corresponding layer

where $s_{newroot}$ is a scaling factor. The root litter rate function, fl_{Rc}, can be calculated with Eq. 10 by exchanging the parameters t_{L1}, t_{L2}, l_{Lc1} and l_{Lc2} to t_{R1}, t_{R2}, l_{Rc1} and l_{Rc2}.

$$z_r = p_{zroot} \left(\frac{B_r}{B_r + \frac{p_{zroot}}{p_{incroot}}} \right)$$

1.13 — Root depth

where p_{zroot} and $p_{incroot}$ are parameters and B_r is the mass of roots i.e. the carbon content in the roots, $C_{Roots} + C_{OldRoots}$.

$$C_{Mobile} = (C_{Leaf \rightarrow LitterSurface} + C_{OldLeaf \rightarrow LitterSurface}) \cdot m_{retain}$$

1.14 — Allocation to the mobile C pool for developing new leaves during litter fall

where m_{retain} is an allocation coefficient.

$$C_{Mobile \rightarrow Leaf} = C_{Mobile} \cdot m_{shoot}$$

1.15 — Allocation from the mobile C pool at leafing between GSI 1 and 2 as an additional supply. This process goes on as long as there is carbon left in the mobile pool.

where m_{shoot} is an allocation coefficient and C_{Mobile} the carbon in the mobile pool.

$$C_{Leaf \rightarrow Harvest} = f_{leafharvest} \cdot C_{Leaf}$$

1.16 — Amount of harvested carbon, removed from the system

where $f_{leafharvest}$ is a parameter. Harvest from the stem pool is calculated analogously by exchanging $f_{leafharvest}$ with $f_{stemharvest}$. These parameters are also used to calculate the harvest fractions from the old stem and leaves perennials.

$$C_{Leaf \rightarrow LitterSurface} = f_{leaflittharv} \cdot (C_{Leaf} - C_{Leaf \rightarrow Harvest})$$

1.17 — Amount of plant parts, which are removed from the plant and enter the surface litter pool at harvest

where $f_{leaflittharv}$ is a parameter. Similar flows are calculated for stem and roots by exchanging $f_{leaflittharv}$ to $f_{stemlittharv}$

$$C_{Mobile} = (C_{Leaf \rightarrow LitterSurface} + C_{OldLeaf \rightarrow LitterSurface}) \cdot m_{retain}$$

1.18 — Allocation to the mobile C pool for developing new leaves during litter fall

where m_{retain} is an allocation coefficient.

$$C_{Mobile \rightarrow Leaf} = C_{Mobile} \cdot m_{shoot}$$

1.19 — Allocation from the mobile C pool at leafing between GSI 1 and 2 as an additional supply. This process goes on as long as there is carbon left in the mobile pool.

where m_{shoot} is an allocation coefficient and C_{Mobile} the carbon in the mobile pool.

$$C_{Roots \rightarrow Leaf} = m_{Root} \cdot (C_{Roots} - C_{Leaf} \cdot r_{rl})$$

1.20 — Allocation of C in the roots to leaves, taking place after a harvest event as long as root:leaf ratio is smaller than the value of the parameter r_{rl} or until the plant goes to dormancy.

where m_{Root} and r_{rl} are parameters and C_{Roots} and C_{Leaf} the carbon in the root and leaf pool

$$C_{OldLeaf \rightarrow LitterSurface} = f(l_{Lc}) \cdot (C_{OldLeaf} - C_{RemainLeaf}) s_{oldleaf}$$

1.21 — Litter fall from roots, leaves and stems in the "old" biomass in perennial plants are calculated similarly to the "new" biomass but with the important exception that some of the old leaves may be retained

where or $s_{oldleaf}$ is a scaling factor. The litter fall for stems and roots is calculated analogously.

$$C_{RemainLeaf} = C_{OldLeaf} \left(1 - \frac{1}{l_{life} - 1}\right)$$

1.22 — Fraction of the whole $C_{OldLeaf}$ pool that will be excluded from the calculation of the litterfall from the old leaves

where l_{life} is a parameter

Plant abiotic processes

Appendix to materials and methods

Equation	No.	Definition
$$R_{s,pl} = (1 - e^{-k_{rn}\frac{A_l}{f_{cc}}}) \cdot f_{cc}(1 - a_{pl})R_{is}$$ where k_{rn} is the light use extinction coefficient given as a single parameter common for all plants, f_{cc} is the surface canopy cover, a_{pl} is the plant albedo and R_{is}, is the global qion. The plant albedo is calculated from the parameters: albedo vegetative stage, $apveg$, and/or albedo grain stage, $apgrain$, depending on plant development.	2.1	Plant interception of global radiation MJ m^{-2} day^{-1}
$$f_{cc} = p_{c\,max}(1 - e^{-p_{ck}A_l})$$ Where p_{cmax} is a parameter that determines the maximum surface cover and p_{ck} is a parameter that governs the speed at which the maximum surface cover is reached. A_l is the leaf area index of the plant.	2.2	Surface canopy cover m^2 m^{-2}
$$A_l = \frac{B_l}{p_{l,sp}}$$ Where $p_{l,sp}$ is a parameter and B_l is the total mass of leaf.	2.3	Leaf area index m^2 m^{-2} as function of leaf mass
$$L_v E_{tp} = \frac{\Delta R_n + \rho_a c_p \frac{(e_s - e_a)}{r_a}}{\Delta + \gamma\left(1 + \frac{r_s}{r_a}\right)}$$ where R_n is net radiation available for transpiration, e_s is the vapour pressure at saturation, e_a is the actual vapour pressure, ρ_a is air density, c_p is the specific heat of air at constant pressure, L_v is the latent heat of vaporisation, Δ is the slope of saturated vapour pressure versus temperature curve, γ is the psychrometer 'constant', r_s is 'effective' surface resistance and r_a is the aerodynamic resistance.	2.5	Potential transpiration E_{tp} mm day^{-1}
$$r_a^* = \frac{\ln^2\left(\frac{z_{ref} - d}{z_0}\right)}{k^2 u} + \Delta z_{snow}$$ where the wind speed, u, is given at the reference height, z_{ref}, k is von Karman's constant, d is the displacement height and z_o is the roughness length.	2.6	The aerodynamic resistance r_a as calculated without stability correction
$z_0 = z_{0max}$ $\quad\quad z_0 > z_{0max}$ $$z_0 = (H_p - \Delta z_{snow}\min(f_1, f_2)) + \Delta z_{snow}\quad z_{0min} > z_0 > z_{0max}$$ $z_0 = z_{0min}$ $\quad\quad z_0 < z_{0min}$ where z_{0max} and z_{0min} are parameters, f_1 and f_2 are functions describing the dependency on leaf area index and canopy density, Δz_{snow} is the snow depth and H_p is the canopy height.	2.7	The roughness length, z_0, is calculated according to the function derived from Shaw and Pereira 1982
$$d = \min\begin{pmatrix} z_{ref} - 0.5 \\ \left((0.80 + 0.11 p_{densm}) - \atop (0.46 - 0.09 p_{densm})e^{-(0.16 + 0.28 p_{densm})^{PAI}}\right)(H_p - \Delta z_{snow}) \end{pmatrix} + \Delta z_{snow}$$ p_{densm} is density maximum of canopy in relation to the canopy height, Δz_{snow} is the snow depth. PAI is the plant area index, H_p is the canopy height.	2.8	Displacement height d, as calculated by the Shaw and Pereira 1982 function
$$r_s = \frac{1}{\max(A_l g_l, 0.001)}$$ where g_l is the leaf conductance and A_l the leaf area index.	2.9	Stomatal resistance s m^{-1}
$$g_l = \frac{R_{is}}{R_{is} + g_{ris}}\frac{g_{max}}{1 + \frac{(e_s - e_a)}{g_{vpd}}}$$ where g_{ris}, g_{max} and g_{vpd} are parameter values, g_{maxwin} corresponds to g_{vpd} in winter. R_{is}, is the global radiation and $e_s - e_a$ the vapour pressure deficit.	2.10	Stomatal conductance per leaf area m s^{-1}

Equation	No.	Definition
$$E_{ta} = E_{tp}^* \int_{z_r}^{0} f\big(\psi(z)\big)\big(T(z)\big) r(z)$$ z_r is root depth Eq. 16, $f\big(\psi(z)\big)$ and fTz are response functions for soil water potential, and soil temperature and rz is the relative root density distribution which is exponentially decreasing from soil surface to the root depth.	2.11	Actual transpiration without flexibility of water transportation within the root system.
$$f\big(\psi(z)\big) = \left(\frac{\psi_c}{\psi(z)}\right)^{p_1 E_{tp} + p_2}$$ where p_1, p_2 and ψ_c are parameters. If the soil water potential is reaching the wilting point, ψ_{wilt}, the uptake is assigned to be zero from that horizon.	2.12	Transpiration response to water stress
$$f\big(T(z)\big) = 1 - e^{-t_{WA}\, \max(0,\, T(z) - T_{trig})^{t_{WB}}}$$ where t_{WA} and t_{WB} and the trigging temperature T_{trig} are parameters.	2.13	Transpiration response to temperature as proposed by Axelsson and Ågren 1976

Surface Energy balance

Equation	No.	Definition
$$R_{ns} = L_v E_s + H_s + q_h$$	3.1	The physically based approach, for calculating soil evaporation, originates from the idea of solving an energy balance equation for the soil surface. According to the law of conservation of energy the net radiation at the soil surface, R_{ns}, is assumed to be equal to the sum of latent heat flux, $L_v E_s$, sensible heat flux, H_s and heat flux to the soil, q_h. The three different heat fluxes are estimated by an iterative procedure where the soil surface temperature, T_s, is varied according to a given scheme until the equation is balanced
$$H_s = \rho_a c_p \frac{(T_s - T_a)}{r_{as}}$$ where air density, ρ_a and the specific heat of air at constant pressure, c_p are considered as physical constants, r_{as} is the aerodynamic resistance calculated as a function of wind and temperature gradients	3.2	sensible heat flux, H_s
$$r_{as} = r_{aa} + r_{ab}$$ where r_{aa} is a function of wind speed and temperature gradients, which is corrected for atmospheric stability, and r_{ab} is an additional resistance representing the influence of the crop cover,	3.3	Aerodynamic resistance above the soil surface, r_{as}, is calculated as a sum of two components
$$r_{aa} = \frac{1}{k^2 u} \left\{ \ln\left(\frac{z_{ref} - d}{z_{0M}}\right) - \psi_M\left(\frac{z_{ref} - d}{L_O}\right) + \psi_M\left(\frac{z_{0M}}{L_0}\right) \right\} \times$$ $$\times \left\{ \ln\left(\frac{z_{ref} - d}{z_{0H}}\right) - \psi_H\left(\frac{z_{ref} - d}{L_O}\right) + \psi_H\left(\frac{z_{0H}}{L_0}\right) \right\}$$ where u is the wind speed at the reference height, z_{ref}, d is the zero level displacement height c.f. potential transpiration of plant, k is the von Karmans constant and z_{0M} and z_{0H} are the surface roughness lengths for momentum and heat respectively. If z_{0M} is exchanged to $z_{0M,snow}$ the equation can be used for snow surfaces. L_O is the Obukhov length and ψ_M and ψ_H are empirical stability functions for momentum and heat respectively. Furthermore, an upper limit of the aerodynamic resistance in extreme stable conditions is set by the "windless exchange" coefficient, $r_{a,soil,max}^{-1}$	3.4	Stability function for aerodynamic resistance at neutral conditions

Appendix to materials and methods

Equation	No.	Definition

$$r_{ab} = r_{aLai} A_l$$

where r_{alai} is an empirical parameter

3.5 — Additional aerodynamic resistance representing the influence of the crop cover

$$L_v E_s = \frac{\rho_a c_p (e_{surf} - e_a)}{\gamma \cdot r_{as}}$$

Where e_{surf} is the vapour pressure at the soil surface and e_a is the actual vapour pressure in the air.

3.6 — Sum of latent heat flux, $L_v E_s$

$$e_{surf} = e_s(T_s) e^{\left(\frac{-\psi_l M_{water}\, g \cdot e_{corr}}{R(T_s + T_{abszero})}\right)}$$

where R is the gas constant, M_{water} is the molar mass of water, g is the gravity constant and e_s is the vapour pressure at saturation.
The empirical correction factor, e_{corr}, depends on an empirical parameter ψ_{eg} and a calculated mass balance at the soil surface, δ_{surf}, which is allowed to vary between the parameters s_{def} and s_{excess} given in mm of water.

3.7 — Vapour pressure at the soil surface

$$q_h = k_h \frac{(T_s - T_1)}{\frac{\Delta z_1}{2}} + L q_{v,s}$$

where k_h is the thermal conductivity of the top soil layer, Lv, as well as the psychrometer constant, γ, are considered as physical constants; $q_{v,s}$, is the vapor flow from the soil surface to the central point of the uppermost compartment

3.8 — Heat flux to the soil, q_h.

$$q_{v,s} = -d_{vapd} f_a D_0(T) \frac{c_{vl} - c_{vs})}{\frac{\Delta z}{2}}$$

where d_{vapb} is the tortuosity given as an empirical parameter, D_0 is the diffusion coefficient for a given temperature, f_a is the fraction of air filled pores $\theta_s - \theta_s$ and c_{vs} and c_{vl} are the concentrations of water vapour at the soil surface and at the middle of the uppermost compartment respectively.

3.9 — Vapor flow from the soil surface to the central point of the uppermost compartment

---

Snow

$$k_{snow} = s_k \rho_{snow}^2$$

where s_k is an empirical parameter.

4.1 — Thermal conductivity of snow

$$\rho_{snow} = \frac{\rho_{prec}\Delta z_{prec} + \rho_{old}\Delta z_{old}}{\Delta z_{snow}}$$

4.2 — Density of snow is a weighted average of the old snow pack i.e. the density of snow remaining from the previous day ρ_{old} and precipitation density, ρ_{prec}

$$\rho_{prec} = \rho_{smin} + 181\frac{(1 - Q_p)}{f_{liqmax}}$$

where ρ_{smin} is the density of new snow, Q_p is the thermal quality of precipitation and f_{liqmax} is a parameter that defines the maximum liquid water content of falling snow that is automatically put to 0.5.

4.3 — Density of new-fallen snow as a function of air temperature, T_a

$$Q_P = \begin{cases} \min\left(1, (1 - f_{liqmax}) + f_{liqmax}\dfrac{T_a - T_{RainL}}{T_{SnowL} - T_{RainL}}\right) & T_a \leq T_{RainL} \\ 0 & T_a > T_{RainL} \end{cases}$$

where f_{liqmax} is a parameter that defines the maximum liquid water content of falling snow and is automatically put to 0.5. T_{RainL} and T_{SnowL} are the temperature range where precipitation is regarded as a mixture of ice and liquid water.

4.4 — Thermal quality of precipitation its fractional frozen water content

Equation	No.	Definition
$$\rho_{old} = \rho_{smin} + s_{dl}\frac{S_{wl}}{S_{wlmax}} + s_{dw}S_{res}$$ where s_{dl} and s_{dw} are parameters, S_{wlmax} is the retention capacity and S_{res} is the water equivalent of the snow.	4.5	Density of the old snow pack increases with the relative amount of free water in the pack and with overburden pressure, i.e., with increasing water equivalent. Density also generally increases with age. The age dependency is accounted for by updating density as the maximum density of the previous time step
$$\Delta z_{old} = \frac{S_{res}}{\rho_{old}}$$	4.6	Depth of old snow pack
$$f_{bare} = \begin{cases} \dfrac{\Delta z_{snow}}{\Delta z_{cov}} & \Delta z_{snow} < \Delta z_{cov} \\[2mm] 0 & \Delta z_{snow} \geq \Delta z_{cov} \end{cases}$$ where Δz_{cov} is a threshold parameter.	4.7	The fraction of snow free ground is used the estimate the average soil surface temperature, and the average surface albedo, during conditions of "patchy" snow cover.
$$M = M_T T_a + M_R R_{is} + \frac{f_{qh}q_h(0)}{L_f}$$ where Ta is air temperature, Ris is global radiation, fqh is a scaling coefficient and Lf is the latent heat of freezing. Melting will affect the whole snow pack, whereas refreezing will only affect a limited surface layer.	4.8	The fundamental part of the empirically based snow model is the melting-freezing function, which combines the mass and heat budgets. The amount of snow melt, M, is made up by a temperature function, MT, a function accounting for influence of solar radiation, MR, and the soil surface heat flow, $qh0$:
$$M_T = \begin{cases} m_T & T_a \geq 0 \\[2mm] \dfrac{m_T}{\Delta z_{snow}m_f} & T_a < 0 \end{cases}$$ where Ta is air temperature and mT And mf are parameters.	4.9	Refreezing efficiency is, inversely proportional to snow depth, $\Delta zsnow$:
$$M_R = m_{Rmin}(1 + s_1(1 - e^{-s_2 s_{age}}))$$ where $mRmin$, $s1$ and $s2$ are parameters. Age of surface snow, $sage$, is determined by the number of days since the last snowfall. To reduce the influence of mixed precipitation and minor showers, snowfall is counted in this context only for snow spells larger than a critical value, $psamin$, and for precipitation with thermal quality, Qp, above a threshold value	4.10	Global radiation dependence of snow melt

Soil carbon and nitrogen processes

Equation	No.	Definition
$$C_{DecompL} = k_l \cdot f(T) \cdot f(\theta) \cdot C_{Litter}$$ Where k_l is a parameter and $f(T)$ and $f(\theta)$ are response functions for soil temperature and moisture in the certain layer.	5.1	Decomposition of the SOC pools for plant litter g C m^{-2} day^{-1}
$$C_{DecompH} = k_h \cdot f(T) \cdot f(\theta) \cdot C_{Humus}$$ Where k_h is a parameter and $f(T)$ and $f(\theta)$ are response functions for soil temperature and moisture in the certain layer.	5.2	Decomposition of the SOC pools for more stable material g C m^{-2} day^{-1}

Appendix to materials and methods

Equation	No.	Definition
$$f(\mathrm{T}) = 1 \qquad T > t_{\max}$$ $$f(\mathrm{T}) = \left(\frac{T - t_{\min}}{t_{\max} - t_{\min}}\right)^2 \quad t_{\min} < T < t_{\max}$$ $$f(\mathrm{T}) = 0 \qquad T < t_{\min}$$ Where t_{min} and t_{max} are parameters and T the soil temperature in the certain layer.	5.3	Response function for soil temperature according Ratkowsky. –
$$f(\theta) = \min \begin{pmatrix} \left(\dfrac{\theta_s - \theta}{p_{\theta Upp}}\right)^{p_{\theta p}} (1 - p_{\theta satact}) + p_{\theta satact}, \\ \left(\dfrac{\theta - \theta_{wilt}}{p_{\theta Low}}\right)^{p_{\theta p}} \\ 0 \end{pmatrix}$$ $$\begin{matrix}p_{\theta satact} & \theta = \theta_s \\ \\ \theta_{wilt} \le \theta \le \theta_s \\ \\ \theta < \theta_{wilt}\end{matrix}$$ where $p_{\theta Upp}$, $p_{\theta Low}$, $p_{\theta Satact}$, and $p_{\theta p}$ are parameters and the variables, θ_s, θ_{wilt}, and θ, are the soil moisture content at saturation, the soil moisture content at the wilting point, and the actual soil moisture content, respectively.	5.4	Response function for soil moisture –
$$C_{LitterSurface \to Litter1} = l_{ll} \cdot C_{LitterSurface}$$ where l_{ll} is a parameter and $C_{LitterSurface}$ the carbon in the surface litter pool.	5.5	Litter from inactive surface litter pool, entering the fast SOC pool at a continuous rate.
$$C_{Litter \to CO_2} = (1 - f_{e,l}) \cdot C_{DecompL}$$ where $f_{e,l}$ is a parameter	5.6	Amount of decomposition products from the fast SOC pools being released as CO_2
$$C_{Litter \to Humus} = f_{e,l} \cdot f_{h,l} \cdot C_{DecompL}$$ where $f_{e,l}$ and $f_{h,l}$ are parameters	5.7	Amount of decomposition products from the fast SOC pools entering the slow decomposition pools
$$C_{Litter \to Litter} = f_{e,l}(1 - f_{h,l}) \cdot C_{DecompL}$$ where $f_{e,l}$ and $f_{h,l}$ are parameters	5.8	Amount of decomposition products from the fast SOC pools being returned to the fast decomposition pools
$$C_{Humus \to CO_2} = f_{e,h} \cdot C_{DecompL}$$ where $f_{e,h}$ is a parameter	5.9	Amount of decomposition products from the slow SOC pools being released as CO_2

Soil heat processes

$$q_h = -k_h \frac{\partial T}{\partial z}$$ where k_h is the conductivity, T is the soil temperature and z is depth.	6.1	Soil heat flux J m^{-2} day^{-1}
$$q_h(0) = k_{ho} \frac{(T_s - T_1)}{\Delta z / 2} + C_w(T_s) q_{in} + L_v q_{vo}$$ where k_{ho} is the conductivity of the organic material at the surface, T_s is the surface temperature, T_1 is the temperature in the uppermost soil layer, q_{in}, is the water infiltration rate, q_{vo} is the water vapour flow, and L_v is the latent heat.	6.2	Upper boundary condition for soil heat flow J m^{-2} day^{-1}
$$k_{ho} = h_1 + h_2 \theta$$ where h_1 and h_2 are empirical constants	6.3	Heat conductivity of the organic material at the surface
$$T_{ss} = \frac{T_1 + a T_a}{1 + a}$$ where the index 1 means the top soil layer, and the snow surface temperature is assumed to be equal to air temperature. a is a weighting factor depending on snow thickness and conductivity in the snow pack and	6.4	Soil surface temperature under the snow pack, during periods with snow cover °C

Equation	No.	Definition

in the uppermost soil layer.

$$T_{LowB} = T_{amean} - T_{aamp}e^{-\frac{z}{d_a}} \cos\left(\left(t - t_{ph}\right)\omega - \frac{z}{d_a}\right)$$

6.5 — Temperature at the lower boundary for heat conduction °C

where T_{amean} and T_{aamp} are parameters, t is the time, t_{ph} is the phase shift, ω is the frequency of the cycle and d_a is the damping depth.

Soil water processes

$$q_w = -k_w\left(\frac{\partial \psi}{\partial z} - 1\right) - D_v \frac{\partial c_v}{\partial z}$$

6.6 — The total water flow, q_w, is the sum of the matrix flow, q_{mat} and the vapour flow, q_v, mm day^{-1}

where k_w is the unsaturated hydraulic conductivity, ψ is the water tension, z is depth, c_v is the concentration of vapour in soil air and D_v is the diffusion coefficient for vapour in the soil

$$\frac{\partial \theta}{\partial t} = -\frac{\partial q_w}{\partial z} + s_w$$

6.7 — The general equation for unsaturated water flow follows from the law of mass conservation and eq. 30

where θ is the soil water content and s_w is a source/sink term for e.g. horizontal in and outflow or root water uptake.

$$S_e = \left(\frac{\psi}{\psi_a}\right)^{-\lambda}$$

6.8 — Water tension ψ according to Brooks and Corey 1965, between the threshold values ψ_x and ψ_{mat}.

where ψ_a is the air-entry tension, λ is the pore size distribution index and S_e the effective saturation.

$$S_e = \frac{\theta - \theta_r}{\theta_s - \theta_r}$$

6.9 — Effective saturation S_e between the threshold values ψ_x and ψ_{mat}.

where θ_s is the porosity, θ_r is porosity content and θ is the actual water content.

$$k_w^* = k_{mat}\left(\frac{\psi_a}{\psi}\right)^{2+(2+n)\lambda}$$

6.10 — Unsaturated hydraulic conductivity k_w^* mm day^{-1} according Brooks and Corey 1965.

Where the matrix conductivity k_{mat} is a function of the total conductivity, n is a parameter accounting for pore correlation and flow path tortuosity and λ is the pore size distribution index.

$$k_{mat} = 10^{(\log k_{sat} - \log h_{com})h_{sens} + \log k_{sat}}$$

6.11 — Matrix conductivity as function of total conductivity

where h_{com} and h_{sens} are parameters and k_{sat} is the total saturated conductivity.

$$q_{wp} = \int_{z_p}^{z_{sat}} k_s \frac{\left(z_{sat} - z_p\right)}{d_u d_p} dz$$

6.12 — The horizontal flow rate, q_{wp}, is assumed to be proportional to the hydraulic gradient and to the thickness and saturated hydraulic conductivity of each soil layer

where d_u is the unit length of the horizontal element i.e. 1 m, z_p is the lower depth of the drainage pipe i.e. the drainage level, z_{sat} is the simulated depth of the ground water table and d_p is a characteristic distance between drainage pipes. Note that this is a simplification where the actual flow paths and the actual gradients are not represented. Only flows above the drain level z_p are considered

Appendix to materials and methods

Equation	No.	Definition
$$k_w^* = 10^{\left(\log(k_w^*(\theta_s-\theta_m)) + \frac{\theta+\theta_s+\theta_m}{\theta_m} \log\left(\frac{k_{sat}}{k_w(\theta_s-\theta_m)} \right) \right)}$$	6.13	Total conductivity close to saturation above the threshold ψ_s, to account for the conductivity in the macro pores.

where k_{sat} is the saturated total conductivity, which includes the macro pores, and $k_w^* \theta_s - \theta_m$ is the hydraulic conductivity below $\theta_s - \theta_m$ i.e. at ψ_{mat} calculated from Eq. 51

Equation	No.	Definition
$$k_w = (r_{AOT} + r_{A1T} T_s) \max(k_w^*, k_{minuc})$$	6.14	Actual unsaturated hydralic conductivity after temperature corrections

where r_{AOT}, r_{A1T} and k_{minuc} are parameter values. k_w^* is the conductivity according to eqs 51 and 52

Table A1.11. Calibrated parameters of study I.

Symbol	Name	Unit	Eq.	Definition	Min	Max
g_{maxwin}	CondMaxWinter	m s^{-1}	2.10	maximal conductance of fully open stomata to calculate the potential transpiration of plants during winter	0.002	1
g_{ph}	GSI Post Harvest1	-		growth stage to which the plant is set back after harvest	1.3	3
k_{gresp}	GrowthCoef1	day^{-1}	1.6	rate coefficient for growth respiration of the plant respiration relative to amount of assimilates	0.13	0.25
k_l	RateCoefLitter1	a^{-1}	5.1	rate coefficient for the decay of SOC in the fast pools		0.003
$k_{mrespleaf}$	MCoefLeaf1	day^{-1}	1.6	rate coefficient for maintenance respiration of leaves respiration relative to leaf biomass	0.015	0.035
$k_{mresproot}$	MCoefRoot1	day^{-1}	1.6	maintenance respiration coefficient for root respiration relative to root biomass		0.003
$k_{mrespstem}$	MCoefStem1	day^{-1}	1.6	maintenance respiration coefficient for stem respiration relative to stem biomass		0.013
k_{rn}	RntLAI	-	2.1	extinction coefficient in the Beer's law used to calculate the partitioning of net radiation between canopy and soil surface	0.52	1
l_{cl}	Leaf c11	g C^{-1}	1.4, 1.5	fraction of new assimilates which is allocated to the leaves	0.52	0.55
l_{ll}	RateCoefSurf L1	day^{-1}	5.5	fraction of the above ground residues that enter the litter 1 pool of the uppermost soil layer	0.002	0.008
l_{LaiEnh}	LAI Enh Coef1	-	1.11	scaling factor for enhanced leaf litter fall rates when higher LAI values are reached	0.0016	0.6
l_{Lc1}	LeafRate11	day^{-1}	1.10,1.12	rate coefficient for the leaf litter fall before the first threshold temperature sum t_{L1} is reached		0.05
l_{Lc2}	LeafRate21	day^{-1}	1.10,1.12	rate coefficient for the leaf litter fall after the second threshold temperature sum t_{L2} is reached	0.1	0.3
l_{LS}	C Leaf to Stem1	-	1.8	scaling factor for reallocation of C from leaf to stem after the plant reached maturity growth state	0.015	0.025
l_{Rc1}	RootRate11	day^{-1}	1.10,1.12	rate coefficient for the litter fall from roots before the first threshold temperature sum t_{R1} is reached		0.015
l_{Rc2}	RootRate21	day^{-1}	1.10,1.12	rate coefficient for the litter fall from roots after the second threshold temperature sum t_{R2} is reached	0.01	0.05

Symbol	Name	Unit	Eq.	Definition	Min	Max
l_{Sc1}	StemRate11	day^{-1}	1.10	rate coefficient for the litter fall from stems before the first threshold temperature sum t_{S1} is reached	0.003	0.1
l_{Sc2}	StemRate21	day^{-1}	1.10	rate coefficient for the litter fall from stems after the second threshold temperature sum t_{S2} is reached	0.03	0.2
m_{retain}	Mobile Allo Coef	-	1.14	coefficient for determining allocation to mobile internal storage pool	0.4[a], 0.05[bc], 0.01[d]	0.8[ab], 0.5[c], 0.45[d]
m_{Root}	RateCoef_fRoot1	-	1.20	speed at which reallocation of C from roots to leaves after harvest take place	0.005	0.04
m_{shoot}	Shoot Coef	-	1.15	coefficient for the rate at which C is reallocated from the mobile pool to the leaf at leafing	0.05	0.15
p_{ck}	Area kExp1	-	2.2	speed at which the maximum surface cover of the plant canopy is reached	0.5	1
p_{Lsp}	Specific LeafArea	g C m^{-2}	2.3	factor for calculating LAI from leaf biomass, which is actually the inverse of specific leaf area, i.e. leaf mass per unit leaf	44	49
p_{mn}	T LMin1	°C	1.2	minimum mean air temperature at which photosynthesis can take place	0.001	0.5
$p_{\theta p}$	ThetaPowerCoef	vol %	5.4	power coefficient in the response function of microbial activity in dependency of soil moisture	0.65	4.5
$p_{\theta Satact}$	Saturation activity	vol %	5.4	parameter in the soil moisture response function defining the microbial activity under saturated conditions	0.001	0.252, 1[f]
$p_{\theta Upp}$	ThetaUpperRange	vol %	5.4	water content interval in the soil moisture response function for microbial activity	20, 8[f]	77
r_{rl}	Root Leaf Ratio1	-	1.20	threshold value for the root:leaf ratio at which reallocation of C from roots to leaves takes place after an harvest event	5	6.5
$s_{newleaf}$	New Leaf1	-	1.9	scaling factor for litter fall from new leaves	0.15	0.25
$s_{newroot}$	New Roots1	-	1.12	scaling factor for litter fall from new roots	0.1	0.25
$s_{newstem}$	New Stem1	-	1.9	scaling factor for litter fall from new stems	0.1	0.15
T_{amean}	TempAirMean	°C	6.5	assumed value of mean air temperature for the lower boundary condition for heat conduction.	5.5[a], 10.5[b,d], 13[c]	6.2[a], 15.5[b,c], 13[d]
$T_{DormTth}$	Dormancy Tth	°C	1.10	threshold temperature for plant dormancy – if the temperature falls below this value for five consecutive days, the dormancy temperature sum starts to be calculated.	0.1	2.5, 5[f]
$T_{EmergeSum}$	TempSumStart	°C		air temperature sum which is the threshold for start of plant development	0.5	10
$T_{EmergeTh}$	TempSumCrit	°C		critical air temperature that must be exceeded for temperature sum calculation	0.15	1
t_{L1}	LeafTsum11	day°C	1.10,1.12	threshold temperature sum after reaching dormancy state for the lower leaf litter rate. When it is reached, l_{Lc1} starts to change towards the increased litter fall rate l_{Lc2}	10	20

Appendix to materials and methods

Symbol	Name	Unit	Eq.	Definition	Min	Max
t_{L2}	LeafTsum21	day°C	1.10,1.12	threshold temperature sum after reaching dormancy state for the higher leaf litter rate. When it is reached, the full high litter rate is applied.	20	50
$T_{MatureSum}$	Mature Tsum	°C		temperature sum beginning from grain filling stage for plant reaching maturity stage	80[a], 320[b], 750[c], 1050[d]	115[a], 450[b], 850[c], 1350[d]
t_{Q10}	TemQ10	-	1.7	response to a 10 °C soil temperature change on the microbial activity, mineralisation-immobilisation, nitrification and denitrification and plant maintenance respiration	1.95	3.5
t_{Q10bas}	TemQ10Bas	°C	1.7	base temperature for the microbial activity, mineralisation-immobilisation, nitrification and denitrification at which the response is 1	15	26
t_{R1}	RootTsum11	day°C	1.10,1.12	threshold temperature sum after reaching dormancy state for the lower root litter rate. When it is reached, t_{Rc1} starts to change towards the increased litter fall rate t_{Rc2}	10	20
t_{R2}	RootTsum21	day°C	1.10,1.12	threshold temperature sum after reaching dormancy state for the higher root litter rate. When it is reached, the full high litter rate is applied.	20	50
t_{S1}	StemTsum11	day°C	1.10	threshold temperature sum after reaching dormancy state for the lower stem litter rate. When it is reached, t_{Sc1} starts to change towards the increased litter fall rate t_{Sc2}	10	20
t_{S2}	StemTsum21	day°C	1.10	threshold temperature sum after reaching dormancy state for the higher stem litter rate. When it is reached, the full high litter rate is applied.	20	50
ε_L	PhoRadEfficiency	gDw MJ^{-1}	1.1	radiation use efficiency for photosynthesis under optimum temperature, moisture and nutrients conditions	1.5[a], 2.3[b], 1.8[c], 2.5[d]	2.6[ab], 3.2[cd]

[a] at Lom
[b] at Amo
[c] at Hor
[d] at FsA and FsB
[e] Parameter uses opposite values to the linked parameter
[f] range tested in additional multiple runs

133

Table A1.12. Calibrated parameters of study II

Symbol	Unit	Equation cf. Table S2	Module	Definition	Min	Max	Literature or default value
Δz_{cov}	m	4.7	Snow coverage	The thickness of mean snow height that corresponds to a complete cover of the soil.	$1\cdot10^{-3}$	0.02	0.01 default value
$m_{R\,min}$	kg J^{-1}	4.10	Snow melt dependency on radiation	Coefficient in the global radiation response of the empirical snow melt function.	$2.3\cdot10^{-7}$	$3\cdot10^{-7}$	$1.5\cdot10$-7 default value
f_{qh}		4.8	Snow melt dependency on soil heat	Scaling coefficient for the contribution of heat flow from ground on the melting of the snow in the empirical snow melt function.	0.3	0.7	0.5 default value
S_{dw}	m^{-1}	4.5	Snow: density coefficient of old snow	Mass coefficient in the calculation of snow density as a function of liquid and ice content in the "old" snow pack.	0.6	1	0.5 default value
s_{dl}	kg m^{-3}	4.5	Snow: density dependence on liquid an ice content	Liquid water coefficient in the calculation of snow density as a function of liquid and ice content. The snow density increase with this value when the liquid water content in the snow pack becomes equal to the total retention capacity	160	210	200 default value
$\rho_{sm\,in}$	kg m^{-3}	4.3	Snow: density of new snow	Density of new snow.	90	120	100 default value
m_T	kg °C^{-1} m^{-2} day^{-1}	4.9	Snow: melting dependency to temperature	Coefficient for temperature dependance in the empirical snow melt function.	2.5	4	A value of 2 is normal for forests. Similar as for MeltCoefGlobRad a two or three fold increase is expected if adaptation to an open filed is to be done Jansson and Karlberg 2010.
$T_{Ra\,inL}$		4.4	Snow: temperature treshold for rain:snow	Above this temperature all precipitation is rain.	1.7	2.2	2 default value
h_{com}	mm day^{-1}	6.11	Soil hydraulic conductivity under saturated conditions	Unsaturated matrix conductivity dependency on total saturated conductivity	0.01	100	10 default value
ψ_a	cm	6.8	Soil hydraulic properties: shape of water retention in the upper horizon	Air-entry tension. As this was the only calibrated parameter defining the shape pF-curve, it determines unsaturated water distribution in the soil including capillary rise.	1 3	8 10	Range received by comparing resulting pF curves with curves measured in peatlands Kellner and Lundin, 2001; Values in bracket were used for soil horizons < −30 cm
d_p	m	6.12	Soil hydrology: drainage distance	Characteristic distance between drainage pipes, denominator when estimating the gradient necessary for the calculation of the horizontal water flow to drainage pipe	30	330	site specific estimation
$g_{max,\,vasc}$	m^2 s^{-1}	2.10	Transpiration efficiency	Transpiration coefficient for vascular plants: the maximal conductance of fully open stomata in the Lohammar equation Lohammar et al., 1980 for calculating leaf conductance and surface resistance.	0.02	0.1	Results from a pre-study calibration with the site data
$g_{max,\,mos}$	m^2 s^{-1}	2.10	Transpiration efficiency	Transpiration coefficient for mosses: the maximal conductance of fully open stomata in the Lohammar equation Lohammar et al., 1980	0.017	0.03	Results from a pre-study calibration with the site data

Symbol	Unit	Equation cf. Table S2	Module	Definition	Min	Max	Literature or default value
s				for calculating leaf conductance and surface resistance.			
g_{maxwin}	m s^{-1}	2.10	Transpiration efficiency outside the growing season	Maximal conductance of fully open stomata to calculate the potential transpiration of plants during winter	0.001	0.03	Results from a pre-study calibration with the site data
t_{WA}	-	2.13	Transpiration stress due to limited water availability under low temperatures	Temperature coefficient in the temperature response function.	0.8	10	Results from a pre-study calibration with the site data
ψ_c	cm water	2.12	Transpiration stress due to too low water content	Critical pressure head for reduction of potential water uptake. A wide range 100-3000 cm water of values has been reported in the literature. Lower values are expected for sandy soils with low root densities and higher values are expected for clayey soils with high root densities	1	330	Results from a pre-study calibration with the site data
p_1	day^{-1}	2.12	Transpiration stress due to too low water content	Coefficient for the dependence of potential water uptake in the reduction function. The dependence of the potential uptake rate has frequently been reported as an important phenomenon for reduction of water uptake	0.3	2	0.3 default value
ψ_{eg}	-	3.7	Vapour pressure at the soil surface	Factor to account for differences between water tension in the middle of top layer and actual vapour pressure at soil surface	0	2	1 default value
$c_{H0,canopy}$	m s^{-1}	2.6	Aerodynamic resistance of canopy: minimum exchange under stabile conditions	Roughness length used in the calculation of r_a for each plant, corresponds to z_0 in Equation 2.6.	$1 \cdot 10^{-4}$	0.1	0.001 default value
$r_{a, max, snow-1}$	s^{-1}		Aerodynamic resistance of snow: minimum exchange under stabile conditions	Minimum turbulent exchange coefficient inverse of maximum allowed aerodynamic resistance over snow. Avoids exaggerated surface cooling in windless conditions or extreme stable stratification.	0	$1 \cdot 10^{-4}$	Results from a pre-study calibration with the site data
r_{alai}	s m^{-1}	3.5	Aerodynamic resistance: contribution of LAI	The contribution of LAI to the total aerodynamic resistance from measurement height reference level to the soil surface.	100	800	Results from a pre-study calibration with the site data
$z_{0M,snow}$	m	2.7, 2.8	Aerodynamic resistance: roughness length of snow	Roughness length for momentum above snow.	$1 \cdot 10^{-5}$	0.001	Results from a pre-study calibration with the site data
s_k	W m^5 °C^{-1} kg^{-2}	4.1	Soil temperature: thermal conductivity of snow	Thermal conductivity coefficient for snow.	$1.2 \cdot 10^{-6}$	$2.86 \cdot 10^{-6}$	Results from a pre-study calibration with the site data
h_2	-	6.3	Soil temperature – thermal conductivity	Empirical constant in the heat conductivity of the organic material at the surface	0.0045	0.0075	0.005 default value
$T_{a,mean}$	°C	6.5	Soil temperature – lower boundary	Assumed value of mean air temperature for the lower boundary condition for heat conduction.	5.5	8	Based on results from a pre-study calibration with the site data. Should be 1.5-5°C higher than annual mean temperature Metzger et al. 2015 which was 2.3 °C at Degerö during the

Symbol	Unit	Equation cf. Table S2	Module	Definition	Min	Max	Literature or default value
							simulation period
$a_{pg\,rain}$	%	2.1	Radiation interception: plant albedo	Plant albedo during grain stage	20	31	Dry grass and straw up to 29 and 33, respectively Kondratiev et al., 1964
$a_{pve,\,vasc}$	%	2.1	Radiation interception: vascular plant albedo	Plant albedo of vascular plants during vegetative stage	10	25	12-22 for *Carex*; 12.5 for bog, raised edge; 17.8 for bog, depression Petzold and Rencz, 1975
$a_{pve,\,moss}$	%	2.1	Radiation interception: moss albedo	Plant albedo of vascular plants during vegetative stage	10	30	11-16% in a *Sphagnum*-sedge bog Berglund and Mace, 1972, 16.4 for *Sphagnum*, 17.5 for *Carex*, 17.9 for *Pragmites* Zhao et al., 1997
$\varepsilon_{L,\,vasc}$	gDW MJ^{-1}	1.1	Plant assimilation efficiency	Radiation use efficiency of vascular plants for photosynthesis under optimum temperature, moisture and nutrients conditions	1.05	1.31	Based on results from a pre-study calibration with the site data. Ranges were selected in that way, that mosses and vascular plants can contribute approximately similar to photosynthesis during summer Vermeij, 2013. Actual values differ due to the different plant coverage.
$\varepsilon_{L,\,moss}$	gDW MJ^{-1}	1.1	Plant assimilation efficiency	Radiation use efficiency of mosses for photosynthesis under optimum temperature, moisture and nutrients conditions	0.1	0.2	Based on results from a pre-study calibration with the site data. Ranges were selected in that way, that mosses and vascular plants can contribute approximately similar to photosynthesis during summer Vermeij, 2013. Actual values differ due to the different plant coverage.
$p_{mn,\,vasc}$	°C	1.2	Plant assimilation: temperature response	Minimum mean air temperature for photosynthesis for vascular plants	-6	5	-6 reported for some alpine plants Körner, 1999, 5 default value
$p_{mn,\,moss}$	°C	1.2	Plant assimilation: temperature response	Minimum mean air temperature for photosynthesis for mosses	-6	5	-6 reported for some alpine plants Körner, 1999, 5 default value
$p_{ol,}$	°C	1.2	Plant assimilation: temperature	Lower limit mean air temperature for optimum photosynthesis for vascular plants	8	14	Need to be higher than T LMin, but lower

136

Symbol	Unit	Equation cf. Table S2	Module	Definition	Min	Max	Literature or default value
$vasc$			response				T LOpt2
p_{o2}, $vasc$	°C	1.2	Plant assimilation: temperature response	Upper limit mean air temperature for optimum photosynthesis for vascular plants	20	32	23-32° C for different *Poacea*-species Wohlfahrt et al., 1999; 12-22 °C for *Carex* and *Eriophorum* Kummerow and Ellis, 1984
p_{o1}, mos	°C	1.2	Plant assimilation: temperature response	Lower limit mean air temperature for optimum photosynthesis for mosses	5	14	Need to be higher than T LMin, but lower T LOpt2
p_{o2}, mos	°C	1.2	Plant assimilation: temperature response	Upper limit mean air temperature for optimum photosynthesis for mosses	18	32	*Sphagnum*: 18 °C Clymo and Hayward, 1982; depending on water content, at least 27 °C Grace, 1973
$f_{SnowReduceLAI}$			Plant LAI reduction due to snow cover	Minimum fraction of canopy above snow surface to allow transpiration or interception evaporation	$1\cdot10^{-3}$	0.01	Results from a pre-study calibration with the site data
l_{Lc1}	day^{-1}	1.10, 1.12	Plant litter fall: leaf litter fall before the season	Rate coefficient for the leaf litter fall before the first threshold temperature sum t_{L1} is reached	$2.5\cdot10^{-4}$	0.01	Results from a pre-study calibration with the site data
l_{LS}	-	1.8, 1.12	Plant litter fall: rate for leaf yellowing at the end of the vegetation period	Scaling factor for reallocation of C from the photosynthetically active to the passive pool after the plant reached maturity growth state	0.02	0.03	Results from a pre-study calibration with the site data
l_{Rc1}, mos		1.12	Plant litter fall		$2.5\cdot10^{-4}$	0.0025	Results from a pre-study calibration with the site data
l_{Rc2}, mos		1.12	Plant litter fall		$2.5\cdot10^{-4}$	0.0025	Calibrated relative to l_{Rc1}
$T_{MatureSum}$	°C		Plant phenology: start of senescense	Temperature sum beginning from grain filling stage for plant reaching maturity stage	320	330	Metzger et al., 2015 found best values leading to grain filling start around mid to end of July, which corresponds to 320-330 at this site
$k_{gresp, mos}$		1.6	Plant respiration		0.2	0.6	A wider range was selected for mosses compared to vascular plants, as due to the selected conceptual model, moss respiration was only growth depending, while there is an additional LAI depending component for vascular plants. Fraction of assimilates, lost by respiration according to Rice et al. 2008 for different

Symbol	Unit	Equation cf. Table S2	Module	Definition	Min	Max	Literature or default value
							Sphagnum species: 33-62%
$k_{gr.esp.vasc}$	day^{-1}	1.6	Plant respiration	Rate coefficient for growth respiration of the plant respiration relative to amount of assimilates	0.14	0.4	Results from a pre-study calibration with the site data
t_{Q10}	-	1.7	Plant respiration: temperature response	response to a 10 °C soil temperature change on plant maintenance respiration	1.8	3	Dark respiration in *Eriophorum*: 1.1-3.7 van de Weg et al., 2013
$p_{zr.oot,vasc}$	m	1.13	Plant rooting depth – important for water uptake and root litter input within the soil profile	Maximum root depth in the function for calculating the actual root depth	-0.5	-0.14	Estimated maximum rooting depth for this site is 30-45cm Peichl, 2015, personal communication.
$p_{zr.oot,moss}$		1.13	Plant rooting depth – important for water uptake and root litter input within the soil profile	Maximum root depth in the function for calculating the actual root depth	-0.1	-0.01	Estimation
$m_{re.tain}$	-	1.14	Plant storage pool for regrowth in spring	Coefficient for determining ratio of leaf carbon, allocated to the mobile storage pool during leaf litter fall	0.2	0.6	0.01-0.4 was found in Metzger et al., 2015 for several peatland sites, however pre-study results suggested higher values for this site
k_{ll}	a^{-1}	5.1	SOC decomposition	Rate coefficient for the decay of SOC in the plant litter pools for mosses	$2\cdot10^{-4}$	0.02	1·10-5 to 0.03 by calibration Metzger et al., 2015
k_h	day^{-1}	3.8	SOC decomposition	rate coefficient for the decay of C in the slow SOC pools	$1\cdot10^{-9}$	$2\cdot10^{-5}$	1·10-5 default value
t_{min}	°C	5.3	SOC decomposition – temperature response	The temperature in the Ratkowsky function at which microbial activity is 0% .	-10	0	-8 default value
t_{max}	°C	5.3	SOC decomposition – temperature response	The temperature in the Ratkowsky function at which the response on microbial activity is 100%.	20	30	20 default value
$p_{\theta Satact}$	vol %	5.4	SOC decomposition – water response	Parameter in the soil moisture response function defining the microbial activity under saturated conditions	$1\cdot10^{-6}$	0.01	A very low value was chosen to get a strong response to droughts.
$p_{\theta Low}$	vol %	5.4	SOC decomposition – water response	Water content interval in the soil moisture response function for microbial activity, mineralisation−immobilisation, nitrification and denitrification.	3	20	13 default value
$p_{\theta Upp}$	vol %	5.4	SOC decomposition – water response	Water content interval in the soil moisture response function for microbial activity	6	10	8 default value
k_{l2}	a^{-1}	5.1	SOC decomposition	Rate coefficient for the decay of SOC in the plant litter pools for vascular plants	$2\cdot10^{-5}$	0.002	Calibrated relative to k_{ll}

Appendix to materials and methods

Table A1.13. Constant parameters of study I

Symbol	unit	Eq.	Definition	Value
Δz_{humus}	m		Thickness of the humus layer as used as a thermal property	3[abd]; 2.5[c]
a_{pl}	%	2.1	Plant albedo	25
$f_{e,h}$	day^{-1}	5.9	Fraction of decomposition products from the slow SOC pools being released as CO_2	0.5
$f_{e,l}$	day^{-1}	5.6, 5.7, 5.8, 33, 34	Fraction of decomposition products from the fast SOC pools being released as CO_2	0.5
$f_{h,l}$	day^{-1}	5.7, 5.8	Fraction of decomposition products from the fast SOC pools that will enter the slow decomposition pools	0.2
$f_{leafharvest}$	-	1.16	The fraction of leaves that is harvested	0.85
$f_{leaflitharv}$	-	1.17	Fraction of the remaining leaves after harvest that enters the fast SOC pool	0.1
$f_{stemharvest}$	-	1.16	The fraction of stem that is harvested	0.85
$f_{stemlitharv}$	-	1.17	Fraction of the remaining stem after harvest that enters the fast C pool	0.1
g_{max}	m^2 s^{-1}	2.10	The maximal conductance of fully open stomata	0.02
g_{ris}	J m^{-2} day^{-1}	2.10	The global radiation intensity that represents half-light saturation in the light response	
g_{vpd}	Pa	2.10	The vapour pressure deficit that corresponds to a 50 % reduction of stomata conductance	100
$h1$	-	6.3	Empirical constant in the heat conductivity of the organic material at the surface	0.06
$h2$	-	6.3	Empirical constant in the heat conductivity of the organic material at the surface	0.005
k_h	day^{-1}	3.8, 5.2, 6.1	Rate coefficient for the decay of C in the slow SOC pools	$2 \cdot 10^{-8}$
k_{mat}	mm day^{-1}	6.10	Matrix conductivity in the function for unsaturated conductivity	1200[I], 300[II]
k_{sat}	mm day^{-1}	6.11, 6.13	Total conductivity under saturated conditions	1200[I], 300[II]
$llife$	a	1.22	Maximum leaf lifetime	1
n	-	6.10	Parameter for pore correlation and flow path tortuosity in the function for unsaturated hydraulic conductivity	1
p_{cmax}	m^2 m^{-2}	2.2	Maximum surface cover of plant	1
p_{fixedN}	-		Response for leaf C:N ratio. A value of 1 means no N limitation.	1
p_{mx}	°C	1.2	Maximum mean air temperature for photosynthesis	35
p_{o1}	°C	1.2	Lower limit mean air temperature for optimum photosynthesis	15
p_{o2}	°C	1.2	Upper limit mean air temperature for optimum photosynthesis	25
$p_{\theta Low}$	vol %	5.4	Water content interval in the soil moisture response function for microbial activity, mineralisation−immobilisation, nitrification and denitrification.	13
r_{AIT}	°C^{-1}	6.14	The slope coefficient in a linear temperature dependence function for the hydraulic conductivity	0.023
r_{AOT}	-	6.14	Relative hydraulic conductivity at 0°C compared with a reference temperature of 20°C.	0.54
$s_{oldleaf}$	-	1.21	Scaling factor for litter fall of old leaf	1
$s_{oldroot}$	-	1.21	Scaling factor for litter fall of old roots	1
$s_{oldstem}$	-	1.21	Scaling factor for litter fall of old stem	1
T_{aamp}	°C	6.5	Assumed value of the amplitude of the sine curve , representing the lower boundary condition for heat conduction	10
z	m	2.11, 6.1, 6.6	Depth of the border between the upper and lower horizon in respect to hydrological properties	0.3
η	mol C g^{-1} dw	1.1	Conversion factor from biomass to carbon	0.45
θ_m	vol %	6.13	Macro pore volume	4[Iab], 6.5[Ic], 7.38[Id], 4[IIab], 8[IIcd]
θ_r	vol %	6.9	Residual soil water content	0.3[I], 0[II]
θ_s	vol %	3.9, 5.4, 6.9, 6.13	Water content at saturation	84[Iab], 79[Ic], 83[Id], 86[IIab], 90[IIc], 89[IId]
θ_{wil}	vol %	5.4	Water content at wilting point	20[Iab], 2[Ic], 33[Id], 22[II]
λ	-	6.8, 6.10	Pore size distribution index	0.2[ab], 0.07[Id], 0.24[Ic], 0.09[IIcd]
ψ_a	cm	6.8	Air-entry tension	8[Iab], 3.8[Ic], 12[Id], 10[IIab], 24[IIcd]
ψ_x	cm	6.8, 6.9, 6.13	Soil water tension at the upper boundary of Brooks and Corey's expression	8000

[a] at Lom   [b] at Amo   [c] at Hor   [d] at FsA and FsB   [I] upper horizont   [II] lower horizont

Table A1.14. Constant parameters of study II.

Symbol	Unit	Eq.	Module	Definition	Value	Literature or default value
η	mol C g^{-1} dw	1.1	Plant biomass:C ratio	Conversion factor from biomass to carbon	0.45	Default value
p_{mx}	°C	1.2	Plant assimilation: temperature response	Maximum mean air temperature for photosynthesis	45	Based on results from a pre-study calibration with the site data.
l_{cl}	g C^{-1}	1.4, 1.5	Plant allocation of assimilates to the leaves	Fraction of new assimilates which is allocated to the leaves	0.545	Metzger et al., 2015
$k_{mre\,spleaf,\,vasc}$	day^{-1}	1.6	Plant respiration	Rate coefficient for maintenance respiration of vascular plant leaves respiration relative to leaf biomass	0.0025	Based on results from a pre-study calibration with the site data.
$k_{mre\,sproot,\,vasc}$	day^{-1}	1.6	Plant respiration	Maintenance respiration coefficient for vascular plant root respiration relative to root biomass	0.0025	Metzger et al., 2015
$k_{mre\,spstem,\,moss}$	day^{-1}	1.6	Plant respiration	Maintenance respiration coefficient for vascular plant stem = photosynthetically inactive biomass like e.g. senescent leaves that are still attached to the plant respiration relative to stem biomass	0	No respiration, as this represents brown, senescent biomass
$k_{mre\,spleaf,\,moss}$	day^{-1}	1.6	Plant respiration	Rate coefficient for maintenance respiration of moss leaves respiration relative to leaf biomass	0	No leaf respiration for mosses to allow a fixed moss capita
$k_{mre\,sproot,\,moss}$	day^{-1}	1.6	Plant respiration	Maintenance respiration coefficient for moss "root" = leaves and stem below the capita respiration relative to root biomass	0.0025	Based on results from a pre-study calibration with the site data.
$t_{Q10\,bas}$	°C	1.7	Plant respiration: Temperature response	Base temperature for the temperature response of plant respriation, at which the response is 1	20	Default value
$s_{new\,stem}$	-	1.9	Plant litter fall	Scaling factor for litter fall from new stems	1	Full litterfall rate applies, no scaling
l_{Sc1}	day^{-1}	1.10	Plant litter fall	Rate coefficient for the litter fall from stems before the first threshold temperature sum t_{S1} is reached	0.05	Based on results from a pre-study calibration with the site data.
l_{Sc2}	day^{-1}	1.10	Plant litter fall	Rate coefficient for the litter fall from stems after the second threshold temperature sum t_{S2} is reached	0.5	Based on results from a pre-study calibration with the site data.
$s_{newleaf}$	-	1.9	Plant litter fall	Scaling factor for litter fall from new leaves	1	Full litterfall rate applies, no scaling
l_{Lc2}	day^{-1}	1.10	Plant litter fall: leaf litter fall rate at the end of the season	Rate coefficient for the leaf litter fall after the second threshold temperature sum t_{L2} is reached	0.5	Based on results from a pre-study calibration with the site data.
t_{L1}	day°C	1.10	Plant litter fall	Threshold temperature sum after reaching dormancy state for the lower leaf litter rate. When it is reached, l_{Lc1} starts to change towards the increased litter fall rate l_{Lc2}	2	Based on results from a pre-study calibration with the site data.
t_{L2}	day°C	1.10	Plant litter fall	Threshold temperature sum after reaching dormancy state for the higher leaf litter rate. When it is reached, the full high litter rate is applied.	14	Based on results from a pre-study calibration with the site data.
t_{S1}	day°C	1.10	Plant litter fall	Threshold temperature sum after reaching dormancy state for the lower stem litter rate. When it is reached, t_{Sc1} starts to change towards the increased	2	Based on results from a pre-study calibration with the site data.

Appendix to materials and methods

Symbol	Unit	Eq.	Module	Definition	Value	Literature or default value
				litter fall rate t_{Sc2}		
t_{L2}	day°C	1.10	Plant litter fall	Threshold temperature sum after reaching dormancy state for the higher stem litter rate. When it is reached, the full high litter rate is applied.	14	Based on results from a pre-study calibration with the site data.
$T_{DormTth}$	°C	1.10	Plant litter fall	Threshold temperature for plant dormancy – if the temperature falls below this value for five consecutive days, the dormancy temperature sum starts to be calculated.	0.7	Based on results from a pre-study calibration with the site data.
l_{LaiEnh}	-	1.11	Plant litter fall	Scaling factor for enhanced leaf litter fall rates when higher LAI values are reached	0.56	Metzger et al., 2015
t_{R1}	day°C	1.10, 1.12	Plant litter fall	Threshold temperature sum after reaching dormancy state for the lower root litter rate. When it is reached, t_{Rc1} starts to change towards the increased litter fall rate t_{Rc2}	2	Based on results from a pre-study calibration with the site data.
t_{R2}	day°C	1.10, 1.12	Plant litter fall	Threshold temperature sum after reaching dormancy state for the higher root litter rate. When it is reached, the full high litter rate is applied.	14	Based on results from a pre-study calibration with the site data.
$s_{new roots}$	-	1.12	Plant litter fall	Scaling factor for litter fall from new roots	1	Full litterfall rate applies, no scaling
$l_{Rc1, vasc}$	day^{-1}	1.12	Plant litter fall	Rate coefficient for the litter fall from roots before the first threshold temperature sum t_{R1} is reached	0.00125	Based on results from a pre-study calibration with the site data.
$l_{Rc2, vasc}$	day^{-1}	1.12	Plant litter fall	Rate coefficient for the litter fall from roots after the second threshold temperature sum t_{R2} is reached	0.005	Based on results from a pre-study calibration with the site data.
$l_{Rc1, moss}$	day^{-1}	1.12	Plant litter fall	Rate coefficient for the litter fall from moss "roots" =belowground leaves & stems before the first threshold temperature sum t_{R1} is reached	0.0005	Based on results from a pre-study calibration with the site data.
$l_{Rc2, moss}$	day^{-1}	1.12	Plant litter fall	Rate coefficient for the litter fall from moss "roots" after the second threshold temperature sum t_{R2} is reached	0.0005	Based on results from a pre-study calibration with the site data.
$l_{life, vasc}$	a	1.22	Plant litter fall	Maximum leaf lifetime vascular plant	1	Vascular plant leaves were assumed to be renewed after one year
$l_{life, vasc}$	a	1.22	Plant litter fall	Maximum leaf lifetime mosses	300	Moss capita was assumed to be constant and therefore never dies
	g m^{-2}			Initial N content of vascular plant leaves; defines C and therefore biomass by defined C:N ratio	32.5	Based on results from a pre-study calibration with the site data.
	g m^{-2}			Initial N content of moss leaves; defines C and therefore biomass by defined C:N ratio	95	Based on results from a pre-study calibration with the site data.
	g m^{-2}			Initial N content of vascular plant roots defines C and therefore biomass by defined C:N ratio	100	Based on results from a pre-study calibration with the site data.
	g m^{-2}			Initial N content of belowground moss parts "roots" defines C and therefore biomass by defined C:N ratio	95	Based on results from a pre-study calibration with the site data.
$p_{incroot}$	-	1.13	Plants: shape of root distribution	Distribution parameter in the function for calculating the actual root depth – important for water uptake and root litter input within the soil profile	-1	Default value
m_{shoot}	-	1.15	Plant storage pool for regrowth in spring	Coefficient for the rate at which C is reallocated from the mobile pool to the leaf at leafing	0.07	Based on results from a pre-study calibration with the site data.

Symbol	Unit	Eq.	Module	Definition	Value	Literature or default value
k_{rn}	-	2.1	Plant radiation interception: partitioning	Extinction coefficient in the Beer's law used to calculate the partitioning of net radiation between canopy and soil surface	0.8	Based on results from a pre-study calibration with the site data.
$p_{cmax, vasc}$	m^2 m^{-2}	2.2	Radiation interception: Plant coverage	Maximum surface cover of vascular plants	0.6	Visually estimated plant coverage at the site
$p_{cmax, moss}$	m^2 m^{-2}	2.2	Radiation interception: Plant coverage	Maximum surface cover of mosses	1	Visually estimated plant coverage at the site
p_{ck}	-	2.2	Radiation interception: Plant coverage	Speed at which the maximum surface cover of the plant canopy is reached	1	Based on results from a pre-study calibration with the site data.
$p_{l,sp}$	g C m^{-2}	2.3	Plant LAI:phytomass ratio	Factor for calculating LAI from leaf biomass, which is actually the inverse of specific leaf area, i.e. leaf mass per unit leaf	47.5	Metzger et al., 2015
$T_{EmergeT h}$	°C		Plant phenology: start of growing season	Critical air temperature that must be exceeded for temperature sum calculation	5	Default value
$T_{EmergeS um}$	°C		Plant phenology: start of growing season	Air temperature sum which is the threshold for start of plant development	50	Default value
$p_{densm, vasc}$	-	2.8	Plant: density of vascular plant canopy	The density maximum of canopy in relation to the canopy height	0.7	Default value
$p_{densm, moss}$	-	2.8	Plant: density of moss canopy	The density maximum of canopy in relation to the canopy height	0.9	Estimation for the site
g_{ris}	J m^{-2} day^{-1}	2.10	Plant assimilation: radiation saturation	Global radiation intensity that represents half-light saturation in the light response	$5 \cdot 10^6$	Default value
$c_{H0, canopy}$	m s^{-1}	2.6	Aerodynamic resistance of canopy: minimum exchange under stabile conditions	Roughness length used in the calculation of ra for each plant, corresponds to $z0$ in eq. 2.6.	0.001	Default value
z_{ref}	m	2.6	Aerodynamic resistance of canopy: minimum exchange under stabile conditions	Height above ground which represent the level for measured air temperature, air humidity and wind speed.	2	Default value
z_{0max}	m	2.7	Aerodynamic resistance: roughness length of plants	The maximum roughness length used when estimating roughness length of different canopies see "Aerodynamic resistance".	3	Default value
z_{0min}	m	2.7	Aerodynamic resistance: roughness length of plants	The minimum roughness length used when estimating roughness length of different canopies	0.01	Default value
g_{vpd}	Pa	2.10	Transpiration stress due to low air humidity	Vapour pressure deficit that corresponds to a 51 % reduction of stomata conductance	100	Default value
p_2	kg m^{-2} day^{-1}	27	Transpiration stress due to too low water content	Coefficient in moisture reduction function. The degree of reduction when the actual pressure head exceeds the critical threshold, ψ_c, is controlled by this coefficient together with $p1$ and the	0.1	Default value

Appendix to materials and methods

Symbol	Unit	Eq.	Module	Definition	Value	Literature or default value
				potential transpiration rate, *Etp*.		
p_{ox}	-	28	Transpiration and assimilation stress due to high water content	A rate coefficient that governs how rapidly the plant resistance will increase because of the lack of oxygen when the water content of the soil exceeds the value give by the actual soil moisture content, θ	0	The plants are assumed to be well adapted to wet conditions and therefore do not suffer from water stress due to too wet conditions
θ_{Amin}	vol %	29	Transpiration and assimilation stress due to high water content	The minimum amount of air that is necessary to prevent any reduced uptake of water from the soil	0	The plants are assumed to be well adapted to wet conditions and therefore do not suffer from water stress due to too wet conditions
t_{WB}	-	2.13	Transpiration stress due to limited water availability under low temperatures	Temperature coefficient in the temperature response function.	0.4	Default value
t_{WC}	-		Transpiration stress due to limited water availability under low temperatures	Temperature coefficient governing the trigging temperature.	0	Default value
$r_{a,soil,max}$	-	3.4	Aerodynamic resistance: upper limit under windless conditions	Minimum turbulent exchange coefficient inverse of maximum allowed aerodynamic resistance over bare soil. Avoids exaggerated surface cooling in windless conditions or extreme stable stratification.	0.001	Default value
z_{0M}	m	3.4	Aerodynamic resistance: roughness length of bare soil	Surface roughness length for momentum above bare soil.	0.001	Default value
s_{excess}	mm	3.7	Vapour pressure at the soil surface	The highest value allowed for the δ_{surf} variable, which is used in the calculations of soil surface resistance and vapour pressure at the soil surface.	1	Default value
s_{def}	mm	3.7	Vapour pressure at the soil surface	The lowest value allowed for the δ_{surf} variable, which is used in the calculations of soil surface resistance and vapour pressure at the soil surface.	-2	Default value
d_{vapb}	-	3.9		Correction factor because of non-perfect condition for diffusion	0.66	Default value
k_{mat}	mm day^{-1}	6.10	Soil hydraulic conductivity: temperature dependence	Saturated matrix conductivity	100	Default value
θ_s	vol %	5.4, 6.9	Soil hydraulic properties: shape of water retention	Water content at saturation	98 95	Received by comparing resulting pF curves with curves measured in peatlands Kellner and Lundin, 2001 under consideration of the range for the calibrated parameter AirEntry; the value in brackets is used for layers below −30cm
θ_{wilt}	vol %	5.4	Soil hydraulic properties: shape of water retention	Water content at wilting point	30 30	Received by comparing resulting pF curves with curves measured in peatlands Kellner and Lundin 2001 under consideration of the range for the calibrated parameter AirEntry; the value in brackets is used for layers below −30cm
ψ_x	cm	6.8, 6.9, 6.13	Soil hydraulic properties: shape of water retention	Soil water tension at the upper boundary of Brooks and Corey's expression	8000	Default value

Symbol	Unit	Eq.	Module	Definition	Value	Literature or default value
λ	-	6.8, 6.10	Soil hydraulic properties: shape of water retention	Pore size distribution index	0.3 0.2	Received by comparing resulting pF curves with curves measured in peatlands Kellner and Lundin 2001 under consideration of the range for the calibrated parameter AirEntry; the value in brackets is used for layers below −30cm
z	m		Soil hydraulic properties: Border between horizons	Depth of the border between the upper and lower horizon in respect to hydrological properties	0.3	Boundary between acrotelm and catotelm, based on visual differences in the soil profile and water table depth measurements Granberg et al., 1999.
h_1	-	6.3	Soil temperature – thermal conductivity	Empirical constant in the heat conductivity of the organic material at the surface	0.06	Default value
T_{aamp}	°C	6.5	Soil temperature – lower boundary	Assumed value of the amplitude of the sine curve , representing the lower boundary condition for heat conduction	10	Default value
Δz_{humus}	m		Soil thermal properties	Thickness of the humus layer as used as a thermal property	3	Site specific value for peat depth. Measurements at the site indicate a peat depth of 3-4m
θ_r	vol %	6.9	Soil hydraulic properties: shape of water retention	Residual soil water content	1 1	Received by comparing resulting pF curves with curves measured in peatlands Kellner and Lundin 2001 under consideration of the range for the calibrated parameter AirEntry; The value in brackets is used for layers below −30cm
n	-	6.10	Unsaturated soil hydraulic conductivity of soil	Parameter for pore correlation and flow path tortuosity in the function for unsaturated hydraulic conductivity	1 1	Based on results from a pre-study calibration with the site data. The value in brackets is used for layers below −30cm
z_p	m	6.12	Soil water: drainage depth	Lower depth of the drainage	-0.12	Measured water level during wet periods at the site
	m		Soil water: minimum drain level	Lowest possible water level	-0.6	Well below the lowest measured water table at that site 0.4.
θ_m	vol %	6.13	Soil hydraulic properties: shape of water retention	Macro pore volume	4 4	Received by comparing resulting pF curves with curves measured in peatlands Kellner and Lundin 2001 under consideration of the range for the calibrated parameter AirEntry; the value in brackets is used for layers below −30cm
k_{sat}	mm day^{-1}	6.11, 6.13	Saturated soil hydraulic conductivity of soil	Total conductivity under saturated conditions	1610 800	From measured dry bulk density according Päivänen, 1973
r_{AIT}	°C^{-1}	6.14	Soil hydraulic conductivity: temperature dependence	The slope coefficient in a linear temperature dependence function for the hydraulic conductivity	0.023	Default value
r_{AOT}	-	6.14	Soil hydraulic conductivity: temperature dependence	Relative hydraulic conductivity at 0°C compared with a reference temperature of 20°C.	0.55	Default value
k_{minuc}	mm day^{-1}	6.14	Soil hydraulic conductivity	The minimum hydraulic conductivity in the hydraulic conductivity function.	1·10^{-5}	Default value

Appendix to materials and methods

Symbol	Unit	Eq.	Module	Definition	Value	Literature or default value
$f_{e,l}$	day^{-1}	5.6, 5.7, 5.8	SOC decomposition	Fraction of decomposition products from the fast SOC pools being released as CO_2	0.5	Default value
$f_{h,l}$	day^{-1}	5.6, 5.7, 5.8	SOC decomposition	Fraction of decomposition products from the fast SOC pools that will enter the slow decomposition pools	0.2	Default value
$p_{\theta p}$	vol %	5.4	SOC decomposition – water response	Power coefficient in the response function of microbial activity in dependency of soil moisture	1	Default value
l_{ll}	day^{-1}	5.5	SOC decomposition	Fraction of the above ground residues that enter the pool for fast decomposition of the uppermost soil layer	0.005	Default value
$f_{e,h}$	day^{-1}	5.9	SOC decomposition	Fraction of decomposition products from the slow SOC pools being released as CO_2	0.5	Default value
cn_m	-		SOC decomposition	Litter quality at which decomposers shift from immobilisation of mineral N to net mineralisation	30	Based on results from a pre-study calibration with the site data.
	-			Geographic position; used for the calculation of cloudiness	65.18	Location of the site

Table A1.15. Criteria for accepted runs in study I in the basic calibration I a. Lower and upper limits are separated by fore slash. In case of R^2, the upper limit corresponds to the highest value achieved for this site. The criteria were selected to fit for around 75 runs and depend on the different performances achieved for the different sites.

Site	Accepted runs	R_{eco} ME	$R_{eco}R^2$	GPP ME	GPP R^2	LAI ME	LAI R^2	Winter R_{eco} ME	Winter GPP ME	NEE R^2	Root biomass ME
Lom	74	−0.15/0.15	0.72/0.79	−0.15/0.15	0.65/0.70	−0.2/0.2		−0.25/0.25	−0.25/0.25		
Amo	64	−0.2/0.2	0.65/0.71	−0.2/0.2	0.65/0.68	−0.5/0.5		−0.4/0.4	−0.4/0.4		
Hor	74	−0.5/0.5		−0.5/0.5					−2/2	0.48/0.53	−150/150
FsA	68	−0.85/0.85	0.5/0.73	−0.85/0.85	0.32	−0.3/0.3	0.58/0.75	−3/3	−1/1		
FsB	67	−0.8/0.8	0.65/0.87	−0.8/0.8	0.35/0.40	−0.25/0.25	0.65/0.82	−2/2	−1/1		

Table A1.16. Configurations of the selected single value representations C1-C7. Resulting values for k_{ll} and ε_L can be found in the main document, Figure 10.

Identifier	Description	t_{Q10} [-]	t_{Q10bas} [°C]	$p_{\theta Satact}$ [-]	$k_{mrespleaf}$ [day^{-1}]	C:N fast pool [-]	p_{ck} [-]
C1_basic	selected basic common configuration	2.7	18.5	0.05	0.017	27.5	0.42[a], 0.2[b], 0.9[c], 1[d]
C2_↑plant_resp	higher ratio of plant to soil respiration	2.7	18.5	0.05	0.022	27.5	0.42[a], 0.2[b], 0.9[c], 1[d]
C3_↑$p_{\theta Satact}$	higher saturation activity	2.7	18.5	0.40	0.017	27.5	0.42[a], 0.2[b], 0.9[c], 1[d]
C4_↑temp_response	steeper temperature response function	4.0	12.0	0.05	0.008	27.5	0.42[a], 0.2[b], 0.9[c], 1[d]
C5_C3&C4	higher saturation activity and steeper temperature response	4.0	12.0	0.40	0.008	27.5	0.42[a], 0.2[b], 0.9[c], 1[d]
C6_C:N_60	C:N of 60 for the fast decomposition pools	2.7	18.5	0.05	0.017	60	0.42[a], 0.2[b], 0.9[c], 1[d]
C7_common_p_{ck}	same p_{ck} value for all sites	2.7	18.5	0.05	0.017	27.5	1

[a] at Lom   [b] at Amo   [c] at Hor   [d] at FsA and FsB

Appendix to materials and methods

Table A1.17. Variables and related parameter as used for further parameter constraint in step I c and III

Variable	Site	Parameter
R_{eco}	Lom, Amo, Hor, FsA, FsB	l_{cl}, l_{Sc1}, l_{Sc2}, l_{Lc1}, l_{Lc2}, l_{LaiEnh}, $T_{MatureSum}$, $T_{DormTth}$, t_{R1}, t_{R2}, t_{S1}, t_{S2}, g_{maxwin}, $k_{mrespstem}$, $k_{mresproot}$, $p_{\theta Satact}$, $p_{\theta Upp}$, l_{l1}, p_{θ}, k_l, $T_{EmergeSum}$, t_{Q10}, t_{Q10bas}
GPP	Lom, Amo, Hor, FsA, FsB	k_{rn}, p_{ck}, ε_L, $p_{l,sp}$, l_{cl}, $s_{newroot}$, $s_{newleaf}$, $s_{newstem}$, l_{Rc1}, l_{Rc2}, l_{Sc1}, l_{Sc2}, l_{Lc1}, l_{Lc2}, l_{LaiEnh}, $T_{MatureSum}$, l_{LS}, $T_{DormTth}$, t_{L1}, t_{L2}, t_{R1}, t_{R2}, t_{S1}, t_{S2}, m_{shoot}, m_{retain}, $T_{EmergeTh}$, $T_{EmergeSum}$, p_{mn}, g_{maxwin}, g_{ph}, $k_{mrespstem}$, $k_{mresproot}$, k_{gresp}, $k_{mrespleaf}$, t_{Q10}, t_{Q10bas}
winter R_{eco}	Lom, Amo, Hor, FsA, FsB	t_{R1}, t_{R2}, t_{S1}, t_{S2}, k_{gresp}, $p_{\theta Satact}$, $p_{\theta Upp}$, l_{l1}, p_{θ}, k_l, $T_{EmergeSum}$, t_{Q10}, t_{Q10bas}
winter GPP	Lom, Amo, Hor, FsA, FsB	l_{cl}, $s_{newstem}$, l_{Sc2}, l_{Lc1}, $T_{MatureSum}$, l_{LS}, $T_{DormTth}$, t_{L1}, t_{L2}, t_{R1}, t_{R2}, t_{S1}, t_{S2}, p_{mn}, g_{maxwin}, g_{ph}, k_{gresp}, $k_{mrespleaf}$
upper most soil temperature	Lom, Amo, Hor, FsA, FsB	k_{rn}, p_{ck}, ε_L
lowest soil temperature	Lom, Amo, Hor, FsA, FsB	T_{amean}
LAI	Lom, Hor, FsA, FsB	k_{rn}, p_{ck}, ε_L, $p_{l,sp}$, l_{cl}, $s_{newleaf}$, l_{LaiEnh}, $T_{MatureSum}$, $T_{DormTth}$, t_{L1}, t_{L2}, m_{shoot}, m_{retain}, $T_{EmergeTh}$, $T_{EmergeSum}$, m_{Root}, , $k_{mrespleaf}$ r_{rl}, g_{ph}
snow depth	Lom	
green above ground biomass	Hor, FsA, FsB	ε_L, $p_{l,sp}$, $s_{newroot}$, $s_{newleaf}$, $s_{newstem}$, g_{ph}
total above ground biomass	Hor, FsA, FsB	$s_{newstem}$, l_{LS}, g_{ph}, $k_{mrespleaf}$
root biomass	Hor	l_{cl}, $s_{newroot}$, l_{Rc1}, l_{Rc2}

Table A1.18. Criteria set for the selection of accepted runs in study II. The first entry describes the basic criteria, all others are applied additional to the basic criteria.

Main component	Variable	R^2	ME
Basic selection these criteria are applied additionally in all following criteria sets	WT < -0.2 m	≥0.40	±0.02 m
	LAI vascular plants	≥0.40	±0.02 m^2 m^{-2}
	daytime NEE		±2 gCO$_2$-C m^{-2}
NEE	Accumulated NEE	≥0.98	
	Daytime NEE		±0.02 gCO$_2$-C m^{-2} d^{-1}
	Night time NEE		±0.07 gCO$_2$-C m^{-2} d^{-1}
Sensible heat	H		±3·10^5 J m^{-2} d^{-1}
	Accumulated H	≥0.97	
Latent heat	LE		±1·10^5 J m^{-2} d^{-1}
	Accumulated LE	≥0.98	
Net radiation	Net radiation	≥0.82	±4·10^4 J m^{-2} d^{-1}
Soil temperature	Temperature -2 cm	≥0.95	±0.22 °C
	Temperature -42 cm		±0.22 °C
Snow	Snow depth	≥0.76	
Water table	WT < -0.15 m	≥0.51	

A2 Appendix to site comparison study I

Figure A2.24. Criteria for accepted runs in study II. The first entry describes the basic criteria, all others are applied additional to the basic criteria

A3 Appendix to the investigation of interactions study II

A3.1 Results: detailed description of sensitivities and interactions per process

Detected sensitivities, connections between performances, and equifinalities showed all strong interactions between the different processes and parameters of different modules. Connections existed between all variables and modules, but most strongly interlinked were LE with WT, Rn with H and Ts Fig. 13 in the main document. H, LE, WT were also linked to each other and to NEE. The impact of the plant is further reflected in the correlations between performances in LAI with performances in many other variables Fig. 16. The implications on the performance for each considered variable will be described in the following sections.

A3.1.1 Water level depth and soil moisture conditions

Performance in water level depth was determined by 12 key parameters Table A3.3.1. It was most strongly connected to the shape of the soil water retention curve ψ_a as well as to the transpiration coefficients for mosses and winter transpiration $g_{max,moss}$, g_{maxwin}. The transpiration coefficient from vascular plants played a smaller role due to the high sensitivities of parameters defining the growth and therefore magnitude of the vascular plant i.e. $k_{gresp,vasc}$, m_{retain}, l_{Lc1}. Equifinalities existed between several of these parameters.

ψ_a had strong effect on the performance of all variables and several strong equifinalities with in particular parameters defining aerodynamic resistance and transpiration; On the other hand ψ_a could not be constraint to an unambiguous range and was therefore the parameter causing the largest overall uncertainty Fig. 13 in the main document.

Performance in WT was further sensitive to parameters defining aerodynamic resistance, i.e. r_{alai} and $c_{H0,canopy}$. Both parameters had equifinalities with ψ_a and moss albedo $a_{pve,moss}$ as well as with timing of snow melt m_T and thermal conductivity of snow s_k. Also the distance between drainage d_p, showed some sensitivity.

A3.1.2 Transpiration and evaporation

The nine most important parameters for WT performance were also key parameters for LE ψ_a, $g_{max,vasc}$, $g_{max,moss}$, g_{maxwin}, $k_{gresp,vasc}$, m_{retain}, l_{Lc1}, r_{alai}, $c_{H0,canopy}$. This explains the strong correlation between the performance in WT and LE ME Fig. 16 in the main document and shows the connections

with plant, WT and H. An additional, sensitive parameter from the aerodynamic resistance module, was the roughness length of snow $z_{0M,snow}$ which correlated with moss albedo, hinting to another connection to R.

Dynamics in WT and LE, but also magnitude of H was improved if the transpiration coefficient was on its lower range in case of mosses and on its upper range in case of vascular plants Fig. A3.4.2. Despite the lower values for mosses, transpiration in the prior was dominated by mosses, due to their higher LAI and coverage Fig. A3.4.4.

Crucial for LE performance was also a parameter defining the aerodynamic resistance of the canopy under stabile conditions $c_{H0,canopy}$: a very small value improved the R^2 of LE and spring LE, but downgraded R^2 of accumulated LE and of winter radiation.

Spring LE was overestimated in most of the runs see Fig. A3.4.1. The strongest sensitivity on spring LE was by the coefficient for winter transpiration g_{maxwin}: the higher the better R^2 and ME. Together with $z_{0M,snow}$ this was also the most important parameter for winter LE.

A3.1.3 NEE & LAI

Seven of the nine parameter which were common for LE and WT were also among the most effective parameters for NEE ψ_a, $g_{max,moss}$, $g_{max,vasc}$,, $k_{gresp,vasc}$, m_{retain}, l_{Lc1}, r_{alai} and belong to four different modules: plant, transpiration, soil hydrology and aerodynamic resistance Table A3.3.1. However the most sensitive parameter for NEE was the rate coefficient for heterotrophic respiration k_{ll}, which was especially important for night time NEE. Further sensitive parameters for night time NEE were the growth respiration coefficient for mosses $k_{gresp,moss}$ and the temperature dependency coefficient for heterotrophic respiration t_{min}.

The rates of photosynthesis and its temperature dependence $\varepsilon_{L,vasc}$, ε_{Lmoss}, $p_{mn,vasc}$ were key parameters for LAI, NEE magnitude or temporal NEE dynamics, respectively. Many strong interactions existed between plant parameters, which were especially visible in the basic selection as mentioned in Section 3.3.3 in the main document.

The rate of leaf litter fall during the growing season l_{Lc1} was one of the parameters with the highest concern, due to its sensitivity on many different processes, its equifinalities and as it could not be constrained to an unambiguous solution Fig. 13 in the main document. Resulting ranges for l_{Lc1} differed especially between the different performance indices within NEE and within LAI, but also between NEE and LAI Fig. A3.4.2.

A3.1.4 Sensible heat fluxes, soil temperatures and net radiation

Many inter-connections existed between H, Ts and Rn, but all three were also linked with LE, WT, snow and NEE. A snow parameter, determining the timing of snow melt m_T was the most crucial parameter for heat fluxes, not only in spring time, but also for the whole year period. Further, m_T was important for Ts in spring time cf. Section A3.1.5. The shape of the soil water retention curve ψ_a was the second most sensitive parameter for both variables.

The aerodynamic resistance dependency factor on LAI r_{alai} was the most sensitive parameter for Ts, and affected also LE, WT and night time NEE, while it strongly correlated with moss albedo $a_{pve,moss}$, the third most sensitive parameter for H and most sensitive parameter for Rn. Accepted ranged for r_{alai} contradicted within the soil temperature variables, depending on the chosen performance index and considered season: high values were important for Ts ME and R^2 during winter, but low ones improved Ts R^2 during spring and during the whole period. Therefore, r_{alai} was the parameter causing the largest overall uncertainty after ψ_a. This was followed by $a_{pve,moss}$, which had low values for accepted ranges in case of H, Rn and Ts during the whole period, but high values in case of winter H and Rn. It further showed strong equifinialites with the roughness length of snow $z_{0M,snow}$, which was the second most sensitive parameter for Rn, but also affected H and LE. The coefficient for thermal conductivity of snow s_k affected Rn and Ts, but not H.

The thermal conductance coefficient of soil organic material h_2, the lower boundary mean temperature T_{amean}, the snow melt dependency to radiation coefficient m_{Rmin} and the density of new and old snow ρ_{smin}, S_{dw} affected only soil temperatures, the latter two also snow depth.

Parameters defining moss and winter transpiration $g_{max,moss}$, g_{maxwin} and the growth respiration coefficient of vascular plants with its effect on vascular plant biomass and LAI $k_{gresp,vasc}$ were sensitive to Ts, $g_{max,moss}$ and $k_{gresp,vasc}$ also to H. The most important parameter for LE, $c_{H0,canopy}$ was another key parameter for Rn and H.

A3.1.5 Snow

The temperature coefficient in the snow melt function m_T was the most important parameter for ME in snow and determined timing of snow melt. However, resulting parameter ranges did not overlap between the different performance indices within the snow depth variable and between different other variables. A longer lasting snow cover low $m_T < 3$ was crucial for spring H and reduced mean error in snow depth, but lowered R^2 values in spring Ts and snow depth. m_T interacted with another snow parameter T_{RainL} as well as with parameters from the temperature and transpiration module T_{amean}, g_{maxwin}. The density coefficient for old S_{dw} and new snow ρ_{smin} had medium effect on snow depth performance, and affect also spring and winter soil temperatures in all layers, but the latter could be unambiguously constrained by the available data.

A3.2 Discussion: detailed description of sensitivities and interactions per process

The parameters that were identified as most influential or that showed the strongest equifinalities were related to soil hydrology and water content, to a stabile representation of the plant, to radiation, temperature and heat fluxes or to snow. The introduced index to measure parameter concern includes subjective choices like weighting factors, the choice of considered calibration variables and their sub periods as well as the chosen performance indices. However several tested variations in especially the weighting did not noticeable change the results: ψ_a was always the most important parameter, followed by the group of parameters with medium importance which differed slightly in their ranking among each other.

A3.2.1 Unsaturated water distribution & soil moisture conditions

Our results suggest that model uncertainty could be greatly reduced if data for either soil hydraulic properties, water content or plant transpiration characteristics were available: Despite available data of detailed WT and LE in our study, large uncertainty remained in simulated water content due to the combined uncertainty in estimates of soil hydraulic properties ψ_a and plant water uptake $g_{max,vasc}$, $g_{max,moss}$, g_{maxwin}. Their sensitivity to many processes and the high number of equifinalities hindered the constraint of other parameters and therefore the uncertainty reduction in all involved processes. For example this might explain why the water response functions for neither plant assimilation nor soil respiration could be constrained. The shape parameter of the water retention curve ψ_a was among the top two most sensitive parameters for NEE, WT, LE, H, Ts, and the third and fifth

most sensitive parameter in case of Rn and snow. Also, the transpiration coefficients $g_{max,vasc}$, $g_{max,moss}$, g_{maxwin} were among the top 10 most important and influential parameters.

Water retention properties are easy and cheap to measure compared to NEE. Previous sensitivity analyses on other ecosystems pointed out their usefulness for modelling carbon dynamics e.g. Wang et al., 2005. Nevertheless, many of the available peatland sites in current databases e.g. European Fluxnet Database Cluster, http://gaia.agraria.unitus.it still do not contain information on water retention properties. Water content would be even more important but also more difficult to measure.

We therefore strongly recommend experimentalists to include water retention measurements in their experimental set up. This might also help to resolve the strong equifinalities of ψ_a with transpiration coefficients and a parameter in the calculation of aerodynamic resistance of the plant canopy, defining the minimum exchange under stabile conditions $c_{H0,canopy}$.

A3.2.2 C balance of vascular plants

A stable vascular plant that establishes a reasonable amount of biomass every year throughout the simulation period, could only be achieved by certain value combinations for the photosynthetic efficiency $\varepsilon_{L,vasc}$, the respiration coefficient $k_{gresp,vasc}$ and the storage fraction for plant regrowth in spring m_{retain}. Despite their high impact in the basic selection, neither equifinalities, nor sensitivities of these parameters reached high measures in final selections, probably because several parameters were interacting simultaneously. This indicates the need for either calibrating these parameters in dependency of each other or setting at least one of them to a constant value, as the available data was not sufficient to resolve these equifinalities. As ranges for these parameters were well overlapping between the different variables, the ranges and combinations could be narrowed unambiguously, leading to a low ranking for parameter concern, despite several detected sensitivities. Nevertheless, these parameters would be of high importance for predictions, if none of the constraining variables are available.

Compared to previous application of the CoupModel on five different, open peatlands Metzger et al., 2015, vascular plants had to have a much more effective C balance to produce the measured leaf area given a limited amount of assimilates. This can be realised by low respiration and litter fall losses and a large storage pool for regrowth in spring. Even if respiration losses from vascular plants were 1/10 of the ones used at the sites in

Metzger et al. 2015, the model tended to either underestimate vascular plant LAI, or overestimate CO_2 uptake Fig 13 in the main document. A possible explanation for the differences in parameter value combination of vascular plants might lie in the vegetation communities. Despite Metzger et al. 2015 included several different types of treeless peatland vegetation communities, none of these sites had a similar vegetation community consisting of mainly mosses and *Eriophorum vaginatum*, as at Degerö Stormyr. *Eriophorum vaginatum* is known to be much more effective in maintaining C compared to other sedges and having a highly efficient remobilization from senescing leaves Shaver and Laundre, 1997; Jonasson and Chapin III, 1985. Uncertainties in measurements and the distribution of modelled respiration over the hours of the day might accelerate or diminish this effect. Explanations by differences in model structure can be excluded, as the same effect was observed when using exactly the same structure unpublished data. To identify the difference between the sites, which causes the deviations in the combined parameter value ranges, the model need to be applied to further open peatland sites differing in vegetation community, nutrient status and plant productivity. This might allow finding trends in parameter ranges, which is a necessary precondition for estimation and reducing model uncertainty in predictions on other peatland sites.

Another plant parameter which was important for a stable vascular plant layer and was ranked as one of the overall most important parameters was the rate coefficient for the leaf litter fall during the growing season l_{Lc1}. Probably due to the high number of correlations with other parameters, these correlations did not exceed the threshold value. l_{Lc1} is directly connected to the filling of the storage pool, but also for maintaining C in the leaves. Its strong sensitivity to LAI affects transpiration and thereby water uptake which explains the strong sensitivity to WT in lower layers and the equifinalities with a transpiration parameter and a parameter describing the water response of heterotrophic respiration. In Metzger et al. 2015, a value of $l_{Lc1} = 0.01$ day^{-1} could be used site independent. This contradicts the much lower ranges of our study for several variables, in particular R^2 of LAI, WT in lower layers and ME of spring time NEE. However, *Eriophorum vaginatum* is known to maintaining its leaves and therefore have a very low litter fall rate Jonassson and Chapin 1985. Further investigations are needed to resolve the differences in resulting ranges and equifinialities with other parameters. Thereby, measurements of leaf litter fall throughout the year would be of high value.

A3.2.3 Sensible heat fluxes, soil temperatures and net radiation

The large number of strong connections between H, Ts and Rn and the equifinalities between their determining parameters indicate the importance to consider, model and calibrate these processes together. However the constraint of two of the most important parameters, r_{alai} and $a_{pve,moss}$, failed not due to different ranges between variables but due to the differences depending on which performance index and season was considered. This emphasises the importance of the subjective criteria choice, even if only one variable is considered.

Accepted values for r_{alai} were exceptionally high 200 s m^{-1} for Ts R^2 and 550 to 800 s m^{-1} for Ts$_1$ ME, whereas a r_{alai} of 200 multiplied with the moss LAI of 1.8 leads to an aerodynamic resistance of 360 s m^{-1}. Mosses might form a well insulating layer, but still the values are much higher than the aerodynamic resistance of a bog in South-Sweden 60 s m^{-1}, Kellner, 2001. Price 1991 reported very high resistance, when moss surface moisture is low, e.g. during dry periods, but these values were still lower than ours. A possible explanation might be an interaction with a non-calibrated, fixed parameter. A high aerodynamic resistance causes better temperature insulation leading to higher summer soil temperatures with lower diurnal oscillations. Further, it leads to strongly reduced soil evaporation and therefore reduced LE, even though this is partly compensated by little higher transpiration from mainly mosses, which profit from the higher water contents in upper soil layers. This explains the sensitivities to WT and LE which also supported a higher r_{alai} value. The main cause for the much lower optimum range for dynamics in Ts compared to magnitude in Ts is probably an overestimation of the diurnal amplitude. A lower moss LAI can reduce this overestimation, but the corresponding parameter was not calibrated to avoid further equifinalities: r_{alai} showed already strong interactions with $a_{pve,moss}$ and $z_{0M,snow}$.

The correlations of the conductivity of organic material h_2 with plant, LE and WT parameters might be explained by the dependency of thermal conductivity from peat wetness Kellner, 2001.

Seasonal differences in moss albedo $a_{pve,moss}$ could be expected as their radiation reflection properties vary with moss water content Graham et al., 2006. However higher values would be expected in summer, when the moss surface is dry and lighter, but our calibration resulted in higher values during spring and winter. These values were much higher >22% compared to literature values 11-16.5%, Berglund and Mace, 1972; 16.4%, Zhao et al., 1997; 11%, Kellner, 2001. Interestingly, albedo of vascular plants did not

show any sensitivities, neither during vegetative stage $a_{pve,vasc}$, nor after start of senescence a_{pgrain} when a higher value would have been expected due to leaf yellowing. H in spring tended to be overestimated, which would be compensated by a high albedo during this time, but might be caused in the real world by open water over frozen soil, which was not realized in the model. Another explanation could lay in the strong equifinalities with $z_{0M,snow}$ and r_{alai}. Direct measurements of plant albedo were not available in this study. A time series observation of those would be very helpful for clarification. The detected sensitivity of moss albedo to winter H and Rn probably results from interactions with other parameters, especially $z_{0M,snow}$ as the surface is covered with a thick snow cover.

A3.2.4 Snow

The model performance in simulating snow depth was not connected to performance in any other variable, except to performance in H if exclusively spring time values were considered. This was surprising, as the range for timing of snow melt varied by two weeks and determines the start of temperature rise, water table dropping and biotic activity. A possible explanation might be the poor ability of snow depth R^2 and ME to assert a good fit in duration of snow cover. This is supported by the fact that the most important parameter for timing of snow melt m_T strongly affected performance in dynamics of H, NEE and Ts during spring time. Parameters defining timing of snow depth might be better constrained if future calibrations include an additional variable with a stronger conclusiveness to the timing of snow depth, e.g. by a boolean time series indicating if snow cover is present or not. It needs to be tested if this could also help to solve the disagreements in value ranges between the performance indices in case of the density coefficient of old snow S_{dw} which caused in combination with m_T the low average overlap within snow depth sensitive parameters.

According to Jansson and Karlberg 2010, a high value for m_T 4-6 kg °C^{-1} m^{-2} day^{-1} could be expected for open fields. A possible explanation for the low accepted values <3 kg °C^{-1} m^{-2} day^{-1} of m_T in case of criteria on H in contrast to the high values if criteria were on Ts, could be that high values compensate for overestimated spring time H cf. Fig. A3.4.1. However, the overestimation of spring H might be connected to different reflection properties of mosses during spring time or to missing consideration of radiation reflection and evaporation from open water which might be formed during snow melt on still frozen soils. The latter is further supported by the underestimation of LE during April and May Fig. A3.4.1, which cannot be connected to underestimated plant transpiration, as the model even tended to overestimate CO_2 uptake during this period.

A3.3 Tables

Table A3.3.1. Correlation coefficients between parameters and performance. The maximum value is shown if a parameter correlated with several performance indices or several sub periods of the same variable. The first two digits after decimal point are displayed. Values < 0.14 are not shown.

Module	Symbol	NEE night dynamics	NEE night ME	LAI dynamics	LAI ME	NEE day dynamics	NEE day ME	NEE dynamics	NEE ME	Rad dynamics	Rad ME	Tsi dynamics	Tsi ME	Ts2 dynamics	Ts2 ME	H dynamics	H ME	LE dynamics	LE ME	WT dynamics	WT ME	Snow dynamics	Snow ME
SOC decomposition	$p_{\theta Upp}$																						
	$p_{\theta Low}$																						
	$p_{\theta Satact}$																						
	t_{max}																						
	t_{min}	23							32														
	k_h																						
	k_{ll}	33	31			30	30	70	33														
Plant	m_{retain}						30												32	30	31		21	
	$p_{zroot, moss}$																						
	$p_{zroot, vasc}$																						
	t_{Q10}																						
	$k_{gresp, vasc}$	52		60		55	28	30							28				21		31	45		
	$k_{gresp, moss}$	31	30					23																
	$T_{MatureSum}$																						
	$l_{Rc1, moss}$																						
	l_{LS}																						
	l_{Lc1}	30		86	33	32	49	44	30										32	29	50	28	68	13
	$f_{SnowReduceLAI}$																						
	$p_{o2, moss}$																						
	$p_{o2, vasc}$																						
	$p_{o1, vasc}$																						
	$p_{mn, moss}$																						
	$p_{mn, vasc}$						33																
	$p_{o1, moss}$																						
	$\varepsilon_{L, moss}$						70		32														
	$\varepsilon_{L, vasc}$		51																				
Rn	$a_{pve, vasc}$																						
	$a_{pve, vasc}$									77	76	52						63	62				
	a_{pgrain}																						
Soil	T_{amean}														59								
	h_2										31	30	78	57									
	s_k				20			31				64	54	62	18					25			
Aerodyna	$z_{0M, snow}$								31	67					54	58	72						
	r_{alai}	32									75	77	83	51						30	28	33	25
	$r_{a, max, snow-1}$																						
	$c_{H0, canopy}$							32								56		86	20				
Transpirat	ψ_{eg}																						
	p_l																						
	ψ_c																						
	t_{WA}																						

Module	Symbol	NEE night dynamics	NEE night ME	LAI dynamics	LAI ME	NEE day dynamics	NEE day ME	NEE dynamics	NEE ME	Rad dynamics	Rad ME	T_{S1} dynamics	T_{S1} ME	T_{S2} dynamics	T_{S2} ME	H dynamics	H ME	LE dynamics	LE ME	WT dynamics	WT ME	Snow dynamics	Snow ME
Soil	g_{maxwin}															17	61	72	75	51	32		
	$g_{max,\,moss}$					28						13				45	29	67	59	65	32		
	$g_{max,\,vasc}$	32																49	27	44	27		
	d_p																	13	22				
	ψ_a	66	44		47	52	45	56		50		67		65		64	62	66	77	76	65	30	
	h_{com}																						
Snow	T_{RainL}															23				19			
	m_T											47	17			86					25	78	66
	ρ_{smin}											30	32	23								47	
	s_{dl}																					62	
	S_{dw}											21										61	58
	f_{qh}																						
	m_{Rmin}												21										
	Δz_{cov}																						

Table A3.3.2. Prior and posterior parameter ranges of the basic selection. Deviations of parameter ranges from the prior, after applying the basic criteria. Only parameters with a deviation are shown. The deviation is given in percentage of the prior range.

	Max	ψ_a	$k_{gresp,vasc}$	m_{retain}	$\varepsilon_{L,vasc}$	$g_{max,moss}$	l_{Lc1}	l_{LS}
Min Range deviation	3%	3%	0%	0%	0%	0%	0%	0%
Max Range deviation	1%	1%	0%	0%	0%	0%	0%	0%
Mean Range deviation	13%	8%	13%	8%	10%	8%	9%	7%
St.D range deviation	11%	11%	5%	4%	2%	2%	5%	1%
5 Percentile range deviation	11%	11%	2%	10%	4%	1%	0%	2%
51 Percentile range deviation	17%	10%	17%	10%	12%	10%	9%	10%
95 Percentile range deviation	19%	19%	14%	1%	1%	4%	13%	2%

Table A3.3.3. Correlation coefficients of the detected equifinalities. The first two digits after decimal point are displayed. Values < 0.14 are not shown.

	k_h	$p_{\theta Satact}$	t_{max}	t_{min}	$p_{\theta Low}$	$p_{\theta Upp}$	k_{ll}	$p_{zroot,\,vasc}$	$T_{MatureSum}$	$k_{gresp,\,vasc}$	$p_{mn,\,vasc}$	$p_{o1,\,vasc}$	$p_{o2,\,vasc}$	m_{retain}	$\varepsilon_{L,\,vasc}$	$\varepsilon_{L,\,moss}$	$p_{mn,\,moss}$	$p_{o1,\,moss}$	$p_{o2,\,moss}$	$k_{gresp,\,moss}$	$p_{zroot,\,moss}$	$l_{Rc1,\,moss}$	$f_{SnowReduceLAI}$	t_{Q10}	l_{Lc1}	l_{LS}	$a_{pve,\,vasc}$
$p_{\theta Upp}$																							16				
$p_{\theta Low}$																				16						21	
$p_{\theta Satact}$																			16								
t_{max}									18									21					18				
t_{min}																											19
k_h																											
k_{ll}																						19					
m_{retain}											20						19							17			
$p_{zroot,\,moss}$																	19										
$p_{zroot,\,vasc}$																											
t_{Q10}			18												17			26						19			
$k_{gresp,\,vasc}$											19		20	25													
$k_{gresp,\,moss}$		16					19																				
$T_{MatureSum}$			18																								
$l_{Rc1,\,moss}$					16																			19			
l_{LS}															16												
l_{Lc1}				21																							
$f_{SnowReduceLAI}$																											
l														19													
$p_{o2,\,moss}$			21													19											
$p_{o2,\,vasc}$																											
$p_{o1,\,vasc}$																								19			
$p_{mn,\,moss}$																									26		
$p_{mn,\,vasc}$																			24								
$p_{o1,\,moss}$					16																						
$\varepsilon_{L,\,moss}$															24						19						16
$\varepsilon_{L,\,vasc}$														25		19					19						
$a_{pve,\,vasc}$					19																						
$a_{pve,\,vasc}$																											
a_{pgrain}																											
T_{amean}	14																										
h_2									20																		
s_k																								23			
$z_{0M,\,snow}$																											
r_{alai}																											
$r_{a,\,max,\,snow-1}$							16																				
$c_{H0,\,canopy}$									16	19										16							
ψ_{eg}																											
p_1												19															16
ψ_c																											
t_{WA}																											
g_{maxwin}																17									20		
$g_{max,\,moss}$									21											20							
$g_{max,\,vasc}$																										22	
d_p		16							23	18																	
ψ_a		17																									
h_{com}																											
T_{RainL}																											
m_T																										14	
p_{smin}						14																					
s_{dl}																											
s_{dw}						20				17																	
f_{qh}	16																				28	17					
m_{Rmin}																											
Δz_{cov}																											
Count	2	3	3	1	3	2	2	0	5	3	3	2	1	3	3	3	2	2	2	3	2	2	2	5	2	3	1

Table A3.3.3 continued.

|	a_{pgrain}	$a_{pve, vasc}$	h_2	s_k	$z_{0M,snow}$	r_{alai}	T_{amean}	$r_{a,max,snow-l}$	$C_{H0, canopy}$	$g_{max, vasc}$	ψ_c	p_1	$g_{max, moss}$	ψ_{eg}	g_{maxwin}	t_{WA}	ψ_a	d_p	h_{com}	m_T	T_{RainL}	m_{Rmin}	f_{qh}	Δz_{cov}	ρ_{smin}	s_{dl}	S_{dw}
$p_{\theta Upp}$							16																				
$p_{\theta Low}$																							14				
$p_{\theta Satact}$																17	16										
t_{max}																											
t_{min}																											
k_h							14														16						
k_{ll}																											20
m_{retain}																											
$p_{zroot, moss}$													20														
$p_{zroot, vasc}$																											
t_{Q10}												16															
$k_{gresp, vasc}$											19																
$k_{gresp, moss}$											16																
$T_{MatureSum}$		20									16		21					23									
$l_{Rc1, moss}$																											
l_{LS}										22										14							
l_{Lc1}													20														
$f_{SnowReduceLA}$																											
l				23																							
$p_{o2, moss}$																											
$p_{o2, vasc}$													17														
$p_{o1, vasc}$											19																
$p_{mn, moss}$																							28				
$p_{mn, vasc}$																		18									17
$p_{o1, moss}$																							17				
$\varepsilon_{L, moss}$																											
$\varepsilon_{L, vasc}$																											
$a_{pve, vasc}$					32	30			18																		
a_{pgrain}																		16									
T_{amean}																									21		
h_2													19				20										
s_k												19															
$z_{0M,snow}$		32																									
r_{alai}		30																18									
$r_{a,max,snow-l}$																											
$C_{H0, canopy}$		18																30									
ψ_{eg}																											
p_1																											
ψ_c				19																							
t_{WA}																			17								
g_{maxwin}																	14			14							22
$g_{max, moss}$			19														45						17				
$g_{max, vasc}$																	23										
d_p	16																										
ψ_a		20						18			30	23			45	14											
h_{com}																17											
T_{RainL}																			20								
m_T															14						20						
ρ_{smin}																											
s_{dl}						21									22												
S_{dw}																											
f_{qh}													17														
m_{Rmin}																											
Δz_{cov}																											
Count	1	3	3	2	1	2	2	1	5	2	1	2	5	0	5	1	7	4	1	3	1	0	4	0	1	2	2

A3.4 Figures
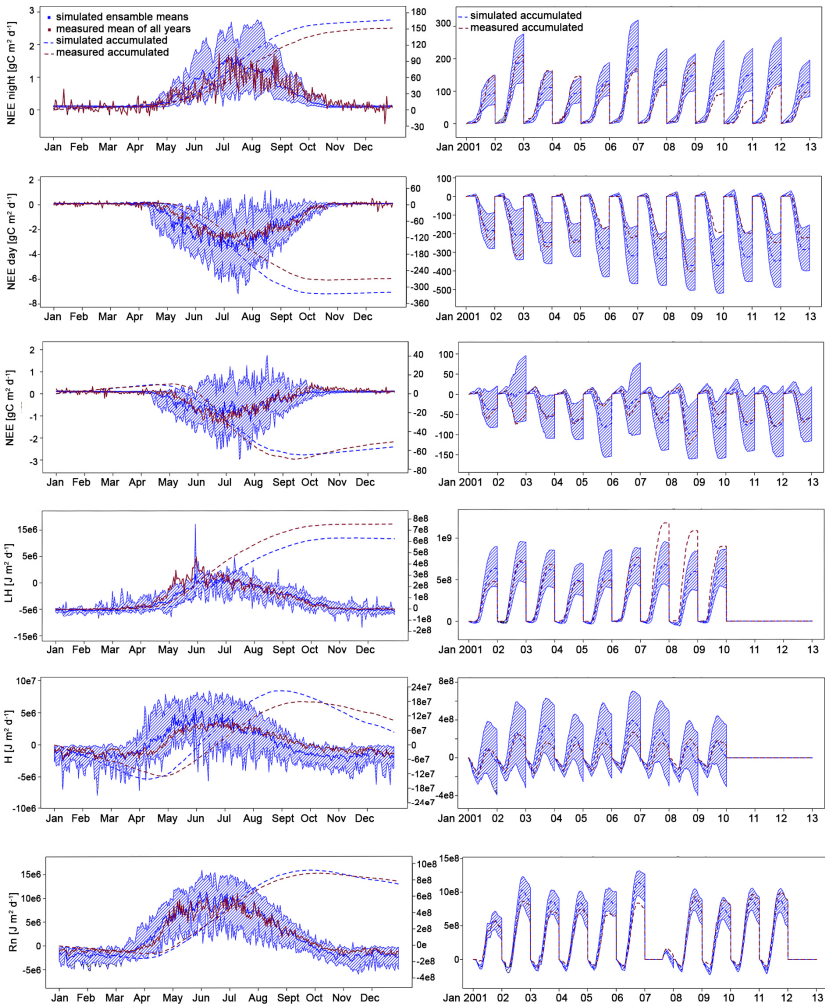
Figure A3.4.1. Model fit to observations. Left column: simulated and measured mean of all years. Right column: cumulated values for each year..
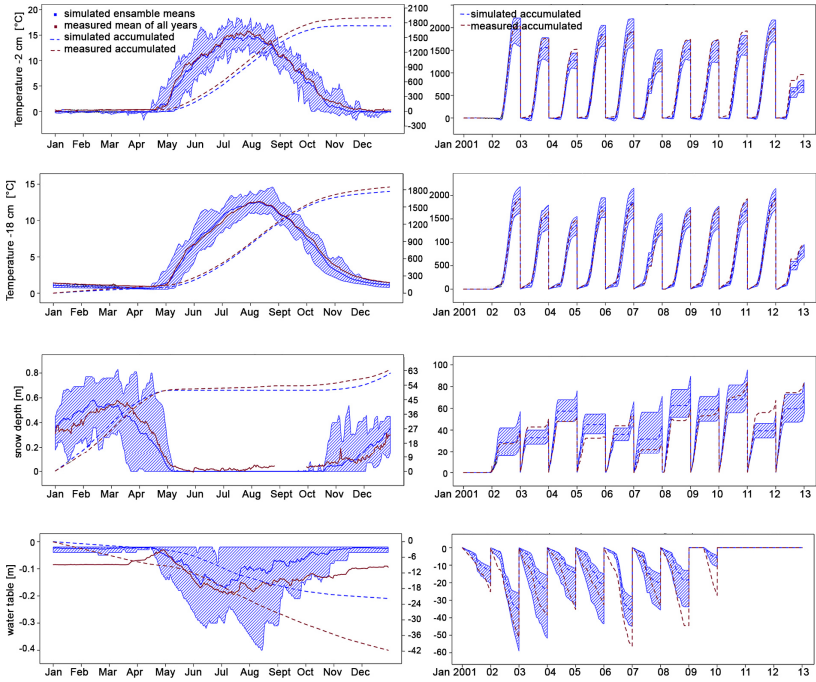
Figure A3.4.1 continued. Model fit to observations. Left column: simulated and measured mean of all years. Right column: cumulated values for each year

Figure A3.4.2. Accepted parameter ranges. The last bar in each bar chart shows the overlapping range. If empty, ranges are not overlapping.
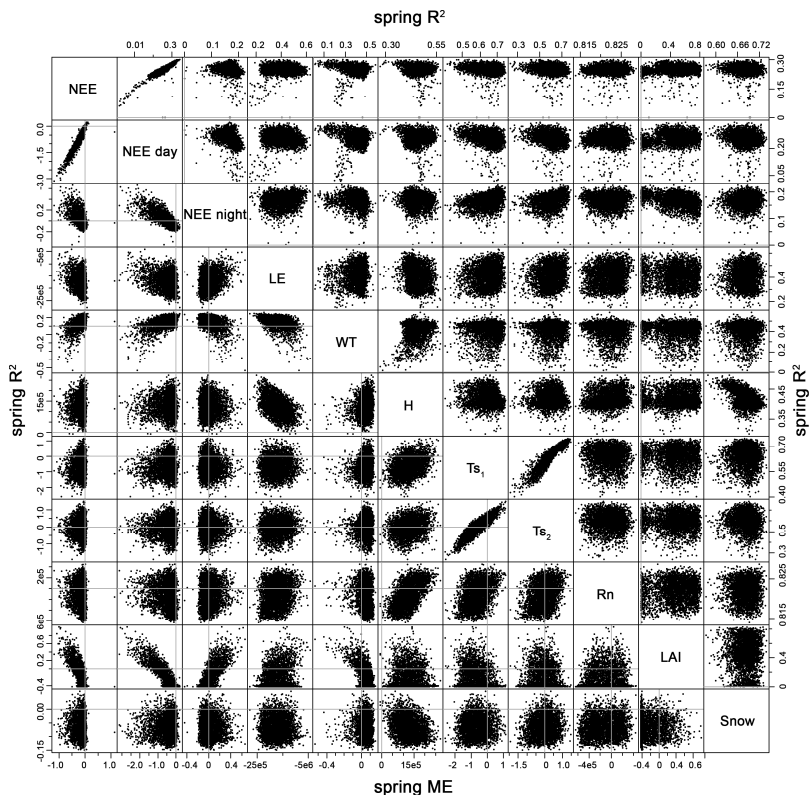
Figure A3.4.3. Correlations between performance indices in the prior distribution during spring time only. Upper panel: R2, lower panel: ME. Each of the dots represents a parameter set. Grey lines indicate the axes through zero.
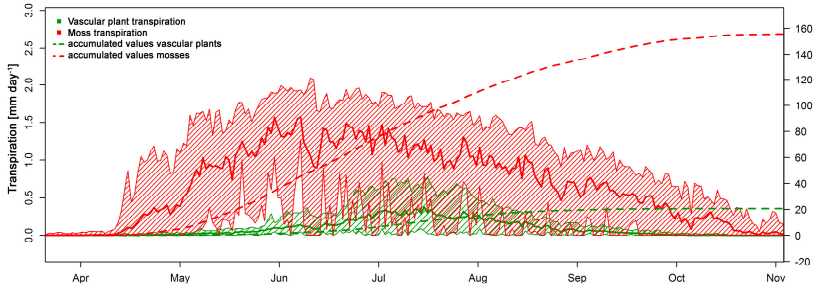
Figure A3.4.4. 12 year mean of transpiration from mosses and vascular plants. The hatched area shows the range of the 51 runs with selected performance in NEE, the solid line its mean.

## A4 Appendix to relationships between vegetation indices and characteristics study III
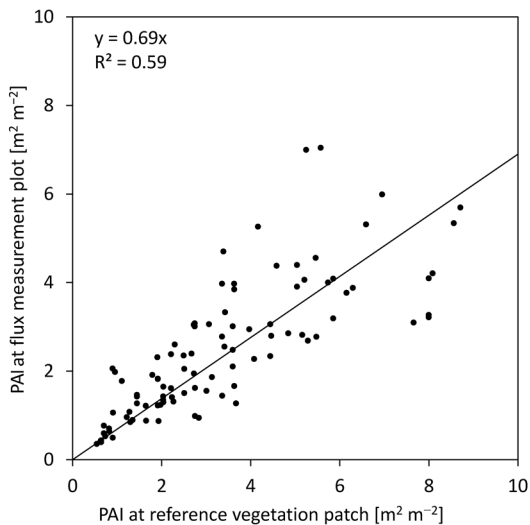
Figure A4.1. Plant area index at chamber plots versus Plant area index at vegetation patches.
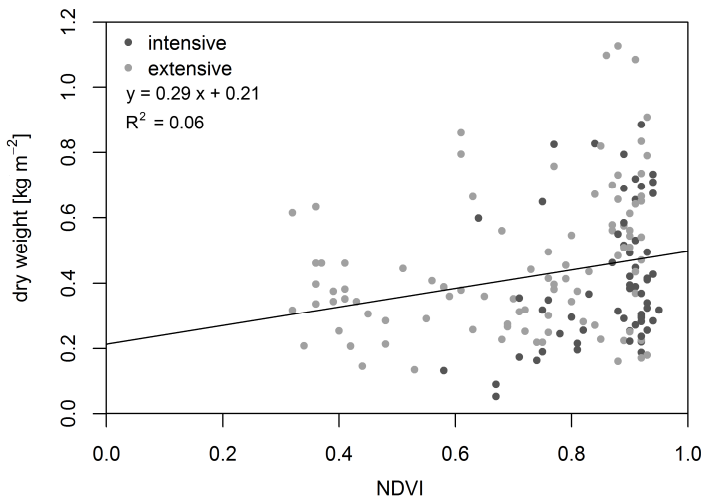
**Figure A4.2.** NDVI versus biomass.
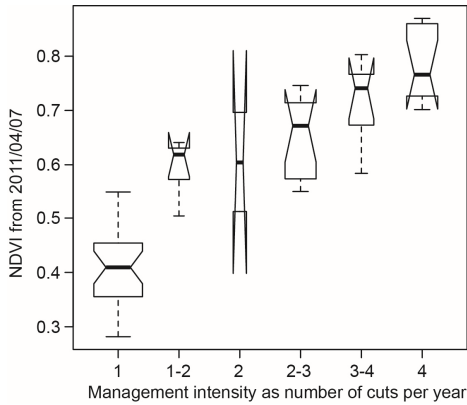
Figure A4.3. Frequency of cutting versus spring time NDVI. Cutting frequency was surveyed by Drösler et al. 2013. Parcels mapped as extensive by Schober and Stein, 2008 but surveyed with more than 2.5 cuts or parcels mapped as intensive but surveyed with less than 2.5 cuts were excluded. The width of the boxes indicates the number of observations in each category. The maximum width corresponds to 27 data points, the minimum to 2.
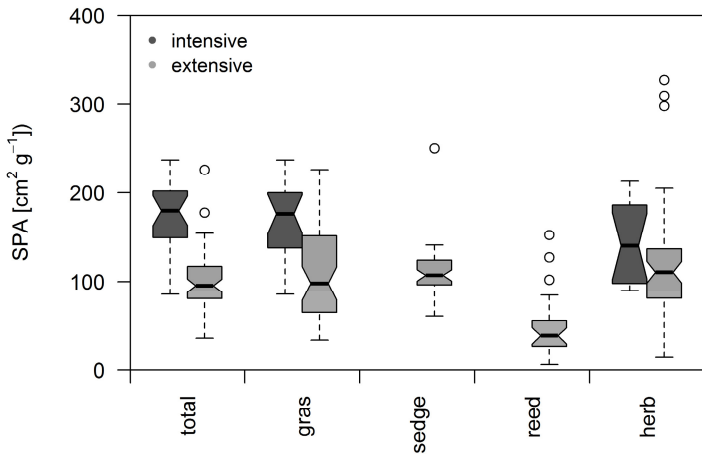

Figure A4.4. Management dependent differences in SPA values for managed grasslands and selected vegetation groups.

Appendix to relationships between vegetation indices and characteristics (study III)
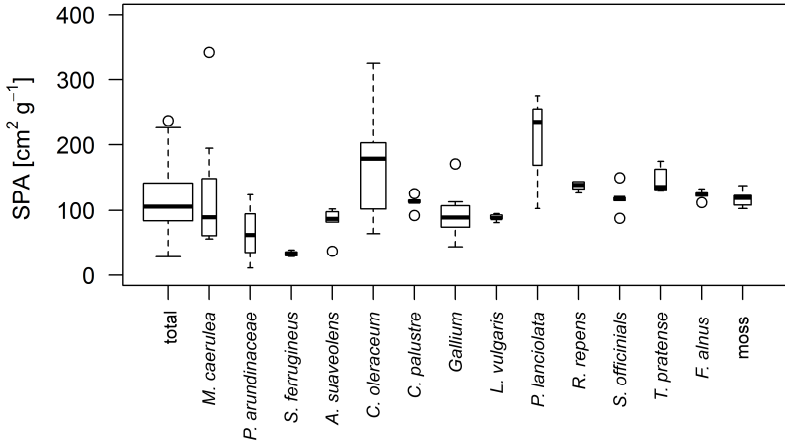
Figure A4.5. Management dependent differences in SPA values for managed grasslands and selected vegetation groups.
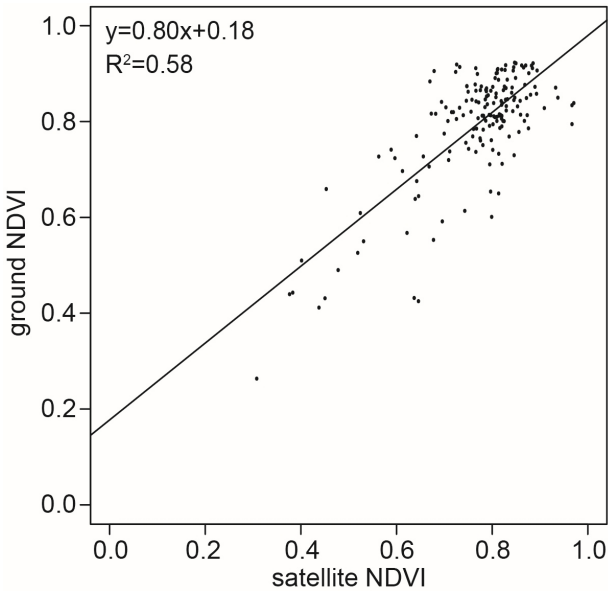
Figure A4.6. Ground versus satellite NDVI.

References to the appendix

Axelsson, B. and Ågren, G.: Tree growth model PT 1 - a development paper. Swedish Coniferous Forest Project. Swedish University of Agricultural Sciences, Department of Ecology and Environmental Research, Uppsala. Sweden, Internal Report 41, 79pp, 1976.

Berglund, E. R. and Mace, A. C.: Seasonal Albedo Variation of Black Spruce and Sphagnum-Sedge Bog Cover Types, Journal of applied meteorology, 806–812, 1972.

Beven, K.: A manifesto for the equifinality thesis, Journal of Hydrology, 320, 18–36, doi:10.1016/j.jhydrol.2005.07.007, 2006.

Beven, K. and Binley, A.: The future of distributed models: Model calibration and uncertainty prediction, Hydrological processes, 6, 279–298, 1992.

Brooks, R. H. and Corey, A. T.: Hydraulic Properties of Porous Media, Hydrology Paper No. 3, Colorado State University, Fort Collins, Colorado, US, 27pp, 1964.

Clymo, R. S. and Hayward, P. M.: The Ecology of Sphagnum, in: Bryophyte Ecology, Smith, A. J. E. Ed., Springer Netherlands, 229–289, 1982.

Drösler, M., Adelmann, W., Augustin, J., Bergman, L., Beyer, C., Chojnicki, B. H., Förster, C., Freibauer, A., Giebels, M., Görlitz, S., Höper, H., Kantelhardt, J., Liebersbach, H., Hahn-Schöfl, M., Minke, M., Petschow, U., Pfadenhauer, J., Schaller, L., Schägner, P., Sommer, M., Thuille, A., and Wehrhan, M.: Klimaschutz durch Moorschutz. Schlussbericht des BMBF-Vorhabens: Klimaschutz-Moornutzungsstrategien 2006-2010: Klimaschutz-Moornutzungsstrategien 2006-2010, TIB/UB-Hannover, Hannover, Germany, 201 pp., 2013.

Grace, J.: The Growth-Physiology of Moorland Plants in relation to their Aerial Environment. Ph.D. thesis, Univ. Sheffield, Sheffield, UK, 1973.

Granberg, G., Grip, H., Löfvenius, M. O., Sundh, I., Svensson, B. H., and Nilsson, M.: A simple model for simulation of water content, soil frost, and soil temperatures in boreal mixed mires, Water Resour. Res., 31, 3371–3382, doi:10.1029/1999WR900216, 1999.

Graham, E. A., Hamilton, M. P., Mishler, B. D., Rundel, P. W., and Hansen, M. H.: Use of a Networked Digital Camera to Estimate Net CO_2 Uptake of a Desiccation-Tolerant Moss, Int. J Plant Sci., 167, 751–758, doi:10.1086/503786, 2006.

Jansson, P.-E. and Karlberg, L.: Coupled heat and mass transfer model for soil–plant–atmosphere systems. Royal Institute of Technology,

Stockholm, 484 pp., accessed: 17 November 2015
https://drive.google.com/file/d/0B0-
WJKp0fmYCZ0JVeVgzRWFIbUk/view?pli=1, 2010.

Jonasson, S. and Stuart Chapin, F. III: Significance of sequential leaf
development for nutrient balance of the cotton sedge,Eriophorum
vaginatum L, Oecologia, 67, 511–518, doi:10.1007/BF00790022, 1985.

Kellner, E.: Surface energy fluxes and control of evapotranspiration from a
Swedish Sphagnum mire, Agricultural and Forest Meteorology, 110, 101–
123, doi:10.1016/S0168-19230100283-0, 2001.

Kellner, E. and Lundin, L.-C.: Calibration of time domain reflectometry for
water content in peat soil, Nordic Hydrology, 32, 315–332, 2001.

Kondratiev, K. Y., Mironova, Z. F., and Otto, A. N.: Spectral albedo of
natural surfaces, pure and applied geophysics, 59, 207–216, 1964.

Körner, C.: Alpine plant life: Functional plant ecology of high mountain
ecosystems, Springer, Berlin, New York, 338 pp, 1999.

Kummerow, J. and Ellis, B. A.: Temperature effect on biomass production
and root/shoot biomass ratios in two arctic sedges under controlled
environmental conditions, Bot., 62, 2150–2153, doi:10.1139/b84-294,
1984.

Metzger, C., Jansson, P.-E., Lohila, A., Aurela, M., Eickenscheidt, T.,
Belelli-Marchesini, L., Dinsmore, K. J., Drewer, J., van Huissteden, J.,
and Drösler, M.: CO_2 fluxes and ecosystem dynamics at five European
treeless peatlands – merging data and process oriented modeling,
Biogeosciences, 12, 125–146, doi:10.5194/bg-12-125-2015, 2015.

Päivänen, J.: Hydraulic conductivity and water retention in peat soils, Acta
Forestalia Fennica, 129, 1973.

Petzold, D. E. and Rencz, A. N.: The albedo of selected subarctic surfaces,
Arctic and Alpine Research, 393–398, 1975.

Price, J.: Evaporation from a blanket bog in a foggy coastal environment,
Boundary-Layer Meteorol, 57, 391-406, doi:10.1007/BF00120056, 1991.

Ratkowsky, D. A., Olley, J., McMeekin, T. A., and Ball, A.: Relationship
between temperature and growth rate of bacterial cultures, Journal of
Bacteriology, 149, 1–5, 1982.

Rice, S. K., Aclander, L., and Hanson, D. T.: Do bryophyte shoot systems
function like vascular plant leaves or canopies?: Functional trait
relationships in Sphagnum mosses Sphagnaceae: Functional trait
relationships in Sphagnum mosses Sphagnaceae, American journal of
botany, 95, 1326–1330, doi:10.3332/ajb.0800019, 2008.

Schober, H. M. and Stein, C.: Freisinger Moos Interkommunales
Flächenmanagement Intercommunal land management in the Freisinger
Moos, final report for LEADER+ -project 06030-081013, Dr. H. M.

References

Schober Büro für Landschaftsarchitektur, Freising, Germany, 56 pp., 2008.

Shaver, G. R. and Laundre, J.: Exsertion, elongation, and senescence of leaves of Eriophorum vaginatum and Carex bigelowii in Northern Alaska, Glob Change Biol, 3, 146–157, doi:10.1111/j.1365-2486.1997.gcb141.x, 1997.

Shaw R.H. and Pereira, A.R.: Aerodynamic roughness of a plant canopy: a numerical experiment. Agricultural Forest Meteorology, 26: 51-65, 1982.

van de Weg, M. J., Fetcher, N., and Shaver, G.: Response of dark respiration to temperature in Eriophorum vaginatum from a 30-year-old transplant experiment in Alaska, Plant Ecology & Diversity, 6, 337–301, doi:10.1080/17560874.2012.729628, 2013.

Vermeij, I.: Relating phenology to the gross primary production in a boreal peatland, using the greenness index, MSc thesis Biology, Wageningen University, Wageningen, 2013.

Wang, X., He, X., Williams, J. R., Izaurralde, R. C., and Atwood, J. D.: Sensitivity and uncertainty analyses of crop yields and soil organic carbon simulated with EPIC, American Society of Agricultural and Biological Engineers, 48, 1041–1054, 2005.

Wohlfahrt, G., Bahn, M., Haubner, E., Horak, I., Michaeler, W., Rottmar, K., Tappeiner, U., and Cernusca, A.: Inter-specific variation of the biochemical limitation to photosynthesis and related leaf traits of 30 species from mountain grassland ecosystems under different land use, Plant, Cell and Environment, 22, 1281–1296, 1999.

Zhao, W., Hidenori, T., and Zhao, H.: Estimation of vegetative surface albedo in the Kushiro Mire with Landsat TM data, Chin. Geograph.Sc., 7, 278-288, doi:10.1007/s11769-997-0056-4, 1997.